Murdoch
UNIVERSITY

Targeting Immune Suppression to Improve the Post-Surgical Outcome of Solid Malignancies

Wayne John Aston
Bachelor of Science (Hons) in Molecular Biology
School of Veterinary and Life Sciences
Murdoch University
2013

Supervisors: Dr Andrea Khong
University of Western Australia
School of Medicine and Pharmacology,
Harry Perkins Institute of Medical Research

Dr Scott Fisher
University of Western Australia
School of Medicine and Pharmacology,
Harry Perkins Institute of Medical Research

Co-Supervisor: Associate Professor Robert Mead
Murdoch University
School of Veterinary and Life Sciences

Declaration

This thesis was completed in accordance with the requirements stated by the School of Veterinary and Life Sciences for the award of Bachelor of Science (Hons) in Molecular Biology.

I declare that this thesis contains the original work of my research unless otherwise stated and referenced and that no part has been submitted for any degree at any other university or institution.

Wayne Aston

Word Count : 22 403

Acknowledgements

Firstly, I would like to sincerely thank my supervisors Dr Andrea Khong and Dr Scott Fisher. Thank you for all the help and support you have provided this year and for the opportunity to undertake this research project. It has been a great year and I have thoroughly enjoyed it. I would also like to thank the research staff within the Tumour Immunology Group and the National Centre for Asbestos Related Diseases for their guidance and support this year, specifically research assistants Catherine Boylen and Joanne Salmons that assisted with my initial training. Also a big thank you to the heads of this group, W/Prof Bruce Robinson and Adj/Prof Richard Lake, for providing a great research and teaching atmosphere as well as their feedback which proved most helpful. I would also like to thank the department laboratory technition Ebony Rouse for everything she did to keep the department running smoothly.

I would also like to acknowledge my family for all their support this year. You have been incredibly understanding and patient and always ready to help with anything you could. Without you, completing this honours year would have been a lot more stressful.

Lastly I would like to thank a close group of friends for being incredibly understanding and for the support offered to me this year. To be able to count on and share with you the highs and low's of this year and the constant encouragement definitely made a huge difference and I sincerely thank you for that.

Abstract

Tumour debulking surgery aims to produce a smaller target for adjuvant therapy whilst also removing much of the tumour associated immunosuppression. Even so, cures are rarely seen in either animal studies or human patients receiving debulking surgery plus adjuvant chemo-immunotherapy, despite evidence of effector T cell activation that should be strong enough to overcome tumour growth. Adjuvant immunotherapies can be used to eradicate distant micro metastases or cancer cells that remain after surgery, but have limited success. This could be due to 'immune brakes' that continue to operate, suppressing the anti-tumour response. This is particularly true for mesothelioma, metastatic melanoma and colorectal cancer, which are the main focus of this project.

Tumour-induced immune suppression may be caused by suppressive immune cells such as regulatory T cells (Tregs) and myeloid derived suppressor cells (MDSCs). Both of these cellular populations suppress the anti-tumour effector T cell responses including the effectiveness of cytolytic CD8+ T cells both systemically and locally. This project will use a combined approach to alleviate immune suppression in combination with debulking surgery through the targeted removal of suppressive Treg and MDSC subsets.

This project aimed to improve the response seen with debulking surgery by removing tumour-associated immune suppression. The hypothesis was that removing these 'brakes' on the anti-tumour immune response would release a stronger, lasting anti-tumour response elicited by adjuvant immunotherapy after surgical debulking. Thus, the results from this study may direct future clinical trials and potentially allow partial debulking surgery to remain a valid treatment option for these patients, especially if followed with the appropriate immunotherapy regimens.

List of Abbreviations

5-FU	5-Fluorouracil
APC	Antigen Presenting Cells
ATCC	American Type Culture Collection
ATRA	All-Trans Retinoic Acid
CSF	Colony Stimulating Factor
CT	Computed Tomography
CTL	Cytotoxic T Lymphocyte
CTLA-4	Cytotoxic T-lymphocytes antigen 4
DAMP	Damage-Associated Molecular Patterns
DC	Dendritic Cell
dLN	Draining Lymph Node
DTx	Diphtheria Toxin
EDTA	Ethylenediaminetetraacetic Acid
ER	Endoplasmic Reticulum
FACS	Fluorescence-activated cell sorting
FCS	Foetal Calf Serum
FMO	Fluorescence Minus One
FoxP3	Forkhead Box 3
gp70	Glycoprotein 70
HA	Haemagglutinin
HTS	High Throughput Sampler
I.p.	Intraperitoneal
ICOS	Inducible T-cell Costimulator

IFN-γ	Interferon Gamma
IL-10	Interlukin-10
IL-2	Interlukin-2
IL-35	Interlukin-35
IMC	Immature Myeloid Cell
iNOS	Inducible Nitric Oxide Synthase
LV	Leucovorin
MDSC	Myeloid Derived Suppressor Cell
MHC	Major Histocompatibility Complex
ndLN	Non-Draining Lymph Node
NK	Natural Killer Cell
PAMP	Pattern-Associated Molecular Patterns
PBS	Phosphate Buffer Saline
PD-1	Programmed death protein-1
PET	Positron Emission Tomography
ROS	Reactive Oxygen Species
S.c.	Subcutaneous
TAA	Tumour-Associated Antigens
TCR	T Cell Receptor
TGF-β	Transforming Growth Factor Beta
TIL	Tumour Infiltrating Lymphocytes
TNF-α	Tumour Necrosis Factor Alpha
TP	Thymidine phosphorylase
Treg	Regulatory T Cell
UV	Ultraviolet
UWA	University of Western Australia

VATS	Video-Assisted Thoracic Surgery
VEGF	Vascular Endothelial Growth Factor

List of Figures and Tables

Table of Contents

Chapter 1: Literature Review

1.1 Cancer

Cancer has become one of the most varied and widespread diseases worldwide with a large proportion of the global population having encountered it either directly or indirectly. It occurs in numerous forms with a large variation in causes, pathogenesis and survival. In Australia, more than 43700 people died from cancer in 2011. Treatment for cancer also places a huge burden on the health system, costing approximately $3.8 billion or 7.2% of the health budget (Australian Institute of Health and Welfare, 2012). Cancer refers to a larger group of varying pathogenic conditions with the common factor being the malignant transformation of normal cells into oncogenic cells that can grow and proliferate uncontrollably. Currently there are more than 200 different types of cancer which can affect every organ of the human body with many of the cell types making up those organs susceptible to malignant transformation (Cancer Research UK, 2012)

Predominantly, cancers present themselves as a solid malignancy in which a mass is made up of one or more oncogenic cell types that has entered a stage of uncontrolled proliferation that leads to the formation of a mass. This occurs as a result of the body's immune system failing to recognise and respond to cells undergoing oncogenic transformation as a result of specific genetic mutations. The cause of these genetic alterations are largely environmental with exposure to certain mutagens as well as lifestyle choices such as dietary intake and alcohol consumption being responsible for tumourigenesis (Sankpal *et al.*, 2012).

Treatments for cancer are varied and include the use of cytotoxic chemotherapeutic agents, radiotherapy, surgery and immunotherapies with the goal of eliminating all traces of the

oncogenic cells while limiting side effects. A combination of these or a combination of different chemotherapy drugs is often used to achieve synergistic effects between individual treatments and has been shown to improve patient outcome especially with the formation of a solid tumour mass (Prados *et al.*, 2012). These solid masses become incredibly resistant to current treatment options and as a result the first point of attack is often surgery with the aim to either completely remove the tumour or reduce its size and impact on the host and then treat with an adjuvant therapy to clear the remaining cells (Yano *et al.*, 2009). The role of immunotherapies for use in the successful treatment of solid cancers has increased dramatically especially in those that are currently resistant to conventional cancer therapy regimes. Several solid cancers have shown a susceptibility to immunotherapeutic agents and include malignant mesothelioma (Bograd *et al.*, 2011), metastatic melanoma (Wolchok *et al.*, 2013) and colorectal carcinoma (Lin *et al.*, 2013) and tumour models of these diseases were used in this study.

1.2 Solid Malignancies

In most cases, carcinogenesis results in the formation of a solid tumour of the tissue type in which the mutations have occurred. These may either be benign and therefore do not spread to other tissues or they may be metastatic where the primary tumour can invade surrounding tissue, enter the circulatory system and spread to other parts of the body.

1.2.1 Malignant Mesothelioma

Malignant mesothelioma is a highly treatment-resistant cancer that is increasing in frequency both in Australia and worldwide (Robinson, Musk*, et al.*, 2005). Mesothelioma is a cancerous tumour that affects the serosal surfaces of the body, namely the pleura, peritoneum and pericardium and is named after its effect on the mesothelium membrane found lining these areas. This cancer is highly associated with asbestos exposure and its

widespread use during the 20th century due to its exceptional fire-resistant properties with its link to mesothelioma only being discovered in 1960 (Ismail-Khan *et al.*, 2006). Detection of mesothelioma is often associated with the development of a pleural effusion and associated chest pain and the median survival for someone diagnosed is 9 to 12 months with a very small number of patients surviving past that. The vast majority of patients affected by mesothelioma are male.

Treatment of mesothelioma depends on the staging of the disease and is mostly palliative due to the cancer not responding well to current treatment protocols. This may involve surgery for either diagnostic, palliative or on rare occasions, the potential cure of the disease (Robinson & Lake, 2005). The goal of surgery in mesothelioma is to perform cytoreductive or debulking surgery to remove all macroscopic evidence of the cancer and then treat with adjuvant therapies (Remon *et al.*, 2013). This is mainly due to the diffuse nature of the cancer with aggressive surgical approaches resulting in the patient being placed under a huge amount of stress. Patients are often excluded from debulking surgery of mesothelioma for various reasons ranging from the extent of the disease and their willingness to receive adjuvant therapy to their general health and wellbeing (Yano *et al.*, 2009).

Chemotherapy is the primary adjuvant therapy option but is not extensively effective and is often used as a palliative approach (Sterman *et al.*, 2005). Chemotherapeutic agents used for the treatment of mesothelioma work more effectively when used in combination with the platinum-containing drugs that have a higher activity than those that do not. The most effective of these are cisplatin and doxorubicin with a response rate of 28.5% versus 11.3% for a single therapy. An exception to this was the response rate of treatment with an antifolate drug methotrexate in which a cohort of patients were treated with a high dose

that resulted in a response rate of 37% compared to 32% showing no change and the remainder having progressive disease (Remon *et al.*, 2013). Other chemotherapy agents in use include cisplatin, raltitrexed and gemcitabine although all of these have response rates below 30% and survival rates often less than 1 year (Lee *et al.*, 2009).

The urgent need for more effective treatment therapies for mesothelioma has prompted researchers to develop treatments that reduce both the incidence and severity of this fatal disease. For this reason the opportunity exists for an immunotherapy to be developed to cause the body's immune system to attack and potentially destroy the cancerous cells. As a surgical approach to mesothelioma cannot remove the entire tumour as some areas are hard to access or diffuse microscopic cancerous deposits are present (Sterman *et al.*, 2005), an immunotherapy designed to attack these remaining cells may prove effective in increasing both patient quality of life and long term survival.

1.2.2 Metastatic Melanoma

Melanoma is a malignant cancer of melanocytes, the cells responsible for the production of the pigment melanin. In Australia, it is the third most common cancer in both men and women and while it makes up only 2.3% of all skin cancers it is responsible for 75% of skin cancer related deaths. When the disease is diagnosed early, the tumour can be removed with little risk however at later stages the prognosis is very poor with a median survival of 6 to 10 months (Read, 2013). The primary cause of melanoma is exposure to ultraviolet (UV) radiation, in particular UV-B that can lead to burns, increased photo ageing of the skin and skin carcinogenesis (Elmageed *et al.*, 2009). Diagnosis of melanomas are usually done visually by identifying moles that may have an irregular shape or colour and a diameter larger than 6 mm and still growing, as well as with a skin biopsy. The confirmation of metastatic melanomas involves diagnostic scanning to detect

metastases with positron emission tomography and computed tomography (PET/CT) rapidly becoming the most accurate diagnostic method. It is also as able to detect a potential response to treatment by measuring changes in the size of metastatic tumours (Read, 2013).

Treatment for non-metastatic melanoma involves surgical resection of the tumour that is often curative with adequate excision margins to ensure the entire mass is removed. A melanoma that has metastasised is much harder to treat and requires the use of adjuvant therapies such as combination chemo-immunotherapy using the chemotherapy agent dacarbazine and the immunotherapy interlukin-2 (IL-2) although this combination has a relatively low response rate between 10-20% (Spagnolo *et al.*, 2012). As melanoma can be quite an immunogenic cancer as a result of detectable tumour-associated antigens (TAA) such as MAGE-1, CDK4 and TYRP1, the possibility of a successful immunotherapy regime looks promising (Gyorki *et al.*, 2013). The latest advances in melanoma immunotherapy are focused on blocking inhibitory molecules such as cytotoxic T-lymphocytes antigen 4 (CTLA-4) and programmed death protein-1 (PD-1) with humanised antibodies already developed against these targets termed Ipilimumab and Nivolumab respectively (Wolchok *et al.*, 2013). Both of these molecules have roles in limiting T cell function and blocking them allows T lymphocytes to remain functional for longer. A recent clinical trial combining both therapies showed that at the maximum doses, 53% of patients had an objective-response with all having a minimum of 80% reduction of tumour mass (Wolchok *et al.*, 2013). This demonstrates a clear link between metastatic melanoma and the potential for immunotherapies to become standard treatment for this cancer.

1.2.3 Colorectal Carcinoma

Colorectal cancer is one of the more common cancers. It results from uncontrolled cellular growth in the colon and rectum with roughly 9.7% of all cancers being in the colon (Harrison *et al.*, 2011). This cancer has a number of risk factors associated with its development such as increasing age, male gender and environmental factors including poor diet and smoking. Roughly two-thirds of the incidence of colorectal cancer can be attributed to inflammatory bowel disease with risk increasing the longer the disease exists as well as the severity of the inflammation. Diagnosis of this cancer is accomplished via a colonoscopy or sigmoidoscopy as well as a tumour biopsy. A CT scan is often done to detect or rule out metastasis (Cunningham *et al.*, 2010).

The treatment of colorectal cancer primarily involves resection of the tumour with the hope that it can be entirely removed with adequate surgical margins. Removal of the lymph nodes aids in the staging of the disease and a higher number of positive nodes removed correlates with a higher patient survival (Le Voyer, 2003). For treatment of metastatic colorectal cancer, adjuvant therapies are used in combination with surgery and mostly include chemotherapy. The most common chemotherapy regime used for this cancer involves 5-fluorouracil (5-FU) in combination with leucovorin (LV) and has been associated with increased survival in patients with stage III disease (Carrato, 2008). Another common chemotherapeutic agent is capecitabine, an oral fluorouracil prodrug that is used to restrict the action of 5-FU to the site of the tumour, as capecitabine is converted to 5-FU by the high abundance of the enzyme thymidine phosphorylase (TP) at the tumour site within the colon (Carrato, 2008). Radiotherapy for colorectal cancer is not recommended as the bowels are highly sensitive to radiation but is used for the closely related rectal cancer (Cunningham *et al.*, 2010). With the lack of adjuvant therapies for colorectal cancer and with surgery the best hope of a cure, the opportunity again exists for

an immunotherapy regime to be developed to eradicate any metastatic disease that remains after surgical resection of the primary tumour mass.

With conventional adjuvant therapies to surgery such as chemotherapy and radiation not being able to sufficiently provide curative options for these cancers, there is the potential to develop effective immunotherapies to induce an immune response to these solid malignancies. As surgery itself can remove a large portion of the tumour thereby reducing its burden on the patient, therapies to either boost an immune response or to remove tumour-associated suppression can promote eradication of any micro metastasis or unresectable tumour left behind after surgery.

1.3 The Role of the Immune System in Cancer

The immune system can detect and eliminate infectious organisms. To be able to use it to combat cancer in a similar way as other therapies, a solid understanding of the tumour immune response is needed to identify key points that can be targeted to either increase the response or remove suppression associated with the presence of a solid tumour. The majority of research into the role of the immune system within the cancer environment focuses on the adaptive response and how cytotoxic T lymphocytes (CTLs) are able to respond to a solid tumour. Evidence also suggests an important role of the innate immune system as well (Liu *et al.*, 2012)

1.3.1 The Immune System

Our immune system plays a vital role in protecting us from infectious organisms as well as initiating the inflammatory response to remove the source of damage and repair that has already occurred. It needs to be able to correctly distinguish a pathogen, such as a virus, from self-antigens to ensure only harmful, foreign molecules are targeted. The immune

system can be separated into the innate and adaptive response with each containing a set of effector cells (Figure 1) that work together to drive the responses to foreign antigens (Dranoff, 2004).

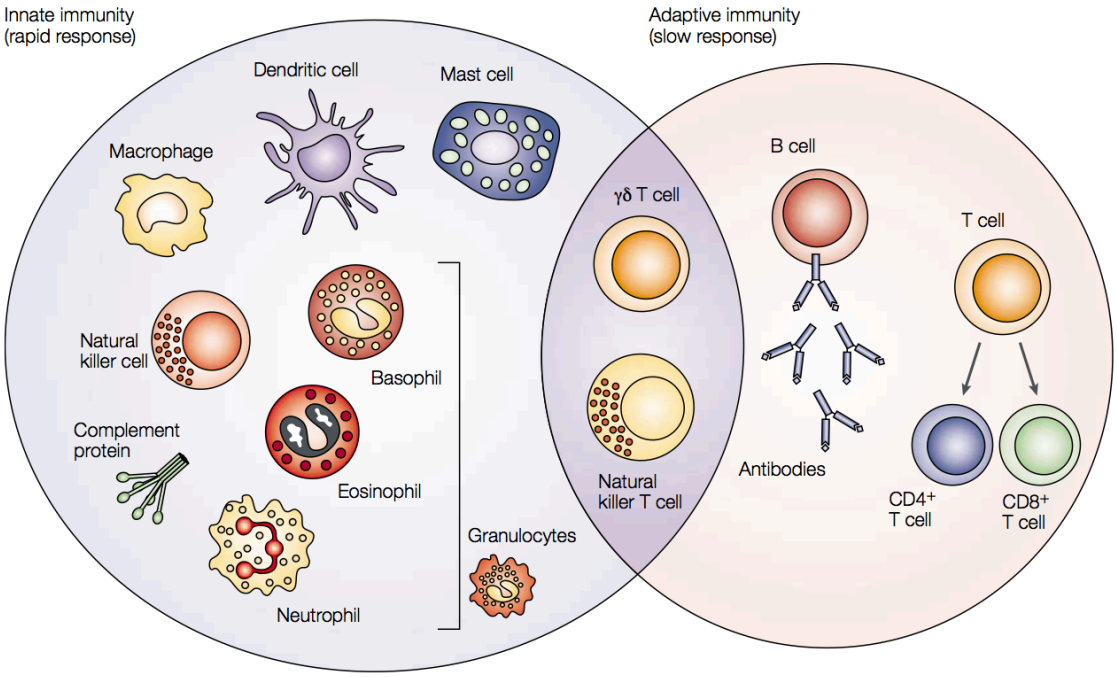

Figure 1: Innate and Adaptive Immunity (Dranoff, 2004)

1.3.1.1 Innate Immunity

The innate immune system is responsible for the fast, non-specific response to a foreign antigen. It has a very short lag time between exposure and response and it does not form immunological memory of encountered pathogens. This system is made up of cellular components such as granulocytes, mast cells, macrophages, dendritic cells (DCs) and natural killer (NK) cells which are the first line effectors in the anti-tumour immune response (Liu *et al.*, 2012). Their response involves the recognition of foreign organisms/antigens and the orchestration of an inflammatory response towards them. Inflammation is mainly initiated by macrophages and DCs when they recognise pattern-associated molecular patterns (PAMPs) or damage-associated molecular patterns (DAMPs) and in response secrete inflammatory mediators that lead to the onset of inflammation

(Janeway, 2001). The innate system also includes soluble factors such as the complement system and is the major humoral component of the innate response. It functions by either binding complement proteins to antibodies already bound to TAAs/microbes or by direct binding that leads to a rapid immune response (Rus *et al.*, 2005). Another feature of the innate immune system that is more relevant to infectious organisms are the barriers such as the skin and gastrointestinal tract. These act to prevent organisms entering the system including oncogenic viruses and contains additional defence mechanisms such as sweat, gastric acid and saliva (Janeway, 2001).

1.3.1.2 Adaptive Immunity

In contrast, the adaptive immune response is antigen-specific and is able to produce memory cells that can be initiated faster responses should that antigen be encountered again. This response is slower than the innate system due to the required expansion of lymphocyte populations. The cells that make up the adaptive immune system include B-lymphocytes that are responsible for antibody production and T-lymphocytes that are involved in the cell-mediated immune response (Dranoff, 2004). The antigen specificity is achieved by the somatic rearrangement of the antigen receptor genes responsible for the production of immunoglobulins for B-lymphocytes and the T cell receptors (TCR) for T-lymphocytes (Narendra *et al.*, 2013). Once these antigen-specific receptors have been produced and activated and the pathogen has been cleared, there exists both memory B cells and memory T cells that retain those receptors and can recognise that same antigen if it is encountered in the future. This forms the basis of vaccination (Niederkorn, 2009).

A key feature of the adaptive immune system is that it differentiates between self and non-self antigens. This allows the adaptive response to only initiate an immune response to antigens that are foreign such as a virus or to a lesser extent a tumour. When this process

fails it can result in non-specific recognition of antigens that may be classed as self-antigens which can then lead to the onset of autoimmune disease (Narendra *et al.*, 2013). This recognition of antigens is accomplished either directly by B-lymphocytes or via a process called antigen presentation for T-lymphocytes that allows them to mount an antigen-specific response against specifically-targeted cells.

1.3.1.3 Antigen Presentation

For the immune system to be able to recognise and respond to non-self antigens, they must be presented to T-lymphocytes via antigen presentation. This is done by antigen presenting cells (APC) such as DCs and macrophages as well as most host cells in terms of cytosolic antigens that bind antigens to the major histocompatibility complex (MHC). The MHC molecule consists of 2 classes, namely class I and class II. In normal antigen presentation, intracellular antigens are broken down into small peptides and loaded onto the MHC Class I molecule on the endoplasmic reticulum (ER) and presented to $CD8^+$ CTLs. Extracellular antigens are captured and processed by APCs such as the DCs and loaded onto MHC class II molecules and presented to $CD4^+$ helper T cells (Savina *et al.*, 2007). There is an exception to this process in that antigens acquired exogenously such as those from a tumour can be presented via Class I to CTLs in a process called cross-presentation (Heath *et al.*, 2004). This process is very important for both anti-viral and anti-tumour immune responses and allows for the induction of central and peripheral tolerance. This process is under very tight control as the activation of CTLs to infection or tumour antigens may lead to autoimmunity and non-specific responses of these CTLs (Flinsenberg *et al.*, 2011). Knowledge of the role of DCs in cross-presentation is continuously expanding with research into this area focusing on the development of therapies to allow cross-presentation to be more effective. To do this requires adequate mouse models that lack

cross-presentation ability while not affecting the other functions of APCs involved in this process (Joffre *et al.*, 2012).

1.3.2 The Tumour Immune Response

The onset of cancer is partly due to the fact that the immune system fails to recognise the oncogenic transformation and is unable to respond and eliminate those proliferating cells before a solid tumour has formed (Whiteside, 2006). To be able to identify therapeutic targets for novel immunotherapies, the immune systems control mechanisms for oncogenesis as well as the response to an already formed solid tumour need to be understood.

1.3.2.1 Immunosurveillance

Burnet and Thomas introduced the theory of immunosurveillance in 1957 (Dunn *et al.*, 2002). The fundamental aspect of this was that the immune system, particularly lymphocytes, are able to patrol around the body and identify neoplastic cells and subsequently eliminate them. This theory has been supported by a number of experimental results showing that transplanted tumours were rejected when implanted into mice (Dunn *et al.*, 2002). The presence of tumour infiltrating lymphocytes (TILs) is further evidence that the immune system can recognise and attack cancer cells (Kim *et al.*, 2007). Despite evidence to suggest that this process is capable of preventing tumour growth, solid malignancies still do occur and therefore a new concept was introduced called immunoediting (Dunn *et al.*, 2002).

1.3.2.2 Immunoediting

This new concept proposed that cancer might edit a person's immune system as to enable escape from immune responses. Immunoediting can be divided into 3 stages: elimination, equilibrium and escape.

1.3.2.2.1 Elimination

This stage involves both innate and adaptive immune responses to the tumour cells. Inflammation is then activated which leads to further recruitment of immune cells to the site of the cancer. Cells such as NK cells are stimulated to produce interferon gamma (IFN-γ) that can result in limited cancer cell death. The tumour antigens are collected by DCs that track to the lymph nodes that initiated the development of CTLs. These then enter the tumour site and attempt to bind with and eliminate the tumour cells expressing that antigen (Kim *et al.*, 2007).

1.3.2.2.2 Equilibrium and Escape

Often some tumour cells are able to survive the elimination stage and enter equilibrium where tumour growth equals tumour death. Eventually, genetic mutations can lead to more of these tumour cells becoming resistant to the elimination processes such as IFN-γ and therefore enter the escape stage in which tumour growth proceeds and solid malignancies form while TILs are still present in the tumour (Vesely *et al.*, 2013).

1.3.3.1 The CTL Response to Tumours

During the elimination phase, there is a response by CTLs, also know as $CD8^+$ T cells. The response of these cells can be outlined in 6 main steps. The tumour immune response (Figure 2) begins with the detection of tumour antigens. These tumour-associated antigens (TAA) (step A) are detected within the tumour microenvironment as well as in the

periphery. They need to reach and be recognised by specialized APCs in the lymph nodes (step B) and presented on the MHC class I molecule to specific $CD8^+$ T cells (step C). These CTL's now proliferate and are programmed to recognise that TAA and enter the systemic circulation (step D) and traffic around the body. Some will enter the tumour blood vessel and pass into the tumour microenvironment where they can recognise the TAA they are specific for and exert their cytotoxic effect (step E). There is also the production of memory T-cells that will stay in the body and will be able to mount a rapid response should that specific antigen be encountered again, with production of both $CD4^+$ and $CD8^+$ cells (step F).

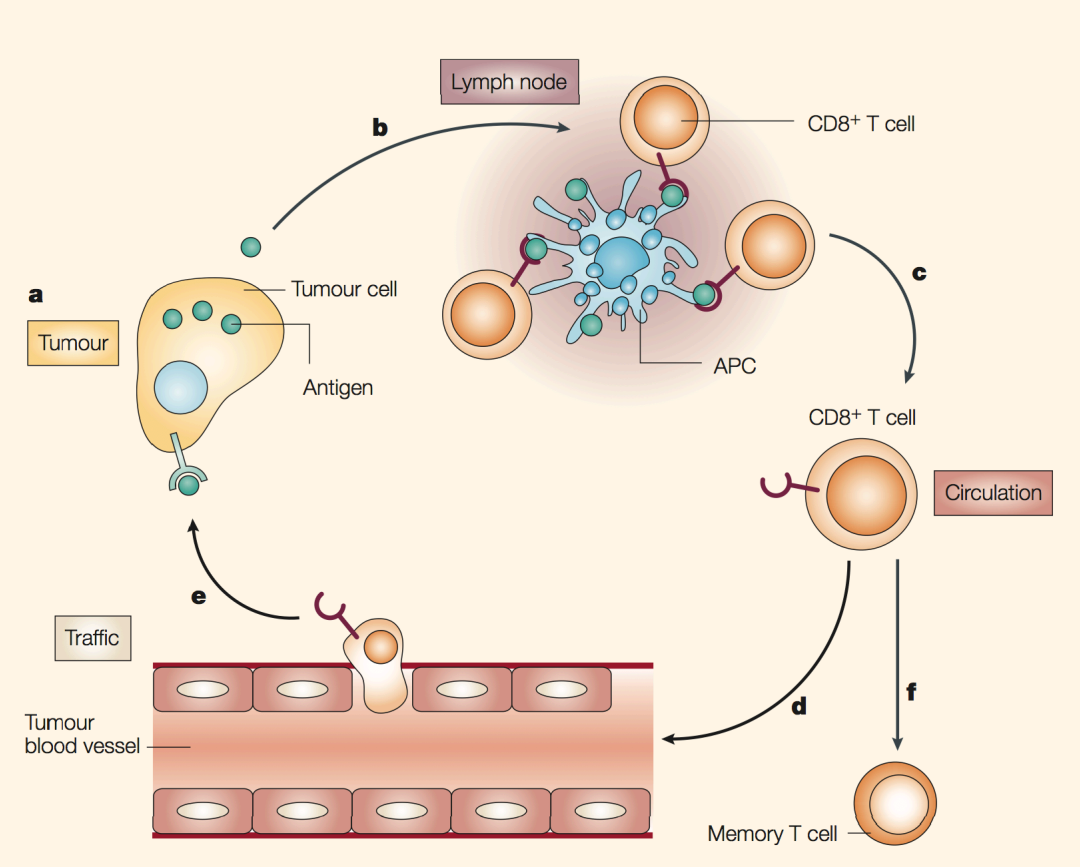

Figure 2: Phases of an Effective $CD8^+$ T-cell Response to a Solid Tumour(Lake *et al.*, 2005)

These $CD8^+$ T cells should preferentially be capable of secreting IFN-γ and tumour necrosis factor-alpha (TNF-α) in order to directly lyse tumour cells (Lake *et al.*, 2005). This response is not perfect and is often inhibited by suppression associated with both the presence of the tumour as well as by the recruitment of immune suppressive cells.

1.3.3.2 Immune Suppression in Cancer

Once the CTL's enter the tumour, they are exposed to suppressive cytokines produced by the tumour itself such as transforming growth factor-beta (TGF-β), Interleukin-10 (IL-10) and vascular endothelial growth factor (VEGF) (Nowak *et al.*, 2006).

The presence of a solid tumour also exerts a systemic suppressive effect on the immune system by a variety of mechanisms (Figure 3).

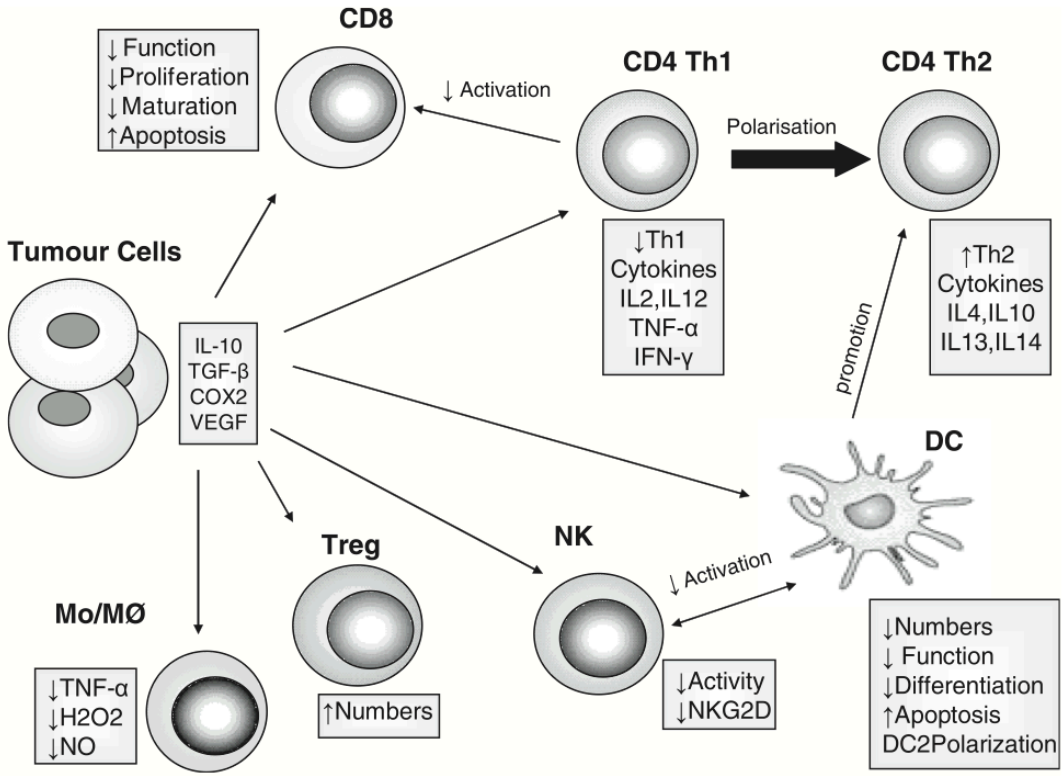

Figure 3: Tumour Suppressive Effects on the Immune System (Evans *et al.*, 2006)

Tumours secrete immune mediators such as IL-10 and TGF-β that are able to reduce the function and number of key immune cells such as CTLs, DCs and NK cells while increasing the presence of Tregs (Evans *et al.*, 2006).

The immune mediator TGF-β inhibits perforin and granzyme mRNA expression that prevents lymphocyte proliferation. IL-10 inhibits the production of cytokines used by CTLs to kill cancer cells such as IFN-γ and TNF-α (Whiteside, 2006). The function, proliferation and maturation of $CD8^+$ T-cells is suppressed which leads to an increase in

their apoptosis, corresponding with a blockade of step C in the tumour immune response. There is also a decrease in the numbers of DCs that leads to less antigen cross-presentation taking place that inhibits this stage of the tumour immune response (Flinsenberg *et al.*, 2011).

The tumour cells are also able to create a shift from Th1 $CD4^+$ T-cells that are able to activate cytotoxic T-cells, natural killer (NK) cells, macrophages and monocytes that would aid in attack of cancer cells to Th2 $CD4^+$ T-cells. These Th2 cells prevent tumour rejection and many malignant cancers are associated with suppression of the Th1 response. Finally the cytokines, especially TGF-β, causes an increase in regulatory T cells (Treg) numbers both in the periphery and within lymphoid organs (Evans *et al.*, 2006). Cellular suppression of the immune system can be accomplished by a number of cells with two of the most potent being Tregs and myeloid derived suppressor cells (MDSC).

1.3.3.2.1 Regulatory T Cells

Tregs are a subset of $CD4^+$ T-cells with their main function being regulation or suppression of the immune system to prevent excessive responses. These functions include prevention of autoimmune disease, suppression of allergies and asthma, induction of tolerance and suppression of pathogen-induced immunopathology (Corthay, 2009). They develop from naïve T cells after exposure to TGF-β or are produced naturally in the thymus and then released into the periphery as a naturally derived Treg (Taams *et al.*, 2006).

To identify these cells, several markers have been suggested and include CD25, CTLA-4 and LAG-3. However there is growing evidence that these are not Treg specific, as CD25 is expressed on activated T-cells and CTLA-4 is up regulated on all $CD4^+$ and $CD8^+$ cells.

This means another, more specific marker was required to ensure correct characterisation and study of this cellular subset. Forkhead box P3 (FoxP3) is a transcription factor involved in the development and production of Tregs and is generally used as a marker for these cells when doing pre-clinical *in vivo* work. In humans there is some evidence that FoxP3 is not exclusive to Tregs and may be transiently expressed by activated $CD4^+$ and $CD8^+$ cells although to a lesser extent than CD25 (Corthay, 2009). The role of Tregs in disease is clearly apparent with many studies looking at their mode of action in autoimmune diseases, allergic disease, infections and of course, cancer (Lin *et al.*, 2013). High numbers of Tregs have been found in patients with lung, pancreatic, breast, liver and skin cancers and in many cases correlates with a decreased survival rate (Wolf *et al.*, 2003). The mode of action of Tregs is complex with a number of mechanisms used to achieve their regulatory or suppressive effects (Figure 4).

Firstly, they are able to suppress the immune system by the release of inhibitory cytokines such as TGF-β, IL-10 and Interlukin-35 (IL-35). It has been well documented that these cytokines have a suppressive nature as well as having a role in the generation of Tregs (Chen *et al.*, 2003). Cytolysis via the secretion of granzyme A or B is a mechanism used by NK cells and CTLs however Treg cells in humans have been shown to express granzyme A while in mice, granzyme B appears to be up regulated in Tregs. Other proposed mechanisms employed by Tregs include metabolic disruption where they consume local cytokines such as IL-2 leaving other cellular populations deprived and they eventually die. There is much debate around this mechanism and more work is needed before it can be regarded as a true ability of Tregs. Lastly, Tregs can target DCs that ultimately affect T-cell activation by inhibiting the maturation of these APCs. Again, there is little data showing this mechanisms in action and so further research is required to validate this (Vignali *et al.*, 2008)

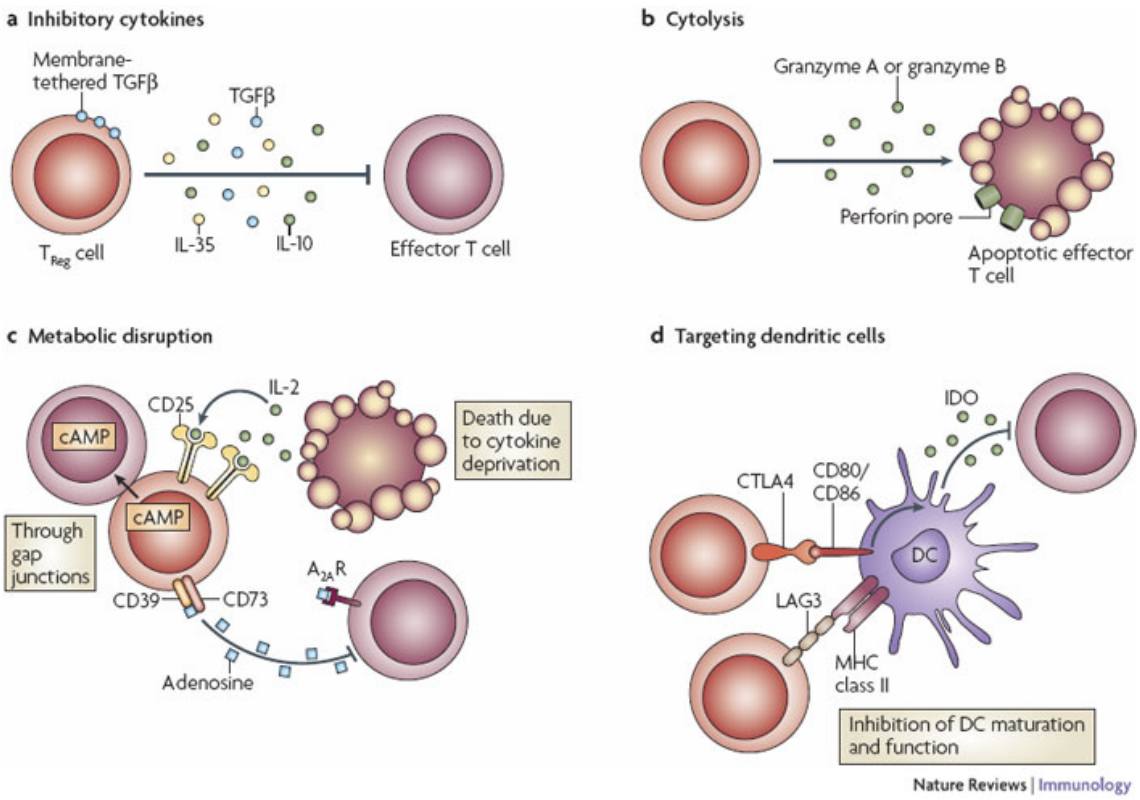

Figure 4: Regulatory T Cell Modes of Action (Vignali *et al.*, 2008)

1.3.3.2.2 Myeloid Derived Suppressor Cells

Immune suppression can also be caused by the presence of myeloid derived suppressor cells (MDSCs). These are a heterogeneous population of immature myeloid cells (IMCs) that consist of the precursors to macrophages, DCs and granulocytes and expand during pathological conditions including cancer. They are mostly found in the bone marrow, making up 20-30% of the cell population in mice. A smaller proportion is found in the spleen and blood, roughly 2-4%. In mice they are characterised by the expression of Gr-1 and CD11b (Gabrilovich *et al.*, 2009). Their suppressive capacity is due to the production of immunosuppressive factors including arginase-1, inducible nitric oxide synthase (iNOS) and reactive oxygen species (ROS). MDSCs are consistently found within most cancers and can be increased up to 10-fold in patients that indicate a major role in immune suppression and may be a possible target for immunotherapies.

1.3.3.2.3 Cancer Specific Immune Suppression

This tumour-associated suppression is evident in the 3 cancer types specific to this study, (mesothelioma, melanoma and colorectal carcinoma). There is also the presence of an anti-tumour immune response that is not effective enough to deal with the solid malignancy (Bograd *et al.*, 2011). Mesothelioma was once considered non-immunogenic but now it is accepted that this is not the case as infiltrating $CD4^+$, $CD8^+$ and Tregs have been found in mesothelioma biopsies (Hegmans *et al.*, 2006). As it has been shown that mesothelioma patients who have an increased tumour-infiltrating $CD8^+$ T cell response survive longer (Anraku *et al.*, 2008), effective therapies to promote TIL recruitment are required. However, Tregs also infiltrate the mesothelioma tumour microenvironment and dampen the anti-tumour response helping to promote tumour progression. Targeting immune suppressors either systemically in the case of this study or possibly locally by intratumoural depletion may result in an effective CTL response within the tumour and lead to regression (Hegmans *et al.*, 2006).

The same principles apply to melanoma as it has been demonstrated that patients with stage IV melanoma had a significantly shorter survival rate when there was a higher proportion of Tregs present. The anti-tumour response being suppressed was the primary factor at work (Baumgartner *et al.*, 2009). While melanoma is usually MHC Class I deficient and therefore poorly immunogenic, there are known melanoma antigens that can be recognised by the immune system. Therefore it is paramount that for the tumour to progress there needs to be suppression of effector and cytotoxic T lymphocytes and again Tregs are one of the primary cell populations that accomplish this. There are already Treg targeting immunotherapies for melanoma but these are not yet effective enough to bring survival past 5 years for many patients (Wolchok *et al.*, 2013).

The role of Tregs in colorectal cancer is slightly different. Suppressive Tregs increase with advancing stages of colorectal cancer and depletion of these would provide an effective strategy for treatment (Lin *et al.*, 2013). There also appears to be a correlation between a high density of Tregs intratumourally and longer survival in patients which is contrasted against the majority of other solid cancers (Salama *et al.*, 2009). An explanation of this is that the Tregs may in fact be dampening tumour development by suppression of the proinflammatory cytokine Th17 which is thought to promote tumour growth and Tregs may be capable of this due to adaptation to the tumour environment (Savage *et al.*, 2013). Therefore it needs to be determined if removal of Tregs and subsequent removal of this proinflammatory suppression results in a CTL response that is more beneficial to the patient than if Tregs were not targeted.

The role of MDSCs has been implicated in all 3 of these cancers types. These cells negatively regulate the immune response and thereby promote tumour growth. (Gabrilovich *et al.*, 2009). Research has looked at both the correct characterisation of these cells as well as potential targeting agents to either remove or force the differentiation of these immature cells into their respective cell types. Treatments used include the anti-Gr-1 antibody for removal of MDSCs in lung cancers represented in mice (Srivastava *et al.*, 2012) and the promotion of differentiation in colorectal cancer by the use of all-trans retinoic acid (ATRA) (Nefedova *et al.*, 2007). The presence of MDSCs is also implicated in melanoma with the use of a PDE-5 inhibitor that suppresses the function of MDSCs and decreases their levels (Umansky *et al.*, 2012).

These 3 suppressive actions, the tumour itself, Tregs and MDSCs present areas in which targeted therapy can act. Possible therapies could focus on inhibiting the suppressive cytokines released by solid tumours in a targeted way as to not cause a systemic effect but

focus the CTL response only to the tumour. Removal of Tregs may also lead to a novel immunotherapy for cancers such as mesothelioma in which other, classical treatments are not effective. The immune response is already used for the defense against viral pathogens via the use of vaccines and so does present an opportunity to translate this to cancer immunotherapy, as this has already been done with the cervical cancer vaccine Gardasil. The role of MDSCs is constantly evolving with better characterisation and targeting therapies required to allow an effective immune response against solid tumours to progress. A further promoter of an immune response, as well as removing some of the tumour-associated immune suppression, is partial debulking surgery and this may be used in combination with an immunotherapy to promote tumour regression.

1.4 Partial Debulking Surgery and the Immune Response

Surgery is one of the primary treatments for solid cancers with the ultimate goal of removing the entire tumour mass. This however is not always possible and certainly with the 3 cancer types mentioned, complete resection is near impossible. This does however allow for the remaining tumour antigens to be used in the administration of immunotherapies which could possible have their effect enhanced by the remaining tumour cells.

Surgical trauma often induces an acute response in patients that can cause cell-mediated immune suppression when there is a release of tumour cells into the system. There is also a risk of disseminated disease as a result of this and the extent of either outcomes has been correlated with the magnitude of surgical trauma (Evans *et al.*, 2009). While this might prove contradictory to the use of immunotherapies, the removal of this suppression will allow an immune response to focus on smaller, more vulnerable tumour cells that have not yet re-established themselves. It has also been shown that newly developed surgical

techniques such as video-assisted thoracic surgery (VATS) has a number of benefits that include reduced recovery time, reduced pain and more importantly to the use of immunotherapies, a reduced extent of immune suppression that returns to normal more quickly than if major surgical techniques are used (Mohiuddin *et al.*, 2013)

1.5 Conclusion

It is well established that the immune system plays a vital role in protection from cancer and is largely suppressed by the presence of a solid tumour. Existing adjuvant therapies to surgery may improve survival in some of the more fatal cancers but a curative option is not yet available for those such as malignant mesothelioma and metastatic melanoma. Surgery often leaves a portion of these cancer cells behind that subsequently grow and become more aggressive. The opportunity for the development of novel immunotherapies for these cancers is great with pre-clinical studies in mice showing promising results. While surgery seeks to target the primary tumour mass, the removal of tumour associated immune suppression such as Tregs or MDSCs will essentially remove the 'brakes' that are in place. This will allow an effective immune response to act upon the tumour or by combining it with another therapy that drives a response. This will hopefully result in a greater survival benefit from treatment and potentially offer a curative option for many fatal cancers.

1.6 Project Hypothesis and Aims

The hypothesis for this study is that targeting immune suppression via removal of Tregs and MDSCs will improve the post-surgical outcome of solid malignancies.

The first aim of this project was to characterise the growth kinetics of the tumour models of mesothelioma, melanoma and colorectal cancer in mice and then develop protocols for partial debulking surgery in these. The second aim was to then use these surgery models in

combination with Treg depletion to determine its effect as well as what time this depletion should occur with reference to tumour size and day of surgery. A trial depletion of MDSCs will be done to determine if this is possible and potentially combine this with surgery. Finally, the last aim was to use the FoxP3.dtr model to characterise the effect of Treg depletion in the lymphoid organs and tumour to gain a better understanding of the systemic CTL response.

1.7 Significance of This Study

With treatment options for late stage mesothelioma, melanoma and colorectal cancer having a low survival and response rate, new treatments need to be investigated. As surgery is a primary treatment option for many cancers, this will be investigated by performing partial debulking surgery in combination with Treg/MDSC depletion immunotherapy with the aim of promoting an immune response capable of successfully eradicating the remaining tumour mass as well as inducing long-term immunological memory. The outcomes of this work showed that surgery in combination with Treg removal is capable of significantly increasing the survival rate of mice that had established tumours when compared to either treatment used alone. It also showed that Treg depletion can be a highly successful treatment option if their transient depletion can be accomplished with either a current or novel immunotherapy.

Chapter 2: Materials and Methods

2.1 Mice

The mice used in this study included the BALB/c and C57BL/6J strains obtained from the Animal Resource Centre (Murdoch, Western Australia) and the BALB/c.Foxp3.dtr.Crslc (referred to as FoxP3.dtr) strain kindly provided by Prof. Ian van Driel (University of Melbourne, VIC). All were housed in pathogen free conditions at the UWA animal house located in M block, QEII Medical Centre. Predominantly, female mice aged between 6-8 weeks were used for the BALB/c and C57BL/6J strains however due to availability, male mice were also used for the FoxP3.dtr strain with ages varying from 6 to 19 weeks. Any procedures and treatments as well as monitoring were approved by the UWA animal ethics committee and were conducted in accordance with the Australian code of practice for the care and use of animals for scientific purposes, 8th edition 2013 developed, by the National Health and Medical Research Council.

2.2 Cell Lines

The AB1-HA cell line was obtained from the National Centre for Asbestos Related Diseases. AB1-HA is a mesothelioma cell line established from in vitro culture of ascetic fluid taken from asbestos exposed BALB/c mice. The resultant AB1 cell line was then transfected with the influenza virus (PR8/34/H1N1 Mt Siani) haemagglutinin gene (HA) to provide a marker antigen and produce the AB1-HA line (Marzo *et al.*, 1999). B16-F10 was obtained from the American Type Culture Collection (ATCC) and is a C57BL/6J mouse melanoma cell line. The BALB/c colorectal cancer cell line CT44, kindly provided by Prof. Kashayarsha Khazaie (Northwestern University, Chicago IL) was generated by transfecting the wild type CT26 cell line with a fusion protein of the HA and enhanced

green fluorescent protein (EGFP) (Khazaie *et al.*, 2006). All cell lines were expanded in culture and frozen down and stored in liquid nitrogen for use in all experiments.

2.3 Cell Culture

The AB1-HA and B16-F10 cell lines were cultured in R10 media (Gibco® RPMI 1640 Cell Culture Media containing L-glutamine with the addition of 0.02M Gibco® Hepes, 0.12 U/mL Benzylpenecillin, 50 μg/mL gentamicin, $5x10^{-5}$M 2ME and 10% Foetal Calf Serum (FCS) v/v). R2 media, used for tumour digestion, contains the same supplements as R10 but instead with only 2% FCS v/v. For AB1-HA only, the media was also supplemented with 0.4 mg/mL of Geneticin. For maintenance of the CT44 cell line, DMEM complete media (Gibco® DMEM media supplemented with 0.02M Gibco® Hepes, 0.12 U/mL Benzylpenecillin, 50 μg/mL gentamicin, $5x10^{-5}$M 2ME, 10% FCS v/v and 1x Glutamax (diluted 1:100 v/v with DMEM media)) was used.

To passage cells, all culture media from the flasks would be removed first by suction and then washed with 1x Phosphate Buffer Saline (PBS) to remove any remaining media. For AB1-HA and B16-F10 cell lines, 0.12% trypsin (Sigma-Aldrich, Castle Hill, NSW) was added to the flasks for 1-2 minutes to remove adherent cells while Cellstripper (Cellgro, Manassas, VA) was used for the CT44 cell line and left for 10 minutes at 37^{o}C to remove cells. Once detached, washing flasks with 10 mL of their respective media then inactivates the trypsin or Cellstripper. These cell suspensions were collected into falcon tubes and spun down at 348 g for 3 minutes and the supernatant removed. Cells were then resuspended in a know volume of their media and split accordingly into new culture flasks. For maintenance of cell culture cells were split when between 80-90% confluency with AB1-HA split 1:30, B16-F10 split 1:40 and CT44 split 1:15.

2.4 Tumour Inoculations

AB1-HA and CT44 were inoculated either into BALB/c or FoxP3.dtr mice while B16-F10 was inoculated into C57Bl/6J mice. Firstly, cells were grown in culture as described above and inoculations were prepared by either trypsinising or using Cellstripper for the CT44 line to remove cells off the culture flasks. Three washes were performed in 1x PBS to remove all traces of growth media. At each wash step, cells were spun down at 348 g for 3 minutes and supernatant removed and resuspended in 20 mL of 1x PBS. Once the wash steps were completed, an aliquot of cell suspension was removed and diluted 1:10. A cell count was then done by diluting the cell suspension 1:2 with 0.4% Trypan Blue (Sigma-Aldrich, Castle Hill, NSW) and counted using the Countess Automated Cell Counter (Life Technologies, Mulgrave, VIC) to determine total live cells and percent viability. The cell suspension was made up to the appropriate volume to give a final concentration of $5x10^6$ cells/mL in PBS. To determine final volume the following calculation was used:

Final volume = (viable cells x current volume)/required concentration.

Each mouse received $5x10^5$ cells (100 μL) subcutaneously by injection on the shaved right hand flank. Surviving mice from AB1-HA tumour experiments were re-challenged on the contralateral flank with inoculations of AB1 to determine immunological memory.

2.5 Monitoring of Tumour Growth

Once inoculated with either cell line, mice were monitored 3x weekly with daily measurements commencing once tumours reached a size of 70 mm^2. Tumour size was determined by measuring the length and width of the tumour mass and multiplying together to give tumour area. Once tumour sizes had exceeded 100 mm^2 while still being under 150 mm^2 mice were euthanised in accordance with the animal ethics permit.

2.6 Diphtheria Toxin Preparation & Administration

Diphtheria toxin (DTx) (Sigma-Aldrich, Castle Hill, NSW) was prepared by dissolving the lyophilised powder into ddH_20 at a concentration of 1 mg/mL and subsequently diluted to a working concentration of 100 ng/µL and stored at -80^oC. For injection, 1 vial was thawed at room temperature and made to a concentration of 1 ng/µL by diluting 1:100 with 1x PBS. This DTx solution was then injected intraperitoneally (i.p.) by inverting mice so as to ensure solution enters the peritoneal cavity.

2.7 Debulking Surgery

2.7.1 Surgical Procedure

The debulking of a solid tumour mass is always done in an axenic environment with the mice being placed under general anaesthesia. Mice were placed in a sealed jar for 1-2 minutes to induce anaesthesia through inhaled methoxyflurane (MDI, Springvale, VIC) at a concentration of 1 mL per 20-25 g mouse. Maintenance of anaesthesia was provided by 5% isoflurane (Abbot, Botany, NSW) in oxygen. Surgery was then performed by making elliptical incisions around the tumour and the skin flaps elevated (Broomfield *et al.*, 2005). The desired amount of tumor is resected, being either a 50% or 75% debulk or a sham were the wound is simply closed by suturing through the tumour without any resection. Partial debulking is performed by removing half the tumour mass which is representative of a 50% debulk and then a further 50% is removed which represents a 75% debulk.

2.7.2 Suturing of Surgical Wound

For suturing of mice inoculated with AB1-HA or CT44, 3/0 polyglycolic sutures were used while for the B16-F10 tumour debulks, 4/0 polypropylene sutures (Surgik, Broken Arrow, OK) were used. Suturing of the wound begins at either end of the surgical site. The skin is brought together and the needle is threaded through. The initial stitch is secured by tying 3

knots, alternating the direction of the knot each time. For Balb/c and Balb/c.Foxp3.dtr.Crslc mouse strains a continuous stitch is done, leaving 2-3 mm between each one. C57BL/6J mice required interrupted suturing to ensure suture integrity. Once the wound is closed, the suture is tied off by tying 3 knots as before and any excess suture is removed.

2.7.3 Recovery

Once surgery has completed, mice are placed in a heat box and are administered 0.1 mg/kg of the analgesic buprenorphine for pain relief by subcutaneous injection near the surgical site. Mice are left to fully wake and once movement has normalised, they are transferred back into their original cage.

2.7.4 Post-Surgical Monitoring

As per the animal ethics permit, all mice that have undergone surgery are monitored 1 hr post-surgery, at the end of the day of surgery as well as the following morning. At each stage, examination for signs of bleeding or gaps in stitching is undertaken. Required resuturing of the surgical site using the protocol described then takes place. Betadine or chlorhexadine is placed onto surgical sites that have opened to prevent any infection. If mice appear in significant pain the following day, euthanasia as per animal ethics is considered.

2.8 Collection and Preparation of Tissues for Flow Cytometry

To harvest organs, mice are euthanised by cervical dislocation after being anaesthetised in methoxyflurane (MDI, Springvale, VIC). They were pinned down and incisions were made to remove the skin from the peritoneum allowing access to the entire internal structure of the mouse.

Target organs (lymph nodes, spleens, tumours) were extracted and placed into 15 mL falcon tubes containing 3 – 4 mL of 1x PBS/2% FCS and placed on ice until required. Blood was collected into 1.5 mL eppendorf tubes containing 15 µL of 1000 U/mL heparin (Pfizer, West Ryde, NSW) to prevent clotting and also placed on ice until required. Once prepared, a 100 µL aliquot of each organ sample or a 50 µL blood sample is added to the corresponding well on a 96 well U-bottom plate. Each organ or blood sample is collected and prepared as follows.

2.8.1 Lymph Nodes

Unless otherwise stated the axillary and inguinal lymph nodes were taken on the tumour bearing side (draining lymph node; dLN) and the non-tumour bearing side (non-draining lymph node; ndLN). The axillary node was located in or on top of the armpit and was visible once the surrounding connective tissue has been removed. The inguinal node is located in the fat pad at the convergence of 3 blood vessels at the left and right flanks. Teasing away the fat pad revealed the node that in tumour bearing mice may be enlarged or involved with the tumour. Draining and non-draining lymph nodes were disaggregated separately using frosted slides into a petri dish and washed with 1x PBS/2% FCS. This was then filtered into filter-top tubes and spun down at 348 g for 3 minutes. The supernatant was removed and the sample resuspended in 300 µL of 1x PBS/2% FCS and placed on ice until required.

2.8.2 Spleen

The spleens were removed by making an incision in the peritoneum on the right hand side. Spleens were disaggregated using frosted slides into a petri dish and collected back into a falcon tube to be spun down at 348 g for 3 minutes. The supernatant was removed and red blood cells lysed by resuspending the cell pellet in 2 mL of 1x Pharm Lyse™ (BD

Bioscience, Lane Cove, NSW) for 3 – 5 minutes. A further 3 mL of 1x PBS/2% FCS is added to deactivate and cells are spun down again at 348 g for 3 minutes. Cells were then resuspended in 5 mL of 1x PBS/2% FCS and placed on ice until required.

2.8.3 Tumour

The tumour is located on the right hand flank of the mouse. There is usually a large deposit of fat and connective tissue surrounding the tumour that needs to be removed. The tumour is then excised from the skin, taking care to remove as much of the skin and hair that is attached to it. To get a single cell suspension from solid tumours they are mechanically digested using 2 scalpel blades in a petri dish. Once the tumours are at a paste like consistency they are collected back into a falcon tube. The 10x Tumour Digest is diluted 1:10 with R2 media and 2 mL is added to each tumour suspension and they are chemically digested for 1 hr on rollers.

After chemical digestion, 50 µL of 0.1 M Ethylenediaminetetraacetic acid (EDTA) is added and further incubated for 15 min on rollers. Once incubation is finished, the suspension is filtered into a new 50 mL falcon tube using 1x PBS/2% FCS to wash the filters allowing for maximum collection of tumour cells. This supernatant is then transferred into filter-top tubes and samples are under laid with 1 mL ice-cold EDTA-FCS to allow samples to be spun at 527 g for 5 min at 4^{o}C. Once spun, the supernatant is removed and samples are resuspended in 200 µL of 1x PBS/2% FCS and placed on ice until required.

2.8.4 Blood

Blood was routinely collected via tail vein bleeds from mice placed into a heat box to dilate the vein to a point where it can easily be viewed. A small nick is made using a

scalpel blade and blood is allowed to drip into the eppendorf tube. No more than 400 µL of blood is obtained for analysis. Once blood has been collected, pressure is applied to the wound and once bleeding has slowed, ferric chloride is applied to cause coagulation and ensures no further bleeding. When necessary blood was obtained via a cardiac puncture. This involves inserting a large gauge needle directly into the heart of the mouse that has been anaesthetised by methoxyfluorane. The needle has punctured the heart when blood enters the syringe without applying any traction. The plunger is slowly pulled back to aspirate a blood sample and once enough is collected, the mouse is euthanised.

Blood samples are placed directly onto the 96-well plate with a 50 µL aliquot into each well corresponding with each sample. Each sample then receives 150 µL of 1x BD FACS™ Lysing Solution (BD Bioscience, Lane Cove, NSW) to lyse the red blood cells and incubated at room temperature for 15 min. The plate is spun down at 348 g for 3 minutes and the supernatant removed. All samples then get resuspended and washed twice with 1x PBS/2% FCS to remove the lysing solution.

2.9 Staining for Flow Cytometry

Samples were prepared as single cell suspensions as per section 2.8 and assessed using flow cytometry. For surface staining, all samples were washed twice in 1x PBS/2% FCS and then stained (Section 2.9.2). Intracellular staining was performed (Section 2.9.1) to detect internal proteins such as FoxP3 and Ki67 when staining for Tregs.

2.9.1 Preparation for Intracellular Staining

Samples are first spun down at 348 g for 3 minutes and the supernatant is removed. All samples are then incubated for 15 minutes with 100 µL of 1x Fix/Perm solution (Jomar Bioscience, Stepney, SA) in the dark. The plate is then spun down again as previously and

washed twice with 1x Perm Buffer (Jomar Bioscience, Stepney, SA) to remove any remaining solution.

2.9.2 Antibody Staining

The antibody solutions are made up to the required volume using their respective dilutions either for the Treg panel or MDSC panel (Appendix Tables 3 and 4 respectively) using either 1x PBS/2% FCS for extracellular staining or 1x Perm Buffer for intracellular staining. A 20 µL aliquot of either the antibody master mix, single stain controls or fluorescence minus one (FMO) controls containing their respective antibodies is placed onto each sample well and mixed. For compensation, positive and negative compensation beads are used and their corresponding single stains are added. The entire plate is then incubated for a minimum of 20 minutes at room temperature in the dark to ensure antibody binding. After the incubation, all wells are made up to 200 µL with 1x Perm Buffer and the plate spun down. A total of 3 washes is done to ensure all antibodies are removed and all samples are resuspended in 200 µL of 1x Stabilising Fixative (BD Bioscience, Lane Cove, NSW) and placed into a 4^{o}C fridge until being run on the flow cytometer.

2.10 Flow Cytometry

All flow cytometry analysis was conducted on a BD FACSCanto II at the Centre for Microscopy, Characterisation and Analysis located at the QEII Medical Centre. This cytometer had 8 fluorescence parameters and contains a 405 nm, a 488 nm and a 633 nm excitation lasers and uses the FACS Diva software package. All samples were prepared on a 96-well U-bottom plate as stated and run on the FACSCanto II using the High Throughput Sampler (HTS). The stopping gate was set to 50, 000 lymphocytes to ensure adequate cell number for analysis. To interpret and analyse the flow cytometry data, FlowJo version 8.8.7 (TreeStar Inc, Ashland, OR) was used.

2.11 Statistical Analysis

Each group of mice contained a minimum of 5 animals unless otherwise stated and statistical analysis was performed using Prism 6 (GraphPad Software, San Diego, CA). All measurements were presented as means ± standard error (SEM). One-way analysis of variance with Dunnett's test was done to compare differences between control and treated experimental groups. Cited P values were at the 95% confidence interval, and differences were considered statistically significant when $P < 0.05$. The extent of statistical significance is represented by the number of asterisks: * represents $P < 0.05$, ** represents $P < 0.01$, *** represents $P < 0.001$ and **** represents $P < 0.0001$.

Chapter 3: Kinetics of Tumour Growth & Surgical Debulking

3.1 Kinetics of Tumour Growth

To test the hypothesis that the removal of suppressive immune cells in combination with debulking surgery will improve the anti-tumour immune response we first needed to develop testable models of solid malignancies. This involved the investigation of tumour growth rates *in vivo* to determine the best time points for both surgery and administration of immunotherapy. To establish these models, BALB/c and C57BL/6J mice were inoculated with different tumour cell lines as described in section 2.4 to determine their respective growth characteristics

To conduct this experiment, $5x10^5$ cells of the relevant tumour cell line was inoculated s.c on the shaved right hand flank of mice. For the AB1-HA and CT44 cell lines, female BALB/c mice were used while B16-F10 was inoculated in the same way into female C57BL/6J mice. All mice were 6-8 weeks old. Tumours were allowed to grow to a maximum of 150 mm^2 with length and width measurements taken and multiplied to give tumour area. Growth curves for AB1-HA and B16-F10 was obtained experimentally in this study while Dr Andrea Khong (UWA Department of Medicine) kindly supplied the growth curve for CT44.

AB1-HA formed solid, spherical tumours that are composed mainly of spindle and polygonal cells (Davis, 1992). The growth of AB1-HA was consistent between all inoculated mice with palpable tumours at day 3 (Figure 5). Tumours reached the maximum allowable size between days 15 and 18. Therefore the day of surgery for the AB1-HA model was set to day 13 at which tumours were large enough to accurately debulk size wise while ensuring that no mice had to be euthanised before surgery could be performed.

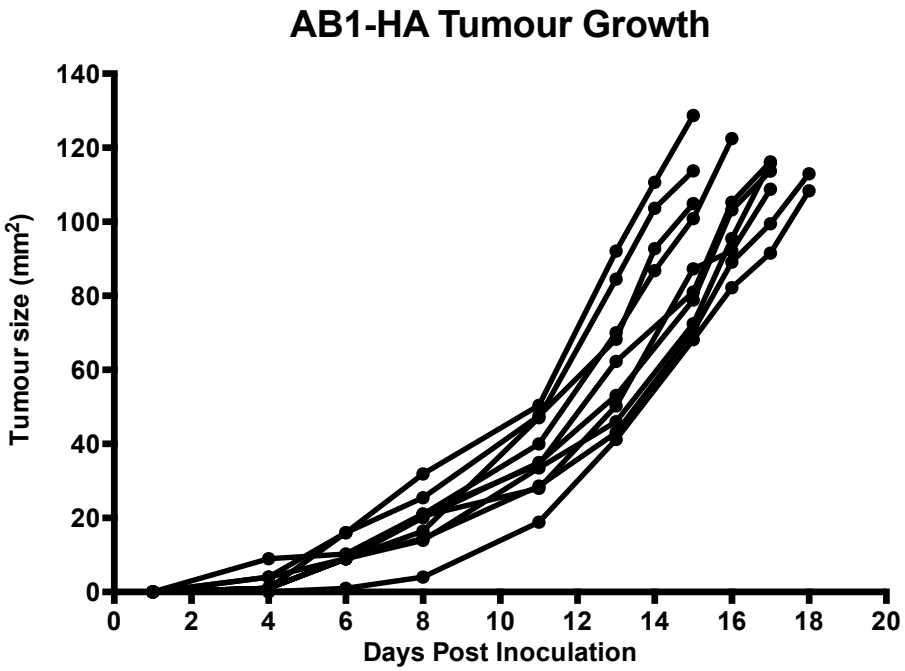

Figure 5: Kinetics of AB1-HA Tumour Growth in BALB/c Mice

A total of 10 BALB/c mice were inoculated with $5x10^5$ cells and growth was measured until tumours reached a size >100 mm^2 in which case they were euthanised. Each line represents an individual mouse.

In contrast, B16-F10 solid tumours were softer and more lobular (Radzi *et al.*, 2012) than AB1-HA and had a much darker colour due to the high concentration of melanin producing melanocytes. The growth of B16-F10 was also consistent between mice but the onset of growth was delayed more than expected and palpable tumours only arose on day 10 and grew for a maximum of 7 days before reaching size, much faster than AB1-HA. In addition to the fast growth rate, once tumours arose we observed increased tumour ulceration in B16-F10 that resulted in these mice being euthanised before reaching maximum size as required by the UWA animal ethics approval.

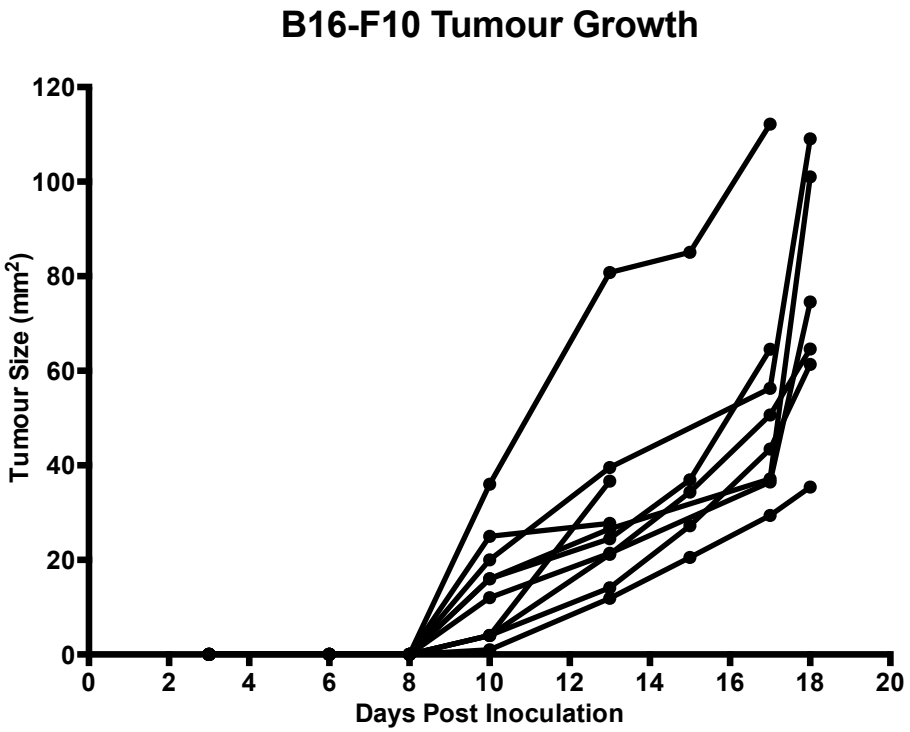

Figure 6: Kinetics of B16-F10 Tumour Growth in C57BL/6J Mice

A total of 10 C57BL/6J mice were inoculated with $5x10^5$ cells and growth was measured. Mice were euthanised when tumours reached a size >100 mm^2 or when they began to ulcerate. Each line represents an individual mouse.

The growth of the colorectal cancer line CT44 was similar to that of AB1-HA with palpable tumours at day 3, however, tumours grew more slowly and reached maximum size between days 15 and 20. The shape of the tumour formed was slightly elongated when compared to AB1-HA and also appeared to be invading the peritoneal cavity.

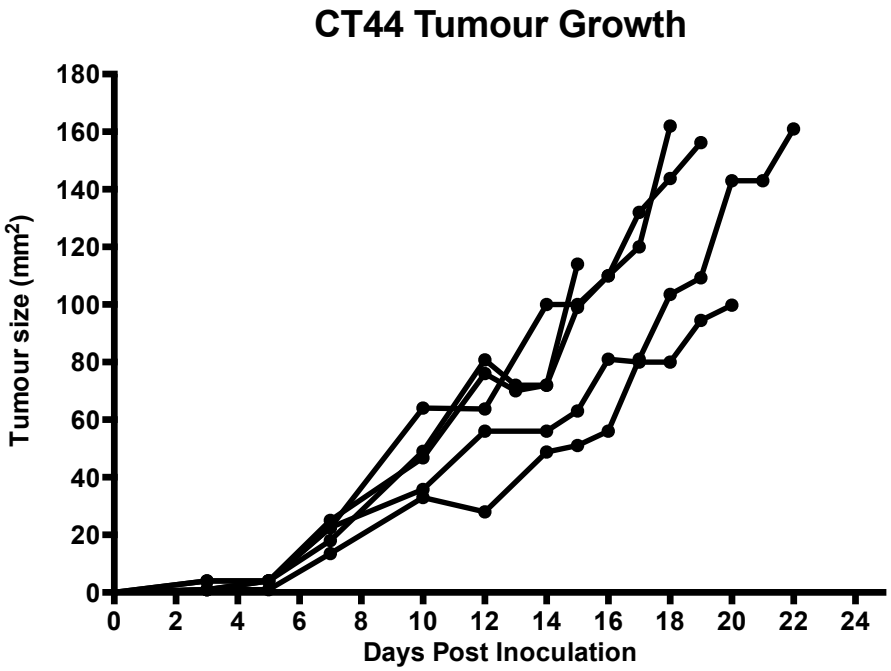

Figure 7: Kinetics of CT44 Tumour Growth in BALB/c Mice.

A total of 5 BALB/c mice were inoculated with $5x10^5$ CT44 tumour cells and growth measured until tumours neared 150 mm^2. Kindly supplied by Dr Andrea Khong (UWA Department of Medicine). Each line represents an individual mouse.

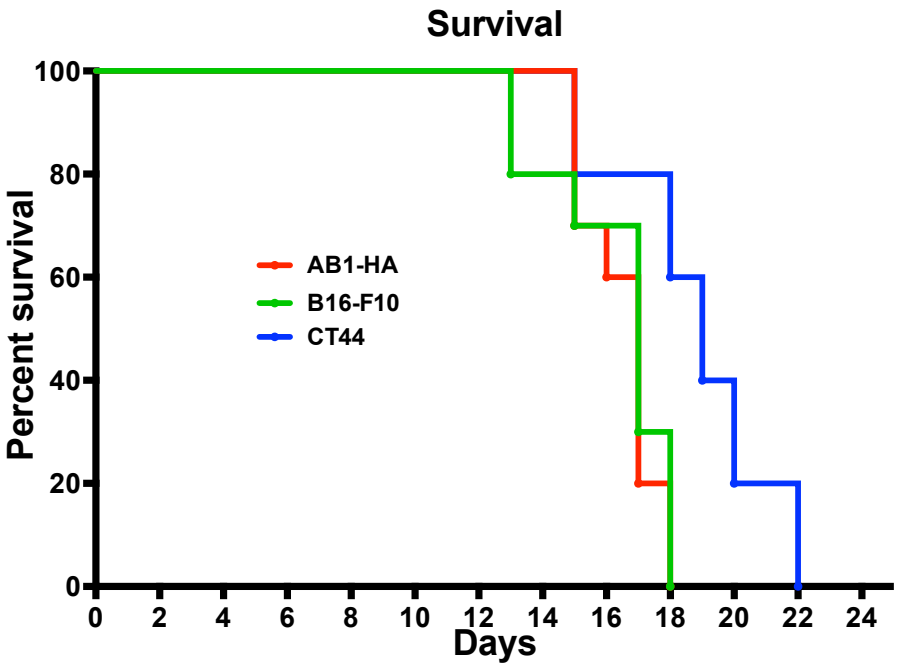

Figure 8: Survival of AB1-HA, B16-F10 and CT44 Inoculated Mice.

Comparison of survival data for AB1-HA, B16-F10 and CT44 tumour bearing mice inoculated with $5x10^5$ respective cells s.c for each cell line.

Due to a high rate of tumour ulceration, the growth rate of B16-F10 was repeated using the tumour line from 3 different sources in this lab to determine if there were any significant differences between them and which would be most suited for future experiments. The three stocks used were my original stock at passage 29 and two others at passage 24 and passage 16. Again, there were high rates of ulceration in all cell lines despite the viability being >90% at inoculation. Results showed consistent growth rates for mice inoculated with either passage 29 or 24 B16-F10 cells relative to passage 16 cells (Figure 9 A, B and C respectively). However, both passage 29 and 24 cells had an increased incidence of ulceration leading to premature euthanasia of the mice. As mice inoculated with the lower passage cells demonstrated less ulceration, those were chosen as the primary stock for the remaining experiments.

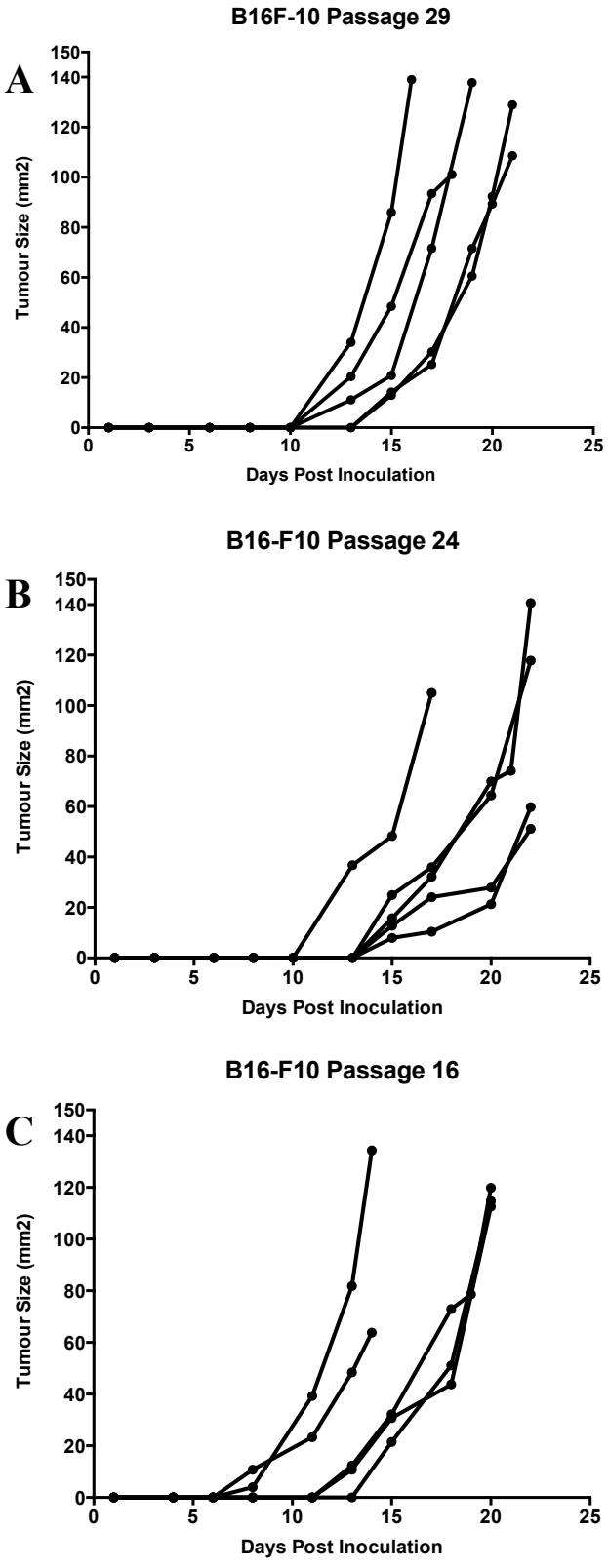

Figure 9: Growth of B16-F10 From 3 Different Sources

B16-F10 was obtained from 3 different research personnel with each having a different passage number. C57BL/6J mice were inoculated s.c. with $5x10^5$ B16-F10 tumour cells. Each line represents an individual mouse.

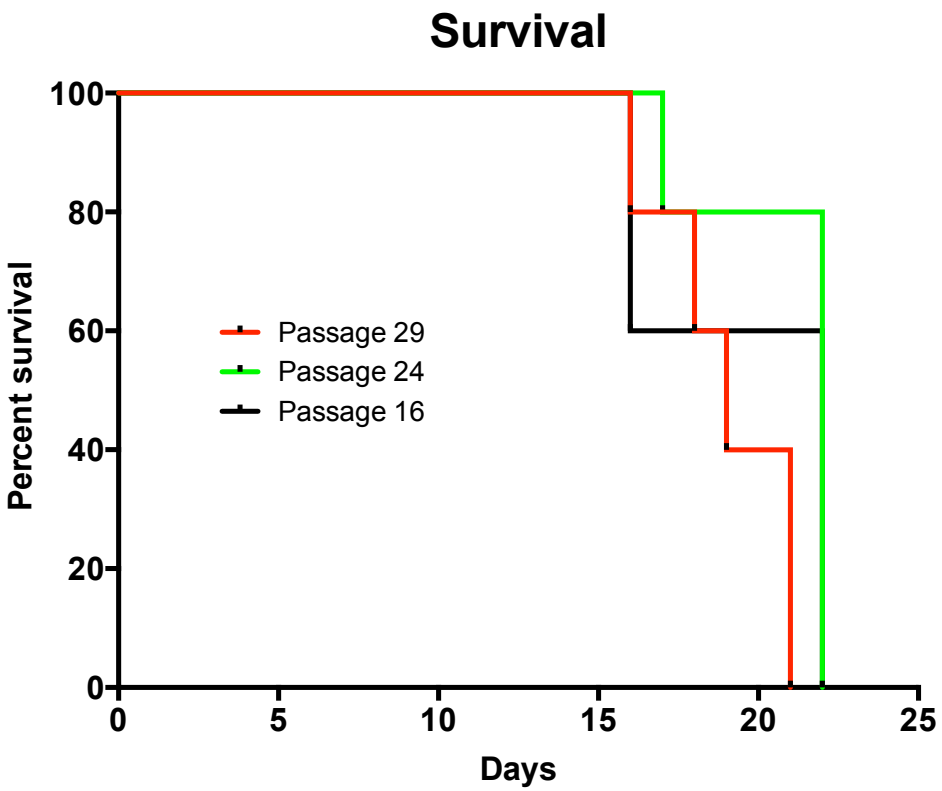

Figure 10: Survival of B16-F10 Comparison

Graph shows the survival of the 3 different groups each inoculated with B16-F10 from a different source at $5x10^5$ cells s.c. per line. The lowest rate of ulceration was observed in the passage 16 cell line.

Summary

The primary aim of this chapter was to establish a number of different mouse models that could be used to assess whether Treg depletion influences the outcome of partial tumour debulking surgery. To achieve this, two different strains of mice were inoculated with three different tumour cell lines to assess growth characteristics.

The growth kinetics of AB1-HA and CT44 were similar however CT44 had a slower rate of growth that extended survival slightly. The B16-F10 melanoma cell line grew very quickly once palpable tumours were evident, however, this was associated with a high rate

of ulceration and tumours rarely reached the maximum allowable size as a result. After repeating the growth of B16-F10 by using cells grown by 3 different personnel, the stock at passage 16 was chosen for use in a pilot debulking experiment to try remove the problem of ulceration by surgically removing tumour mass. A pilot debulking surgery was also done for CT44.

3.2 Surgical Debulking of Solid Tumours

With the growth kinetics of the proposed tumour models for this project characterised, a protocol for performing debulking surgery on these needed to be developed. As surgery for solid tumours is often not curative due to outgrowth of residual tumour cells, we aimed to mimic this scenario by using a partial debulking tumour model in which a predetermined proportion of the tumour is left behind following surgical resection. As this debulking surgery protocol had been previously described in the AB1-HA tumour model (Broomfield *et al.*, 2005) we therefore sought to apply this technique to both the B16-F10 and CT44 models.

Surgical debulking of the solid tumours was performed as described in section 2.7 with either a sham, 50% or 75% debulk done to determine what effect each has on tumour growth and survival. C57BL/6J mice inoculated with B16-F10 and BALB/c mice inoculated with CT44 were used as described previously. There were 3 groups per experiment corresponding with the extent of debulking to be done with 5 mice per group. Where tumours had not grown sufficiently for surgery or an unexpected death resulted from surgery, those mice were excluded from analysis. For the B16-F10 model, mice were inoculated on day 0 and surgery performed on day 13 due to the onset of tumour ulceration in some mice with tumours approximately 40 mm^2 in size. For the CT44 model, mice were inoculated on day 0 and surgery performed on day 15 when tumours were approximately 80 mm^2. All mice were then monitored until tumours grew to sizes >100 mm^2 or the health of mice deteriorated as a result of other complications. In the case of CT44, 2 mice had tumours that regressed after surgery and so were monitored for 4 weeks after tumour regression to ensure no residue tumour cells remained that could give rise to new solid malignancies.

3.2.1 Surgical Debulking of B16-F10 Solid Tumours

The surgical debulking of B16-F10 (Figure 11) was brought forward as a result of ulceration beginning in some mice. Tumours growth was delayed due to surgery as expected but the post-surgery growth rate remained the same with most mice having to be euthanised by day 20 due to ulceration and not that tumours reached maximum size. Growth rates appeared to remain constant pre and post-surgery for all groups. There were no survivors in any of the groups and one mouse that received a 75% debulk did not recover after having to be re-stitched post-op. The outcomes for the B16-F10 debulking model were further complicated by additional issues such as mice chewing sutures and high rates of ulceration and therefore the decision was made to apply the debulking protocol to the CT44 tumour model.

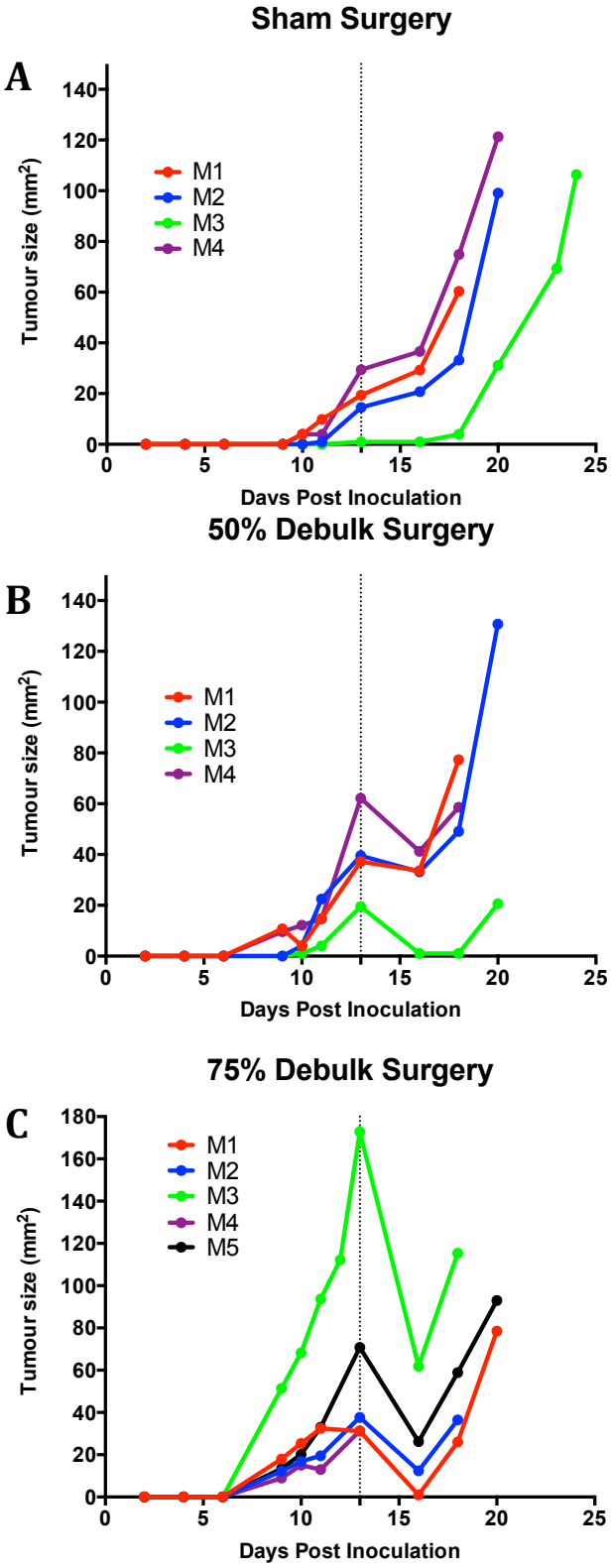

Figure 11: Debulking Surgery of B16-F10 Solid Tumours

Either a sham (A), 50% (B) or 75% (C) debulking surgery was performed on C57BL/6J female mice aged 6-8 weeks that had been inoculated s.c. with $5x10^5$ B16-F10 tumour cells. Each line represents an individual mouse.

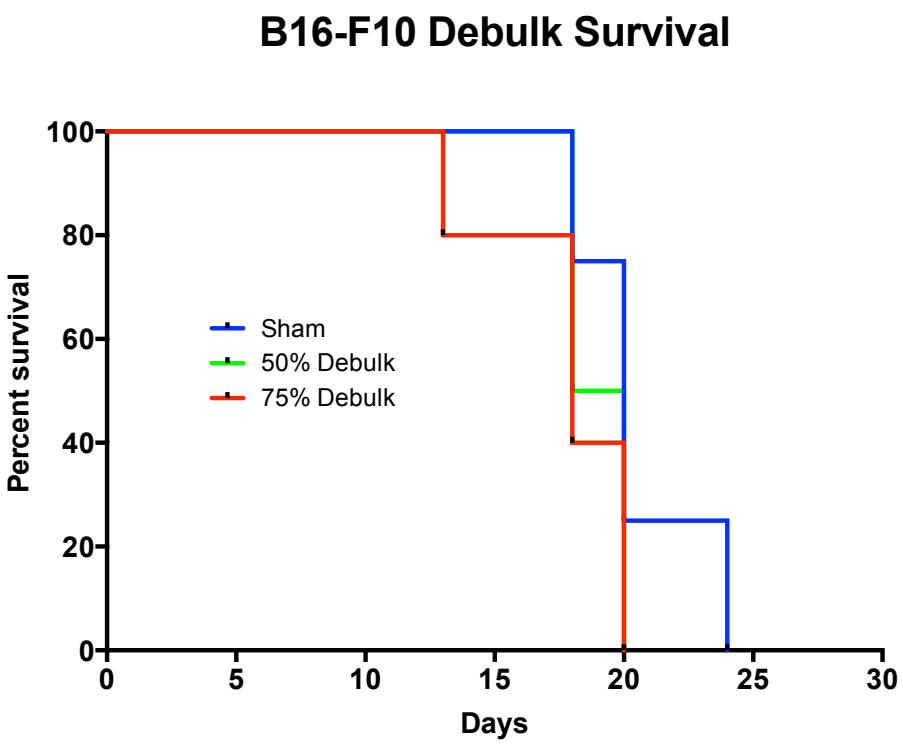

Figure 12: B16-F10 Debulk Survival

Survival plot depicting the influence of partial debulking surgery on B16-F10 bearing C57BL/6J mice.

3.2.2 Debulking of CT44 Solid Tumours

The surgical debulking of CT44 tumours was done in the same way as for AB1-HA (section 2.6.1 & 2.6.2). It was expected that these tumours would be similar in structure as AB1-HA *in vivo,* based on gross observation, however these tumours were slightly more gelatinous although not to the extent of B16-F10. There was also more bleeding from the surgical site both during surgery as well as post-op in a small number of mice. This did not result in any unplanned euthanasia as was managed by irrigation of the wounds before suturing as well as re-suturing of any open areas during post-op monitoring.

Tumour size at the time of surgery (Figure 13 A, B, C) was roughly between 60 and 80 mm^2 with a couple showing very early signs of ulceration. The rate of tumour growth after surgery on CT44 was slowed in 46% (7/15) of mice with complete regression observed in 2 of these. These mice either received a sham or a 50% debulk respectively. Survival was also longer than for the B16-F10 tumour model with all but 3 still alive past day 20. Based on these results a 75% debulking model was chosen to represent an unresectable tumour mass to be used in combination with Treg depletion to determine what effect surgery is having as a treatment.

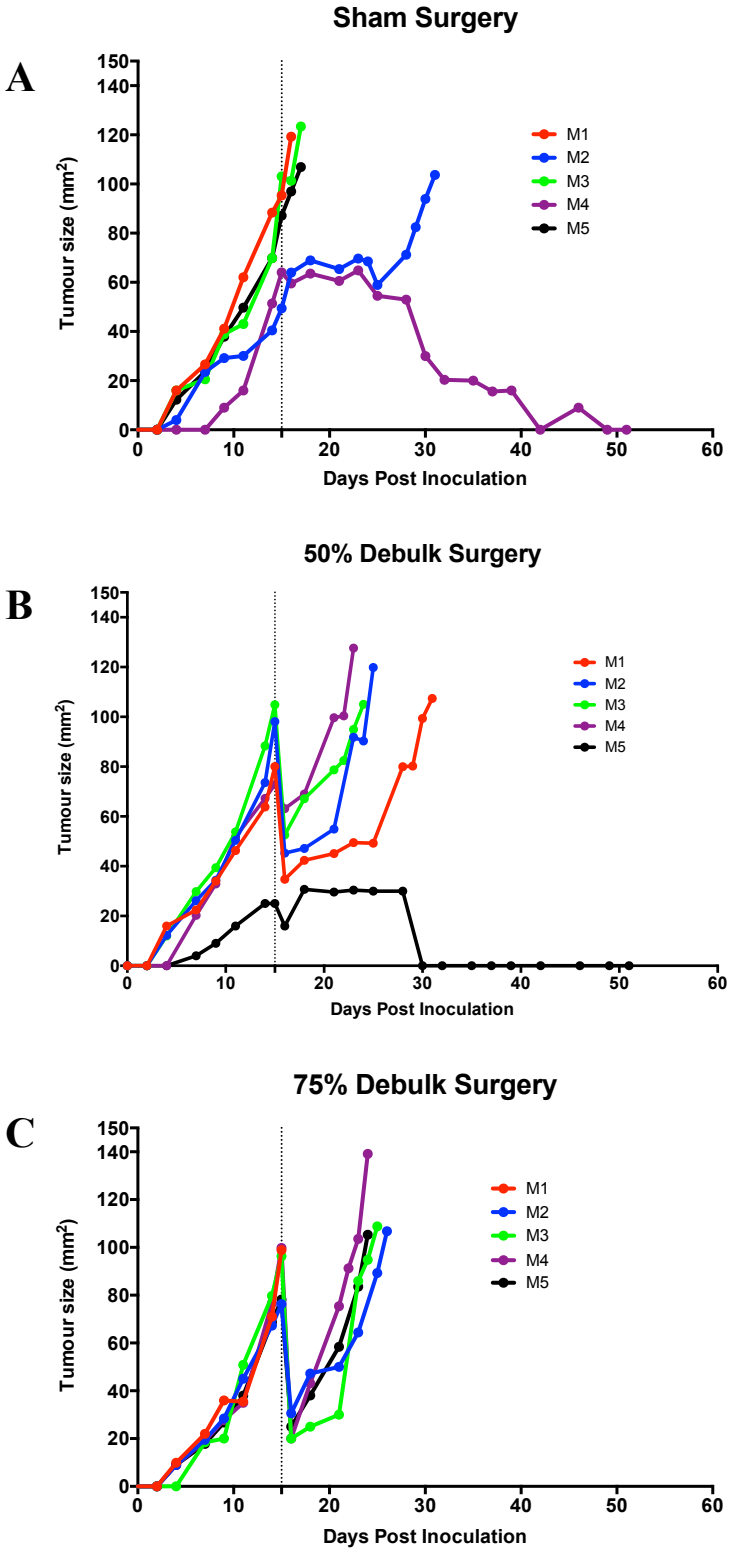

Figure 13: Debulking Surgery of CT44 Solid Tumours

A sham (A), 50% (B) or 75% (C) debulking surgery was performed on BALB/c female mice aged 6-8 weeks that had been inoculated s.c. with $5x10^5$ CT44 tumour cells. Each line represents an individual mouse.

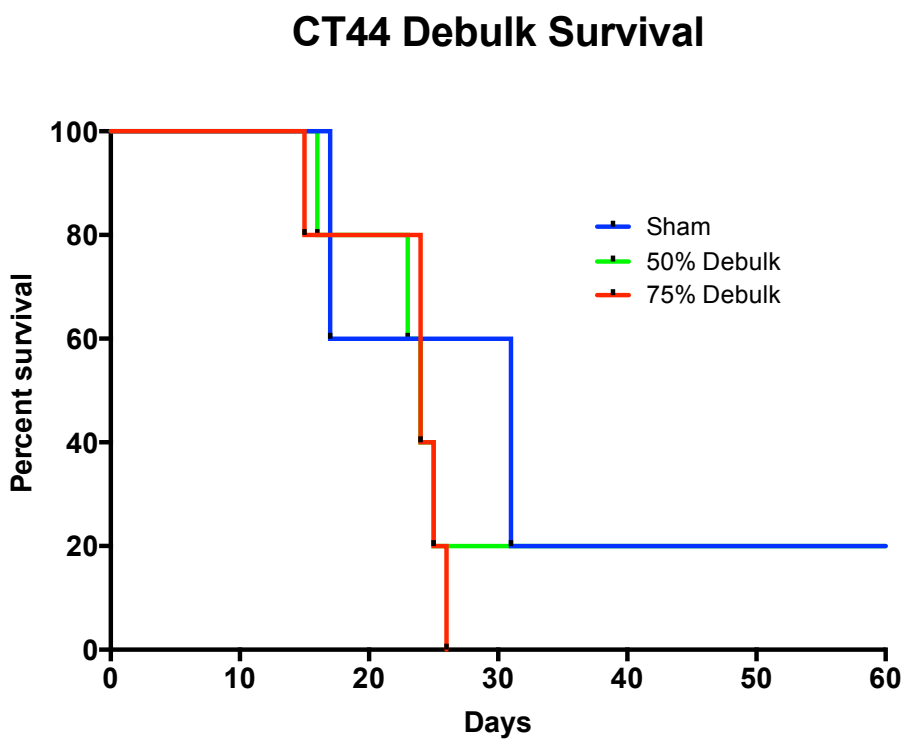

Figure 14: CT44 Debulk Survival

Graph represents the percentage of mice remaining per group and on what day's mice in each of those perspective groups was euthanised due to either tumours reaching maximum size or other negative outcomes such as unexpected death after surgery.

Summary

This chapter aimed to investigate the effect of surgical debulking of solid tumours in both the B16-F10 and CT44 tumour models. The many complications, particularly early onset of ulceration indicated that the B16-F10 model was not conducive to our debulking surgery protocol and therefore we did not pursue this any further. Instead the CT44 tumour model previously established was proposed for surgical debulking.

The CT44 model responded well to surgery with tumours debulked using a similar protocol as for the AB1-HA model. Tumour growth rate was slowed after surgery in some mice with 1 mouse from both the sham and 50% debulk groups having tumours that

completely regressed with no re-growth at a later time point. The excess bleeding from these tumours during surgery did not prove problematic with irrigation added in for later experiments. There was some re-stitching of surgical sites post-op where bleeding had not ceased but again was not problematic. This resulted in the CT44 tumour model being a prime candidate from future experiments looking at the combination of surgery with removal of immune suppression.

Chapter 4: Targeted Removal of Immune Suppression In Combination With Surgery

With the tumour and debulking models now established, the effect of suppressive cell removal needed to be investigated. This includes both MDSCs and Tregs, both of which have suppressive capabilities associated with solid malignancies.

4.1 Myeloid Derived Suppressor Cells

MDSCs are a heterogeneous population of immature myeloid cells that are the progenitors of macrophages, granulocytes and dendritic cells (Gabrilovich *et al.*, 2009). While the majority of MDSC's are located in the bone marrow, small populations, roughly 2-4%, exist in both the spleen and blood (Kong *et al.*, 2013) hence these were used to characterise these cells in both naïve and tumour bearing mice. This cell population is defined as $CD11b^+$ $Gr\text{-}1^+$ in mice although this cell population is both difficult to characterise and target due to their heterogeneity (Kong *et al.*, 2013).

The gating strategy used for flow cytometry analysis is shown in Figure 1. For this study, MDSCs were defined by gating on the negative populations of CD3, CD19 and CD11c cells and then comparing Gr-1 and CD11b to further differentiate this population into Gr-1 low, intermediate and high. The degree of immune suppression capability can be related to the expression of Gr-1 with the most potent being the Gr-1 intermediate population. Gr-1 high MDSCs exert mild suppression against $CD8^+$ T cells but not to the extent of the intermediate population (Youn *et al.*, 2010).

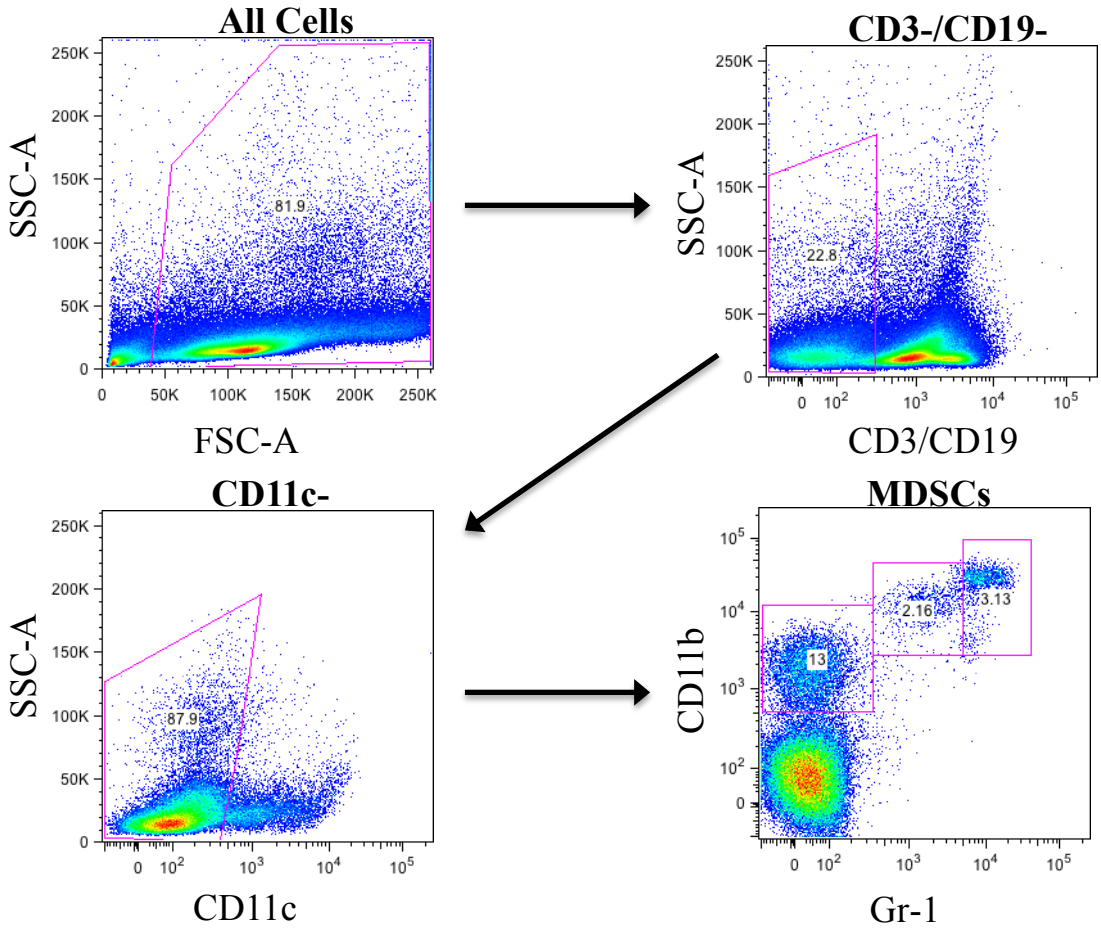

Figure 15: MDSC Gating Strategy

MDSCs were identified in spleens by selecting all cells and then gating on the CD3, CD19 and CD11c negative populations. MDSCs are then separated into the low, intermediate and high populations based on expression of Gr-1.

Firstly, MDSC populations in the spleen and blood needed to be characterised. This experiment was conducted in parallel to a Treg depletion experiment using Foxp3.dtr mice inoculated with $5x10^5$ AB1-HA cells s.c on the shaved right hand flank. Mice were harvested as described (Section 2.8) before tumour inoculation and 16 days post-inoculation. To determine the proportions of MDSCs, the staining panel outlined in table 4 (Chapter 8) was used on blood and spleen samples obtained from naïve and tumour bearing mice to observe any differences between them.

Results show that in the blood there were a higher proportion of Gr-1 high MDSCs relative to the low and intermediate populations (Figure 16 A). When comparing naïve to tumour bearing mice, there is a significant increase in the Gr-1 low and Gr-1 high MDSC proportions in the mice that had established tumours but no increase in the Gr-1 intermediate population.

The spleen showed a higher proportion of Gr-1 low MDSCs both in naïve and tumour bearing mice relative to the Gr-1 intermediate and Gr-1 high populations (Figure 16 B). There was no significant increase in proportions for any of the MDSCs proportions when comparing naïve mice to tumour bearing mice.

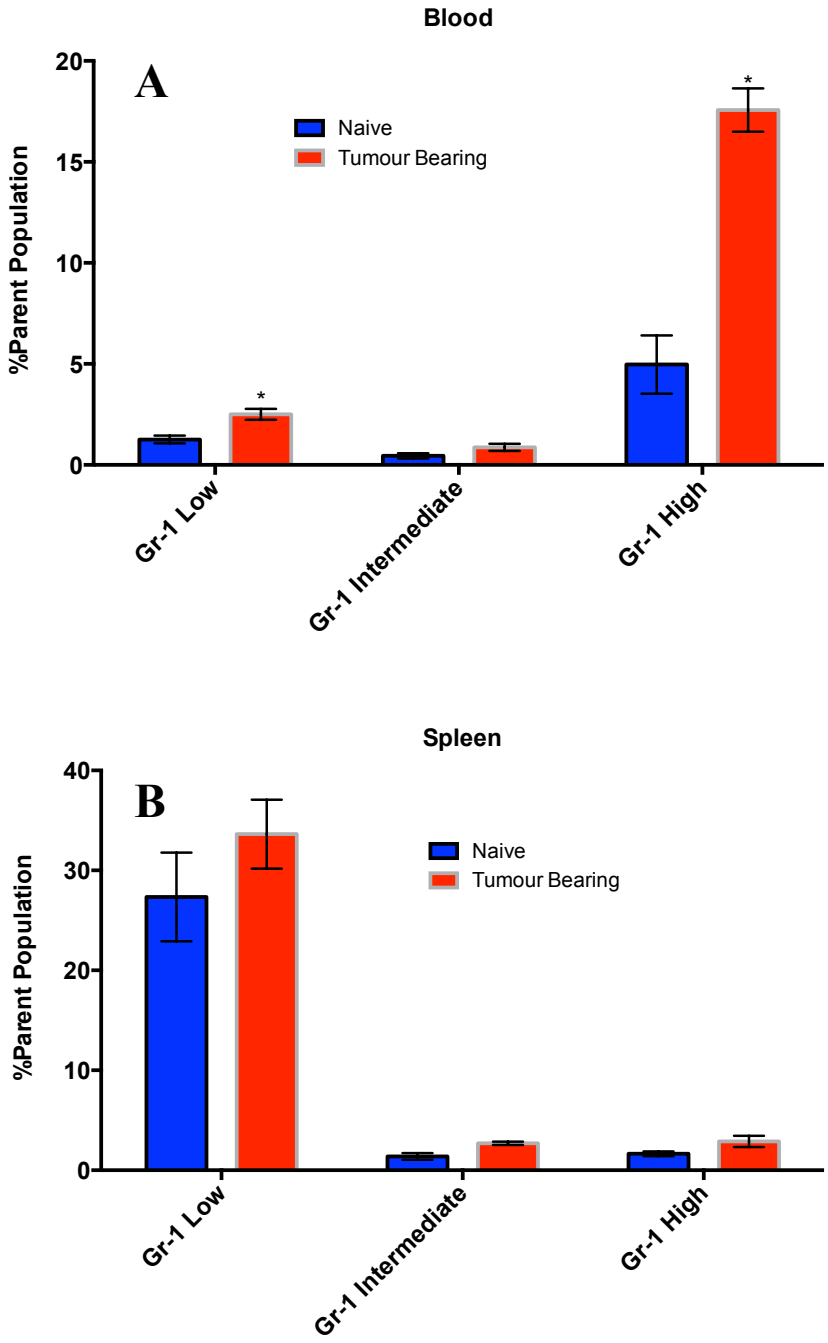

Figure 16: MDSC Characterisation in Blood and Spleen Samples

MDSCs were characterised in the blood (A) and the spleen (B) of naïve and tumour bearing mice. MDSCs were separated based on the level of Gr-1 expression.

To determine what effect the removal of MDSCs have on the survival of mice inoculated with the AB1-HA tumour cell line, a preliminary experiment was carried out by Dr Andrea Khong testing the effect of all-trans retinoic acid (ATRA) and anti-Gr-1 antibody on tumour growth. Described previously in a lung cancer model, the anti-Gr-1 antibody was capable of depleting Gr-1 expressing MDSCs and resulted in 50% (4/8) of the established Lewis Lung (LL) tumours regressing and development of immunological memory against tumour rechallenge as a result of the increased APC, NK and T cell activity (Srivastava *et al.*, 2012). The second compound ATRA has been shown to force MDSCs to differentiate into their respective non-suppressive cell types with studies conducted in both lung cancer (Lee *et al.*, 2012) and in colorectal carcinoma (Nefedova *et al.*, 2007).

ATRA was given at a dose of 10 μg/g per mouse dissolved in dimethyl sulfoxide (DMSO) every day for 10 days and anti-Gr-1 antibody at a dose of 200 μg per mouse every 2nd day for 3 days. The control groups were treated with either DMSO only or PBS only.

The results show that the anti-Gr-1 antibody sufficiently depleted the Gr-1 high population of MDSCs (Figure 17 B) when compared to the DMSO controls (Figure 17 A). ATRA resulted in a higher proportion of the Gr-1 high MDSCs when compared to the control groups (Figure 17 C). The survival of the treated groups was not increased with the use of either treatment relative to the control groups and no delay in tumour was observed (Figure 18)

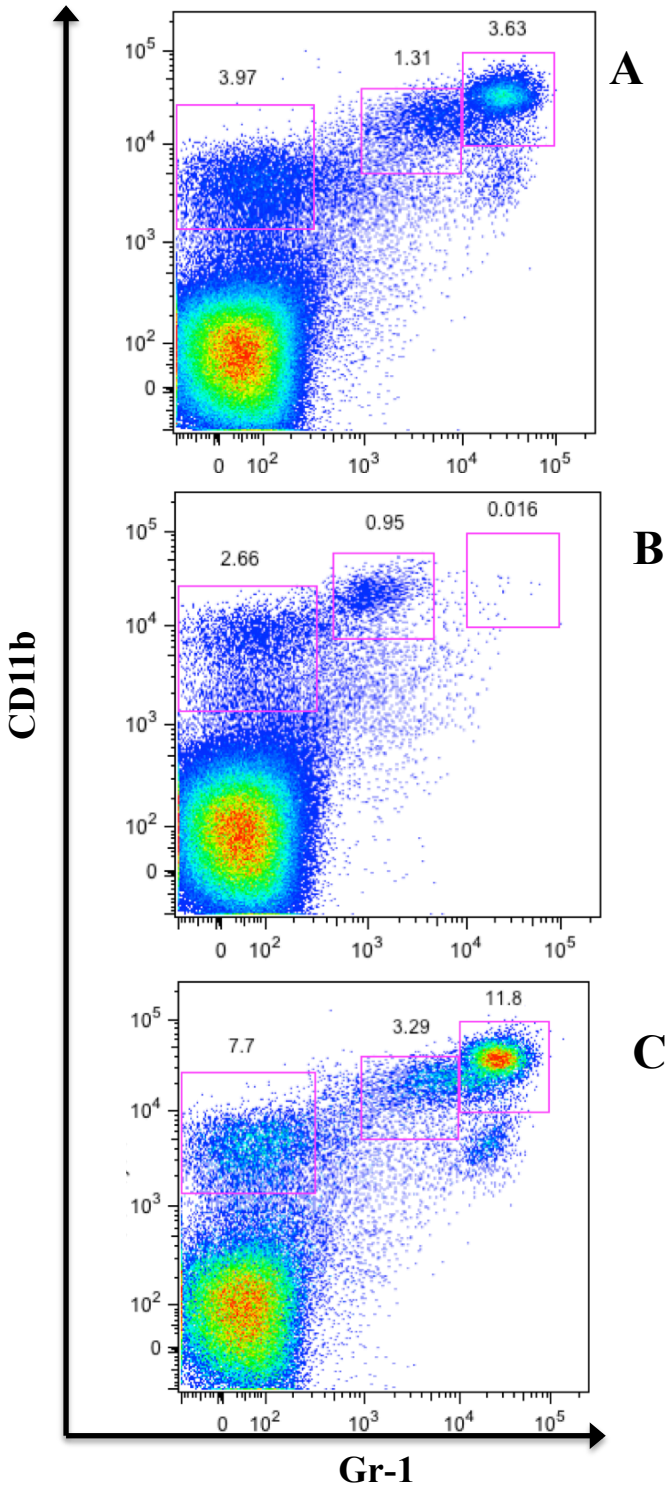

Figure 17: MDSC Depletion With Anti-Gr-1 or ATRA

MDSC depletion was tested by comparing a DMSO control (A) to the anti-Gr-1 treated (B) and ATRA treated (C) mice. MDSC's were analysed from the spleens of AB1-HA tumour bearing BALB/c mice.

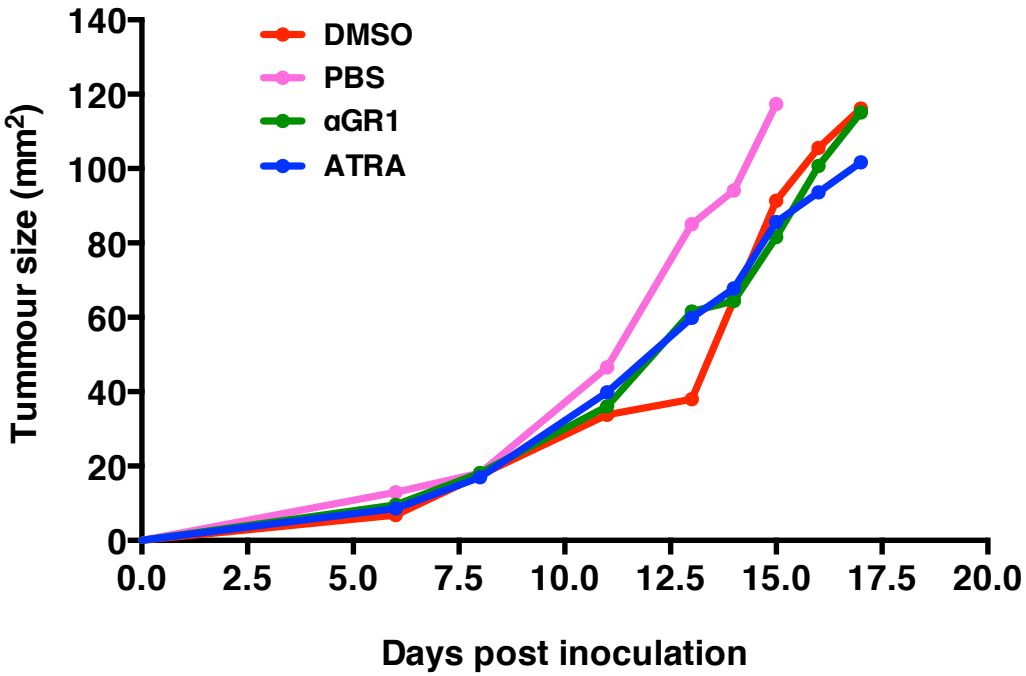

Figure 18: Tumour Growth for MDSC Targeted Mice

Figure shows AB1-HA tumour growth for the DMSO and PBS controls and the anti-Gr-1/ATRA treated mice. Each line represents a group of 3 mice for the controls and 5 mice for the treated groups.

Summary

Flow cytometry analysis of MDSCs in the blood and spleen of naïve and tumour bearing mice showed that there were a higher proportion of Gr-1 high MDSCs in the blood while the spleen had a significantly higher proportion of the Gr-1 low MDSCs in both naïve and tumour bearing mice. The proportion of Gr-1 low and high MDSCs in the blood did significantly increase when comparing naïve mice to tumour bearing mice but this was not mirrored in the spleen samples.

The preliminary experiment by Dr Andrea Khong showed that the use of anti-Gr-1 antibody results in a depletion of only the Gr-1 high MDSC population while those treated with ATRA had an increase in proportion of this same population. Neither treatment

conveyed a survival benefit to mice inoculated with the AB1-HA tumour cell line. Due to the difficulties in obtaining a method which resulted in the clear depletion of MDSCs, it was decided that any future experiments involving MDSC depletion would be ceased and the primary focus would remain with Tregs as a mouse model allowing for their targeted depletion has been established.

4.2 Timing of Treg Depletion In Combination With Surgery

With the debulking models established for both AB1-HA and CT44, the effect of surgery in combination with removing tumour-associated immune suppression needed to be determined. One of these methods is the transient depletion of Tregs to remove one of the 'brakes' placed on the immune system by the presence of solid tumours. Another aim was to determine at what time this Treg depletion should occur when combined with surgery so as to provide the optimal conditions in which an immune response can adequately attack and eradicate established solid tumours. To accomplish this, the FoxP3.dtr mouse model was used. FoxP3 is a transcription factor involved in the development and function of Tregs and was also used as a marker for this cell population. This model allows for a specific depletion of $FoxP3^+$ Tregs by administering DTx.

4.2.1 BALB/c.FoxP3.dtr.Crslc Mouse Model

The FoxP3.dtr mouse model was developed by inserting cDNA encoding the human diphtheria toxin receptor (DTR) that had been fused with sequences coding for the green fluorescent protein (GFP) at the 3' untranslated region of *FoxP3* (Kim *et al.*, 2007). This results in the expression of both proteins on all $FoxP3^+$ cells allowing them to be depleted when a dose of DTx is given as well as detect these Tregs by screening for the presence of GFP. This method allows for precise depletion of only these cells in contrast to other immunotherapies such as low dose cyclophosphamide or anti-CD25 that may affect other

immune cell populations including activated T lymphocytes (Needham *et al.*, 2006). Depletion occurs in a dose dependent manner with higher doses depleting Treg proportions to much lower levels. Figure 19 gives an overview of this model.

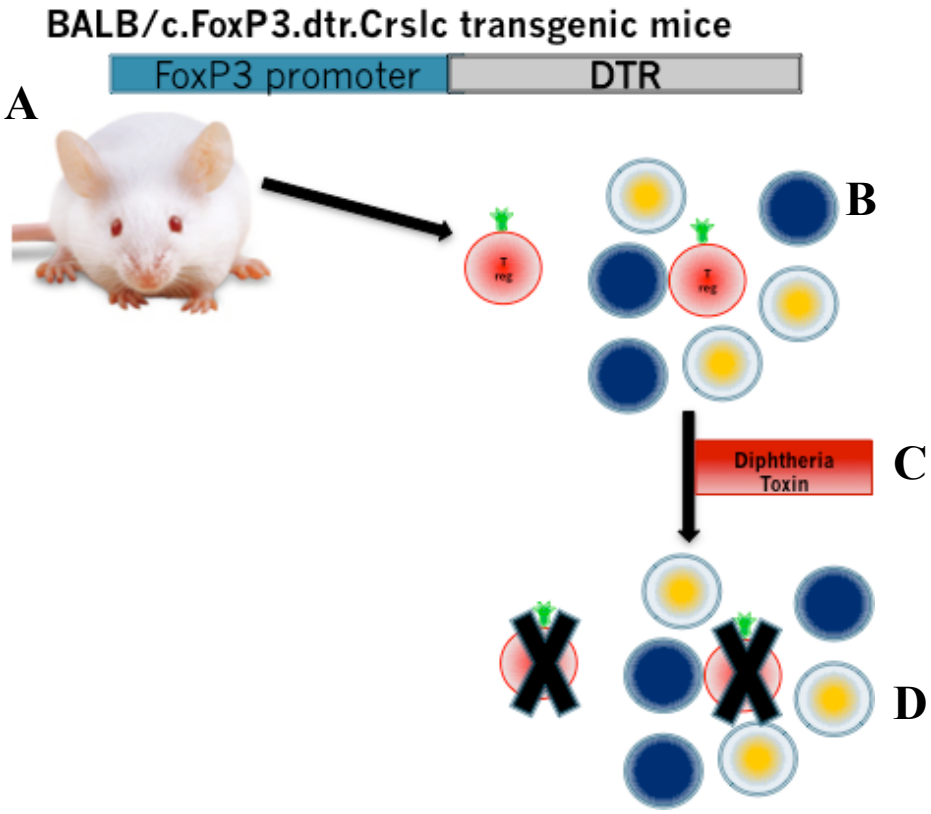

Figure 19: Mode of Action of the FoxP3.dtr Transgenic Mouse Model.

The FoxP3.dtr transgenic mouse (A) has the *DTR* gene inserted under the control of the FoxP3 promoter. All Treg cells now express the cognate receptor for DTx (B). When a dose of DTx is given (C) the result is the depletion of those cells (D).

As observed in Figure 20, DTx was able to deplete Treg proportions in a dose dependent manner in the FoxP3.dtr model. Untreated mice have between 8-12% of their $CD4^+$ T cells as $FoxP3^+$ Tregs and the administration of DTx does not affect the proportions of $CD8^+$ T cells or non-$FoxP3^+$ $CD4^+$ T cells. Based on these results a dose of 5 ng/g/mouse was chosen that would both deplete Tregs and not result in eradication of solid tumours.

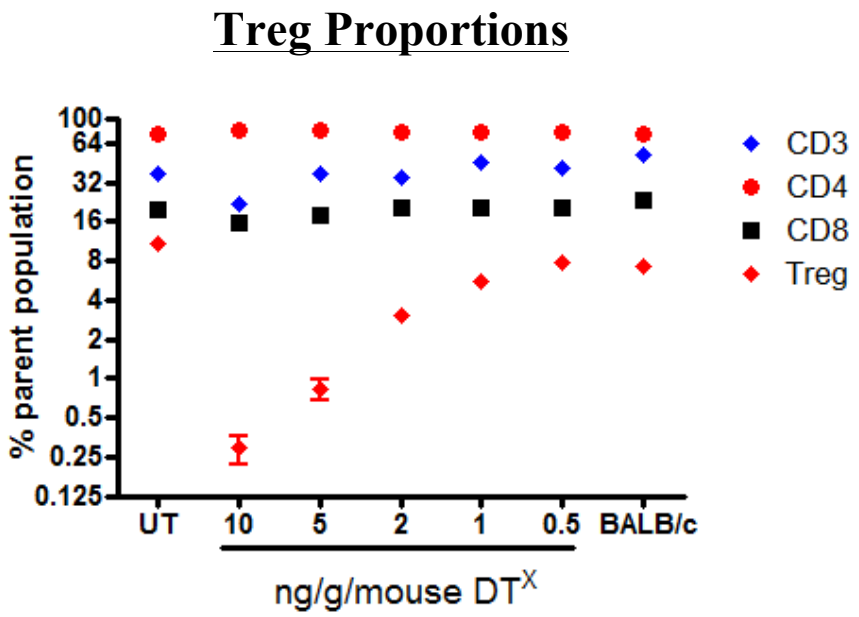

Figure 20: Dose Dependent Treg Depletion in FoxP3.dtr Transgenic Mouse Model.

The dose dependent nature of DTx is show in (E) as was provided by Dr Scott Fisher (UWA Department of Medicine and Pharmacology). Data represented on a log2 scale to separate cellular proportions obtained from blood samples.

4.2.2 Gating Strategy for Tregs

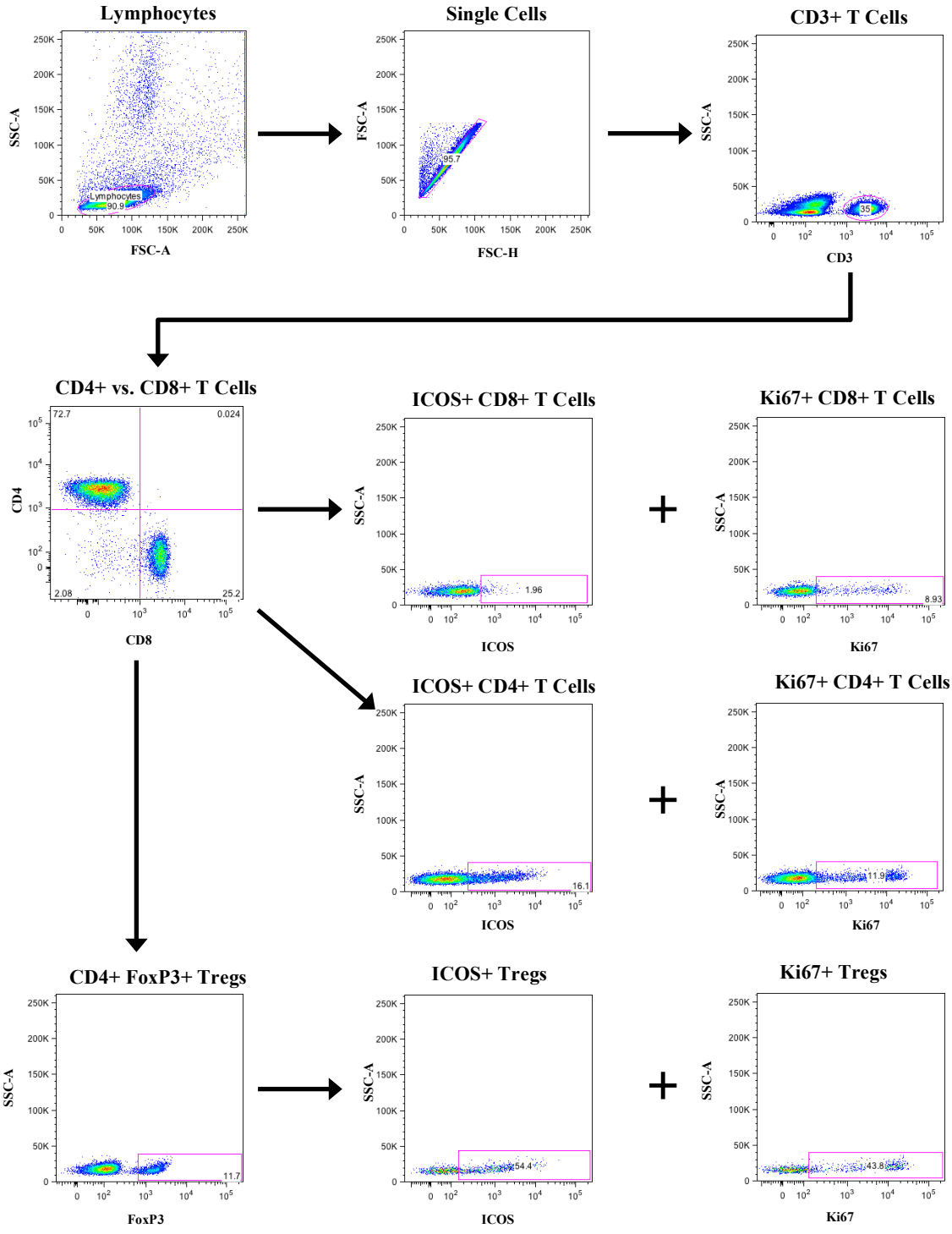

Figure 21: Gating Strategy for FoxP3$^+$ Tregs

Figure shows the gating strategy for analysis of CD4$^+$, CD8$^+$ and FoxP3$^+$ proportions and their respective activation/proliferation status in blood. This same strategy was used for other lymphoid organs and tumours.

To analyse the proportions of $CD4^+$, $CD8^+$ and $FoxP3^+$ T cells and what percentage of each are activated/proliferating, the flow cytometry panel described in table 3 (Chapter 8) was established. To isolate these respective cellular proportions and what percentage of each is activated/proliferating, the gating strategy in Figure 21 was used. Firstly lymphocytes were gated by FSC/SSC and single cells selected. Gating on the $CD3^+$ population allows the analysis of $CD4^+$ and $CD8^+$ T cell proportions. These can then be further analysed to determine the ICOS and Ki67 proportions of both $CD4^+$ and $CD8^+$ T cells that represents activation and proliferating respectively. Finally, $FoxP3^+$ Tregs are analysed by gating on $CD4^+$ T cells and further gating on $FoxP3^+$ cells. Again both ICOS and Ki67 expression can be quantified in this population.

4.2.3 Surgery and Treg Depletion in the AB1-HA Model

This experiment aimed to firstly determine if surgery offers a benefit to the eradication of AB1-HA solid tumours in combination with depletion of Tregs and secondly what the best time to do this was based on tumour size and day of surgery. To conduct this experiment, 6 groups of 5 Foxp3.dtr mice were inoculated with $5x10^5$ AB1-HA cells s.c on the shaved right hand flank. Mice were both male and female between 6-14 weeks of age.

4.2.3.1 Timelines and Growth Kinetics

The 6 groups were separated into 3 different timelines in which DTx was given when tumours were at different sizes either before or after surgery. Surgery was conducted on day 16 for the respective groups. Bloods were taken and stained using the Treg panel at the time points of 1, 4, 7 and 14 days (DTx+1, DTx+4, DTx+7 and DTx+14 respectively) after administration of DTx to measure the proportions of the cell types described as well as their activation and proliferation status. Timelines and growth curves for those groups are show in figures 11, 12 and 13 respectively.

4.2.3.1.1 Neo-adjuvant Small Tumours

The focus of the first timeline was to investigate the effect of giving a dose of DTx when small tumours had grow and compare that to the group who received both the DTx and a 75% debulking surgery. The timeline (Figure 22) shows that tumours were inoculated on day 0 and that a dose of DTx was given on days 9 and 10 with surgery performed on day 16. The surgery only control group was included in this timeline simply for blood sample collection at the same time points and did not receive any DTx.

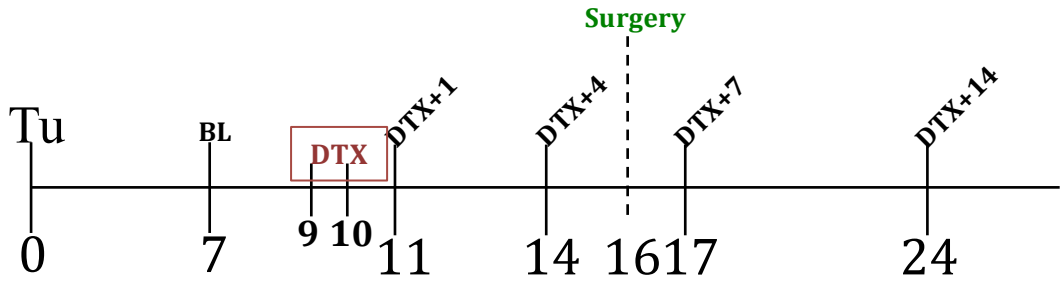

Figure 22: Timeline for Neo-adjuvant DTx Dosing of a AB1-HA Small Tumour

Figure shows the timeline for this group with the respective dosing, surgery and blood collection days.

Results for this group showed that all of the mice that received surgery only (Figure 23 A) eventually developed tumours that reached maximum size and were euthanised by day 35. One mouse was unable to undergo surgery due to spontaneous tumour regression. Survival for the other small sized tumour groups (Figure 24) showed the DTx only group had a slight halt in tumour growth before 80% (4/5) mice had to be euthanised because tumours reached maximum size. This group had a survival of 20% (1/5) in which one mouse had a tumour that began regressing shortly after the DTx dose and did not regrow. The group receiving surgery and DTx had no survivors but had one mouse survive until day 51 post inoculation with a significantly slower tumour growth rate. Another mouse (M4) was euthanised due to injuries sustained by bullying from another mouse.

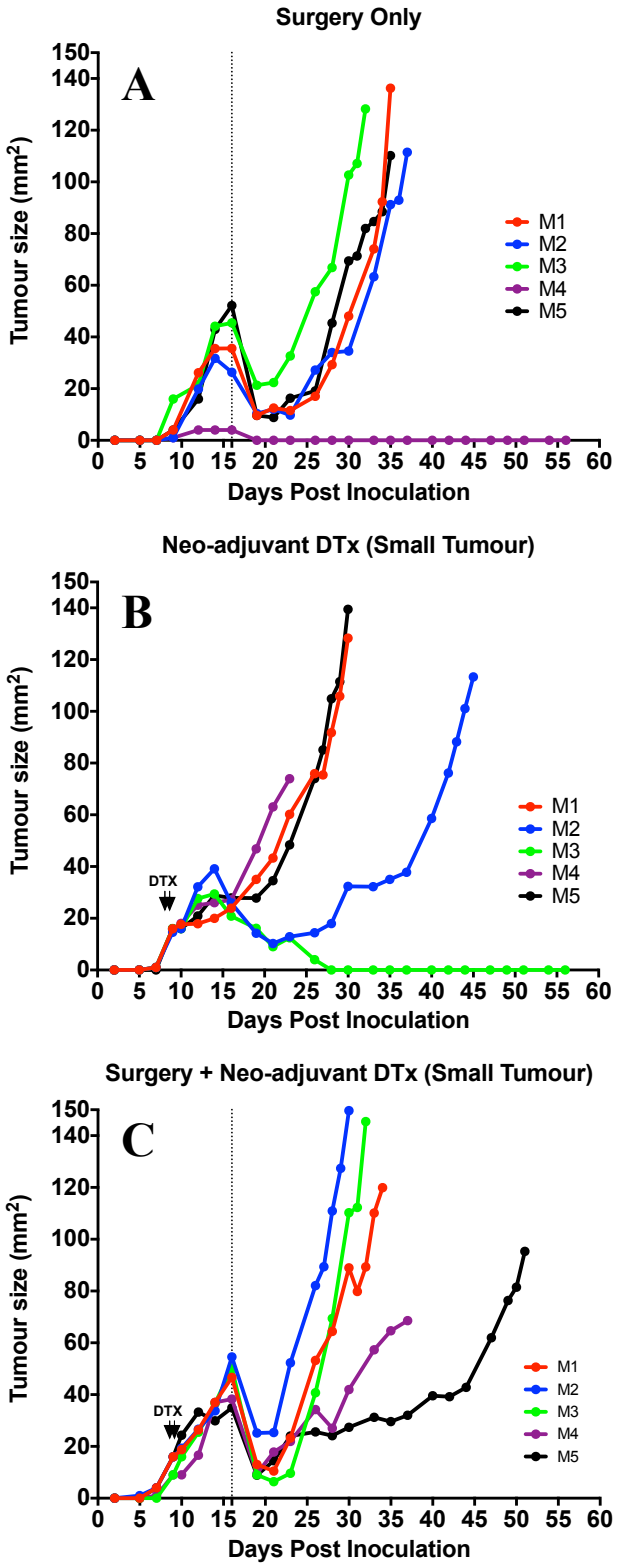

Figure 23: Neo-adjuvant DTx Dosing of a AB1-HA Small Tumour

Figure shows the surgery only control (A), the DTx treated at days 9/10 only (B) and the surgery and DTx treated at days 9/10 (C) groups. Each line represents an individual mouse. The vertical dotted line represents day of surgery and the arrows represent DTx dosing.

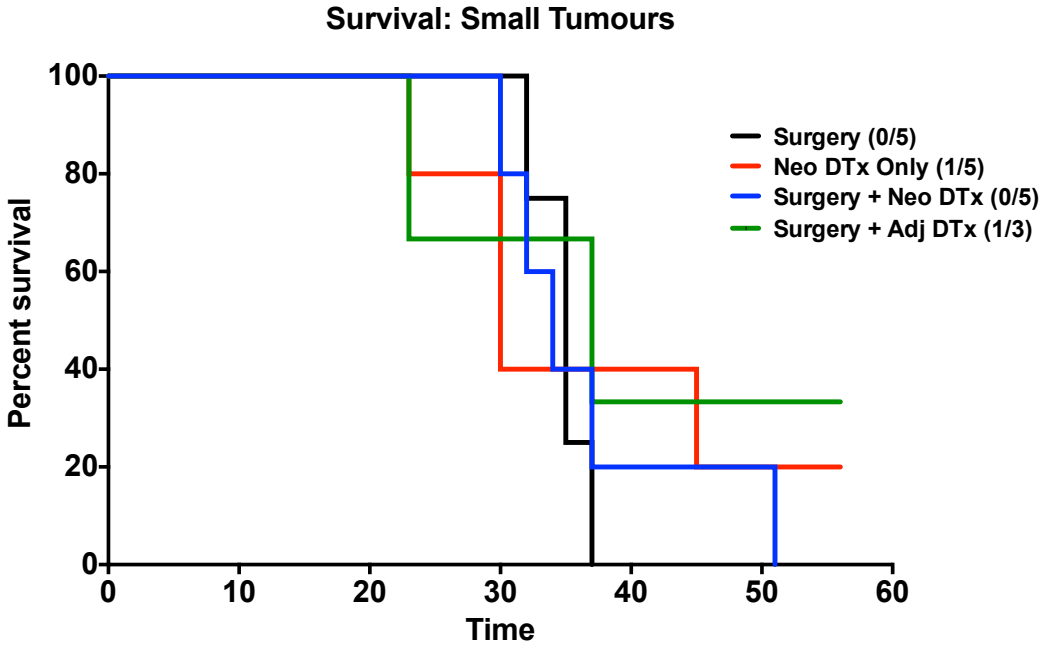

Figure 24: Survival of Small Sized AB1-HA Tumours.

Comparison of survival data for the surgery only group and groups treated with DTx at a small sized tumour.

4.2.3.1.2 Neo-adjuvant Medium Tumours

The second timeline (Figure 25) investigated the effect of giving a dose of DTx when tumours were of a medium size and then comparing the DTx only group with the one that received the combination with surgery. Tumours were again inoculated on day 0 and the DTx doses were given on days 14 and 15 with surgery done on day 16.

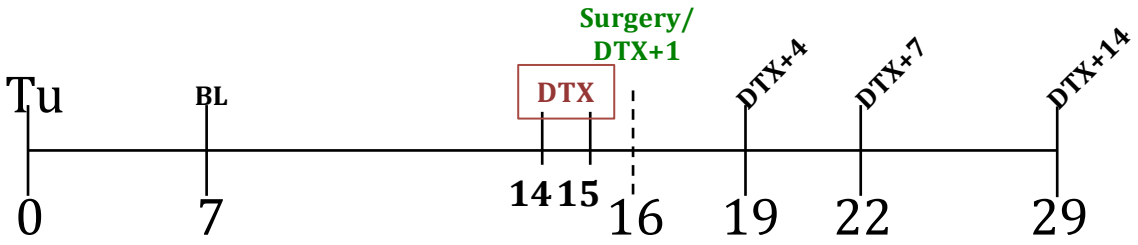

Figure 25: Timeline for Neo-adjuvant DTx Dosing of a AB1-HA Medium Tumour

Figure shows the timeline for this group with the respective dosing, surgery and blood collection days.

The results showed a difference in survival between the two groups (Figure 27) although not significant. The DTx only group had a survival of 25% (1/4) excluding the mouse that did not have a solid tumour while the surgery and DTx group had a survival of 60% (3/5). The two non-survivors in this group did have a slower growth rate after DTx and surgery and their survival was extended by six and eight days respectively when compared to the surgery only group (Figure 23 A). The decline in growth rate was observed with two mice in the DTx only group as well.

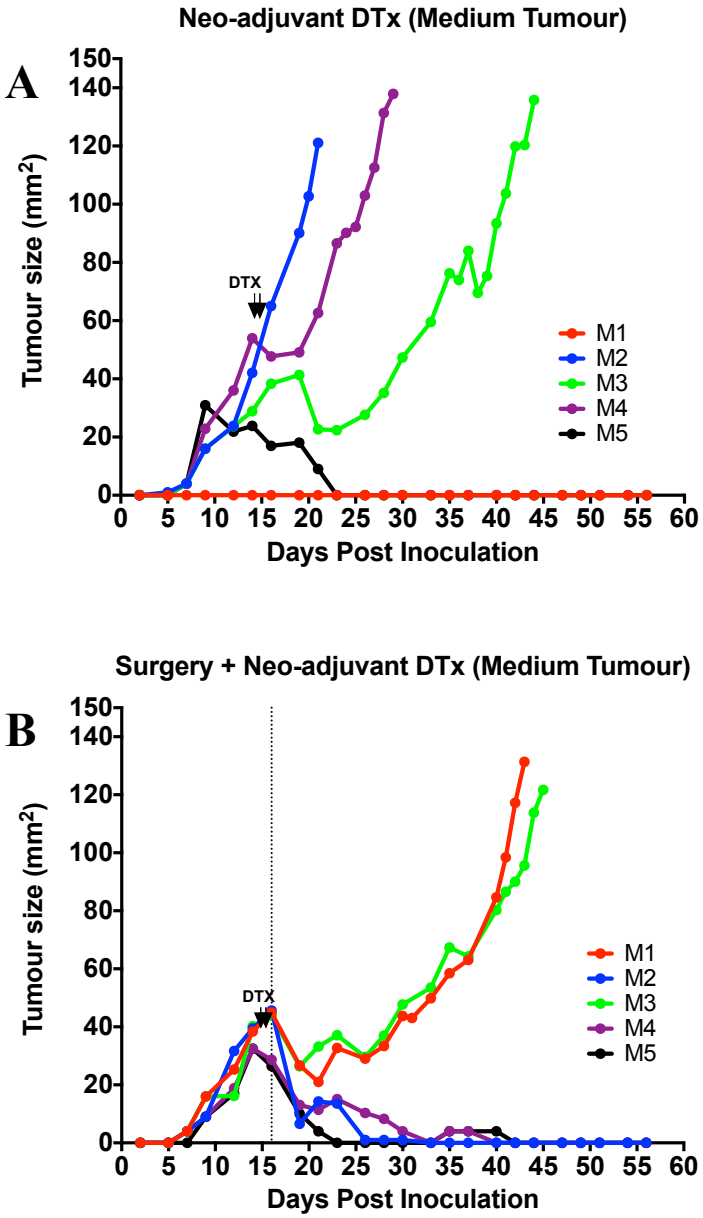

Figure 26: Neo-adjuvant DTx Dosing of a AB1-HA Medium Tumour

Figure shows the DTx treated at days 14/15 only (A) and the surgery and DTx treated at days 14/15 (B) groups. Each line represents an individual mouse. The vertical dotted line represents day of surgery and the arrows represent DTx dosing.

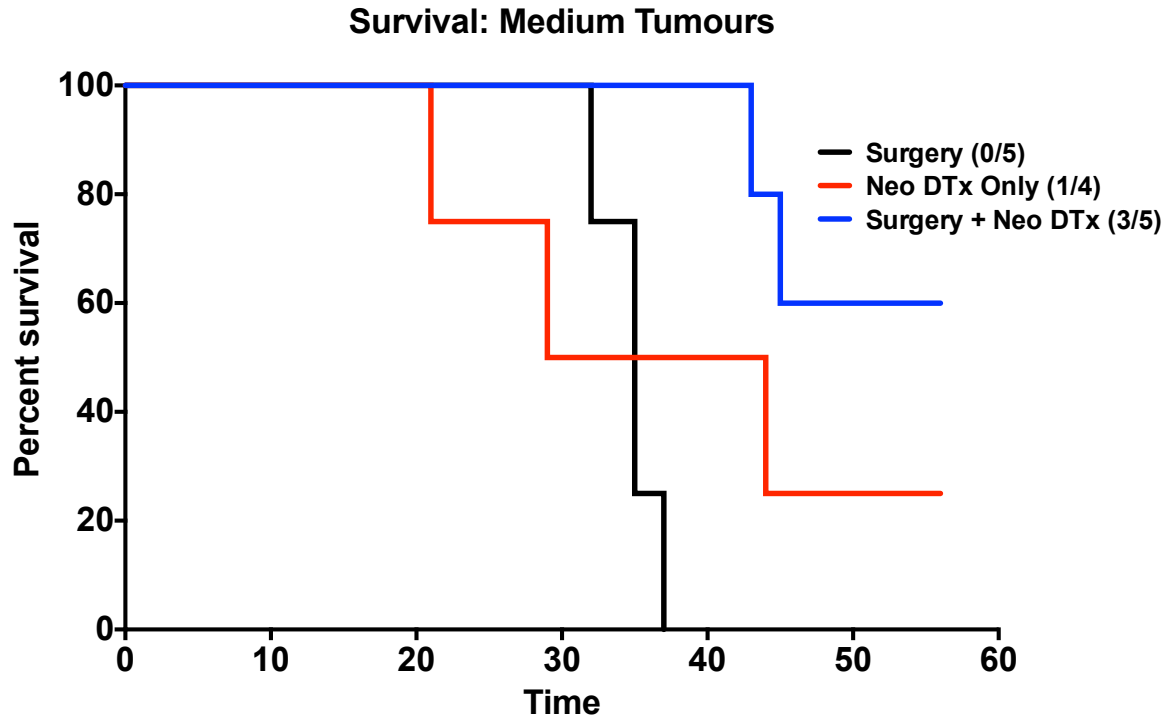

Figure 27: Survival of Medium Sized AB1-HA Tumours

Comparison of survival data for the surgery only group and groups treated with DTx at a medium sized tumour.

4.2.3.1.3 Adjuvant Small Tumours

The final timeline (Figure 28) contained one group investigating the effect of giving the DTx as an adjuvant after surgery when tumours were at a small size. The tumours were inoculated at day 0 with surgery on day 16 and DTx dosing on days 18 and 19.

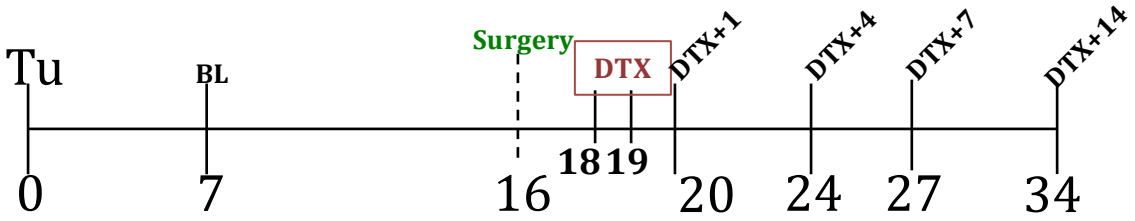

Figure 28: Timeline for Adjuvant DTx Dosing of a AB1-HA Small Tumour

Figure shows the timeline for this group with the respective dosing, surgery and blood collection days.

Tumour growth for this group (Figure 29) showed one mouse that did not have a growing tumour at any stage and one that had a tumour regress before surgery could be done and therefore neither of these received any treatment. Of the three that did, survival was 33% (1/3) while the other 66% (2/3) were euthanised when tumours reached maximum size (Figure 24). Tumour growth was slowed in only one of the mice that had a tumour reach size while DTx had no effect on the other.

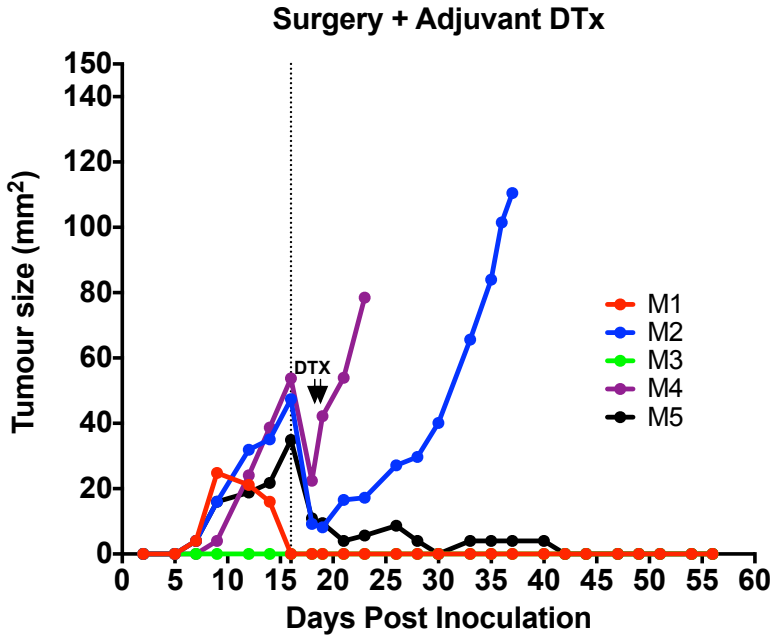

Figure 29: Adjuvant DTx Dosing of a AB1-HA Small Tumour

Figure shows the surgery and DTx treated at days 18/19 group. Each line represents an individual mouse. The vertical dotted line represents day of surgery and the arrows represent DTx dosing.

4.2.3.2 Flow Cytometry Analysis

As mentioned, bloods were taken from mice at the time points specified on each timeline. The purpose of these bloods was to observe the depletion of Treg proportions after DTx had been given and how soon they repopulate. The activation and proliferation status of $CD4^+$, $CD8^+$ and $FoxP3^+$ cells was also investigated to determine what immune response initiates and for how long it remains elevated following Treg depletion.

Firstly, analysis of $CD4^+$, $CD8^+$ and $FoxP3^+$ Treg proportions (Figure 30) showed that at baseline (A), the proportion of $CD4^+$ cells were between 70-80% of total $CD3^+$ cells. The proportion of $CD8^+$ cells was between 20-30% of total $CD3^+$ cells. The Treg proportions sat between 8-12% of total $CD4^+$ cells at baseline which is normal levels in mice.

Once mice had been treated with DTx, proportions were again measured at the DTx+1 time point (B) for each group and showed that the proportion of Tregs of $CD4^+$ cells had dropped down to between 2-3%. The proportions of both $CD4^+$ and $CD8^+$ cells did not change and remained at the same levels as their baseline readings. The surgery only group showed no change in any proportions as it was not treated with DTx. A comparison of the level of Treg depletion compared to the control levels of the surgery group is also shown (Figure 28 C) and shows a significant difference between that and each treated group.

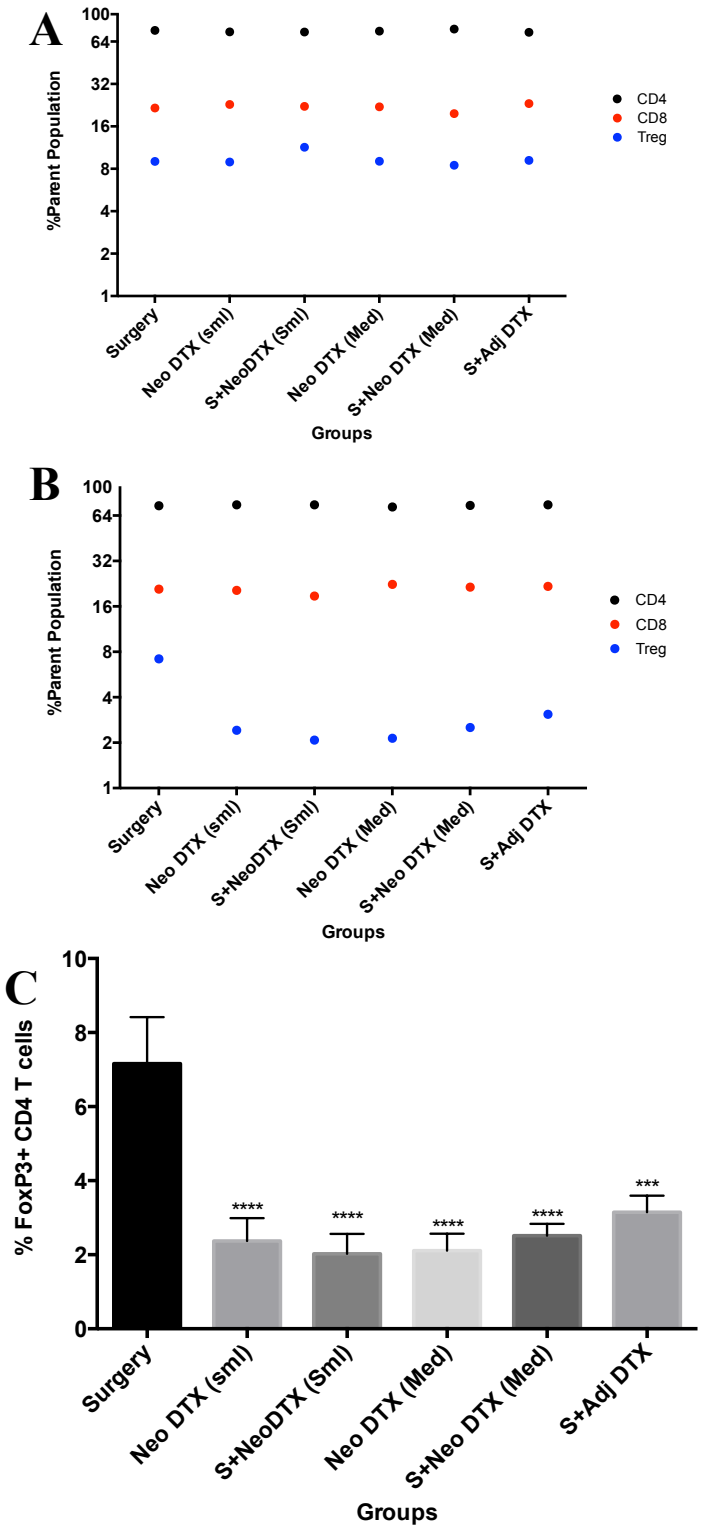

Figure 30: Baseline Proportions and Treg Depletion

Graphs showing baseline proportions for $CD4^+$, $CD8^+$ and $FoxP3^+$ cells (A) and their proportions after dosing with 5 ng/g/mouse DTx (B). Each point represents a mean of all individual results for that group and was placed on a log2 scale to separate cellular proportions.

The drop in Treg proportions lead to an increase in both the proliferation and activation of $CD8^+$ cells. Activation of $CD8^+$ cells was obtained by measuring ICOS expression via flow cytometry while proliferation was measured via Ki67 expression and these were obtained at the DTx+4 time point. The baseline activation levels for $CD8^+$ cells were between 1-2% and increased up to between 8-15%. Proliferation baseline levels were between 5-14% and increased to anywhere between 13-30%. The graphs in Figure 31 don't contain data for this time point from the neo-adjuvant DTx dosing at a small tumour due to an unforeseen complication. Figure 31 (A) is on a log2 axis to better visualise the data while proliferation was adequately represented on a linear scale.

This increased level of $CD8^+$ activation remained elevated for two weeks after the DTx dose despite Treg proportions having already returned to baseline at DTx+4. A representative graph (Figure 31 C) illustrates this and is data obtained for the DTx only treated group with a medium sized tumour.

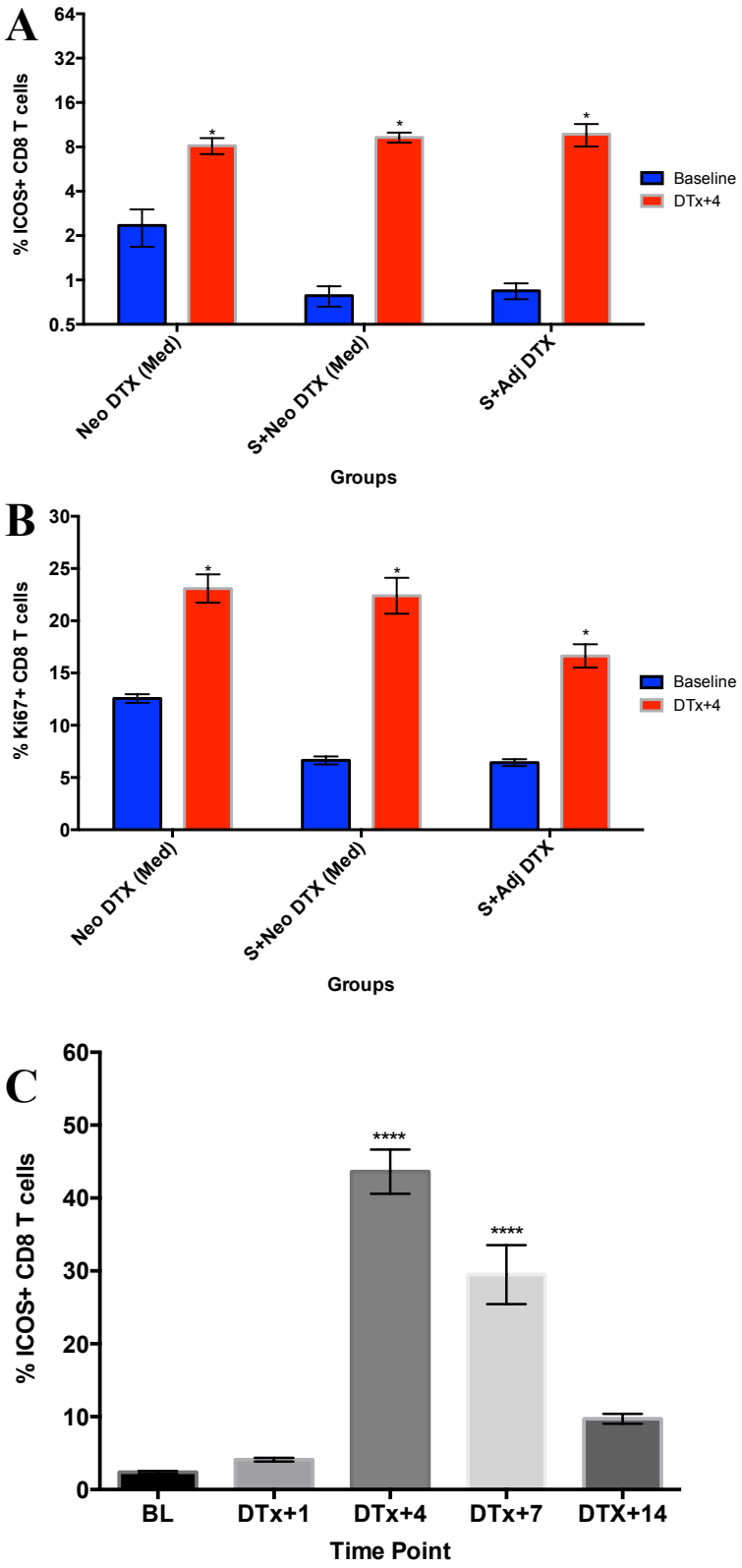

Figure 31: Increase in CD8$^+$ Activation and Proliferation in DTx Treated Tumours

Graphs shows percentage of activated (A) and proliferating (B) CD8$^+$ T cells as well as the increased level of activation of CD8$^+$ T cells over time (C). All DTx+4/DTx+7 levels were significantly different from baseline for all groups with P-values <0.0001.

Summary

These experiments aimed to show a difference between receiving DTx only as a treatment and the combination of DTx and surgery. The surgery only control group had no survivors for those mice that developed tumours where as all other groups did have varying survival rates. When DTx was administered at a small tumour it appeared that DTx alone and DTx in combination with surgery was not effective enough to result in a high survival rate. When DTx is administered to mice with medium tumours that then undergo surgical debulking the following day, the rate of survival increases and is significantly better than the previous two groups. When compared to each other, the group that received surgery had a much better survival rate than the group that didn't. This correlates with the flow cytometry results that show a peak in $CD8^+$ activation would have occurred three days after those mice had received surgery where the group that had DTx earlier would already have activation coming down, being at DTx+2 on the day of surgery. The final group that received DTx post-surgery was slightly inconsistent as only 3/5 mice were able to undergo surgery and subsequently only had one of those survive. Their peak $CD8^+$ activation occurred eight days after surgery in those mice that were treated.

4.2.4 Surgery and Treg Depletion in the CT44 Model

This experiment had the same aims as for the AB1-HA model to firstly determine if surgery offers a benefit to the eradication of CT44 solid tumours in combination with depletion of Tregs and secondly what the best time to do this was based on tumour size and day of surgery. It also allowed for the comparison of the response of the two different tumour models to surgery and DTx therapy.

To conduct this experiment, 6 groups of Foxp3.dtr mice were set up all with 5 mice except the surgery only group that had 3 due to the low number of mice available. All were inoculated with $5x10^5$ CT44 cells s.c on the shaved right hand flank.

4.2.4.1 Timelines and Growth Kinetics

The experimental setup for Treg depletion in the CT44 model was identical to the work done in the AB1-HA model (Section 4.2.1)

4.2.4.1.1 Neo-adjuvant Small Tumours

The first timeline looked to investigate the effect of giving a dose of DTx when small tumours had grow and compare that to the group who received both the DTx and a 75% debulking surgery. The timeline (Figure 32) shows that tumours were inoculated on day 0 and that a dose of DTx was given on days 6 and 7 with surgery performed on day 13. The surgery only control group was included in this timeline simply for blood sample collection at the same time points and did not receive any DTx.

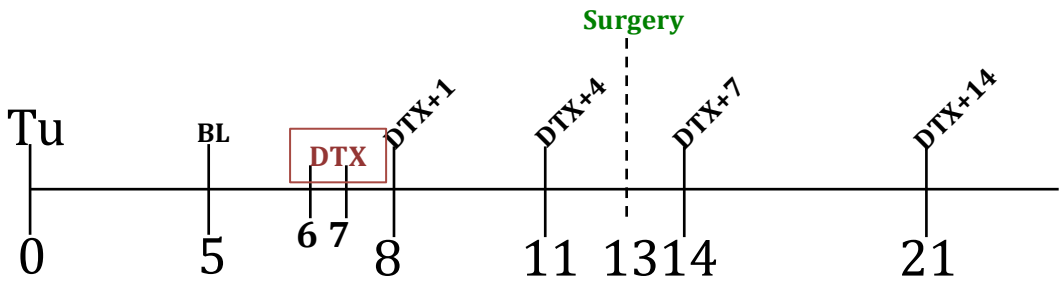

Figure 32: Timeline for Neo-adjuvant DTx Dosing of a Small CT44 Tumour

Figure shows the timeline for this group with the respective dosing, surgery and blood collection days.

Results show that all mice in the surgery only group (Figure 33 A) had tumours that grew to maximum size with one mouse having a tumour that regressed and subsequently regrew, increasing its survival time significantly compared to the other two. The DTx only group (Figure 34) had a high survival rate of 80% (4/5) with only one mouse having to be euthanised. These survivors remained tumour free once they had completely regressed and no regrowth occurred. The DTx and surgery group for this timeline had a slightly lower survival rate of 60% (3/5) when compared to the DTx treated only. Tumour growth was reduced for one mouse with tumour size reduced to 9 mm^2 but then started to grow at the same rate as before surgery was done (M1).

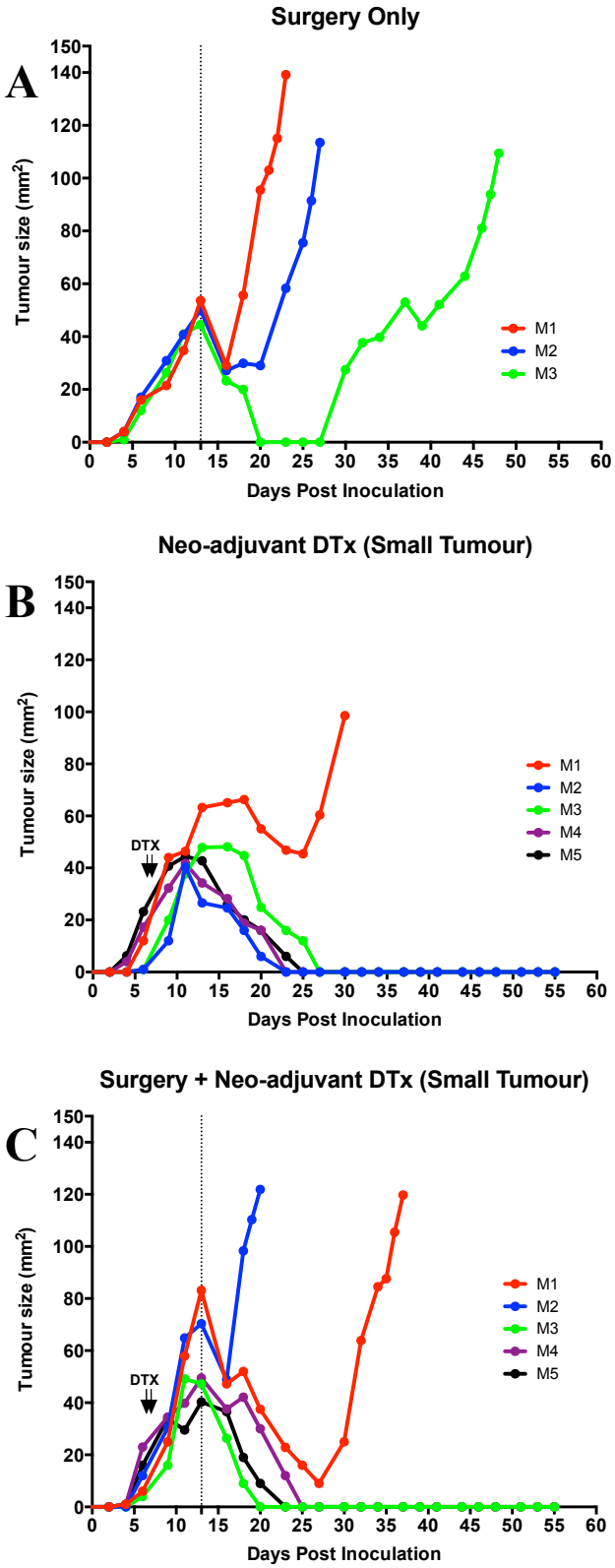

Figure 33: Neo-adjuvant DTx Dosing of a CT44 Small Tumour

Figure shows the surgery only control (A), the DTx treated at days 6/7 only (B) and the surgery and DTx treated at days 6/7 (C) groups. Each line represents an individual mouse. The vertical dotted line represents day of surgery and the arrows represent DTx dosing.

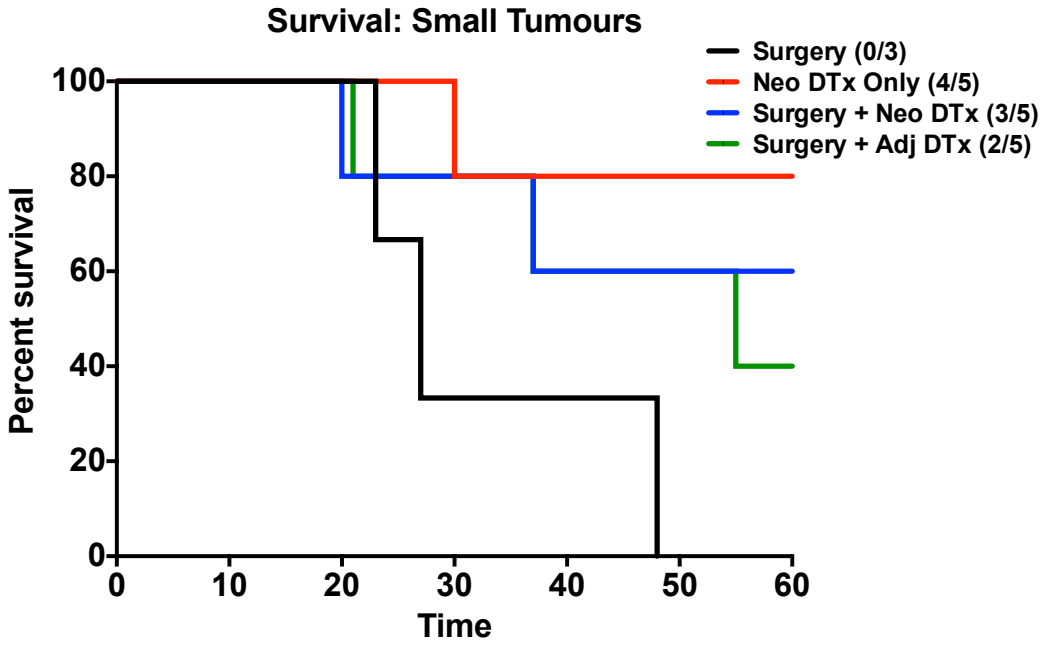

Figure 34: Survival of Small Sized CT44 Tumours

Comparison of survival data for the surgery only group and groups treated with DTx at a small sized CT44 tumour.

4.2.4.1.2 Neo-adjuvant Medium Tumours

The second timeline (Figure 35) where DTx was given when tumours were at a medium size showed no difference between the survival of the DTx treated only and the surgery plus DTx treated groups (Figure 37). Both had a survival of 40% (2/5) with the surgery extending survival time by 10 days for 2/5 of the mice compared to the DTx only group. When compared back to the AB1-HA model for this timeline, there was a clear between DTx only and the combination of surgery and DTx. One mouse in the DTx only group had a tumour approximately 108 mm^2 that then responded to the DTx therapy and regressed down to 0 mm^2 before regrowth started (Figure 36 A).

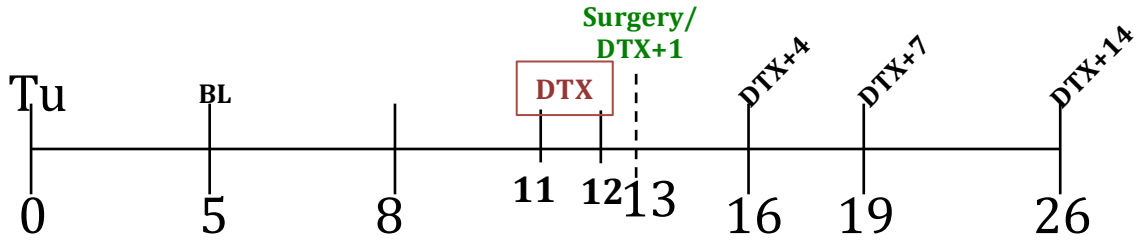

Figure 35: Timeline for Neo-adjuvant DTx Dosing of a Medium CT44 Tumour

Figure shows the timeline for this group with the respective dosing, surgery and blood collection days.

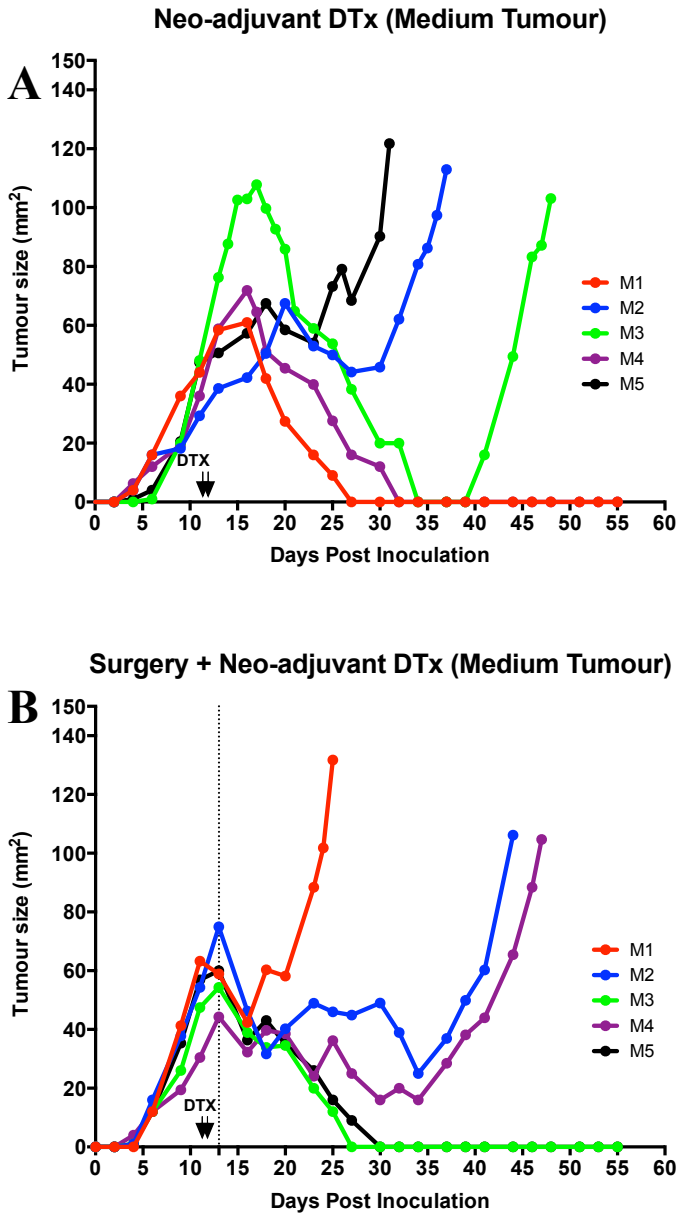

Figure 36: Neo-adjuvant DTx Dosing of a CT44 Small Tumour

Figure shows the timeline for this group (A), the surgery only (B), the DTx treated at days 6/7 only (C) and the surgery and DTx treated at days 6/7 (D) groups. Each line represents an individual mouse. The vertical dotted line represents day of surgery and the arrows represent DTx dosing.

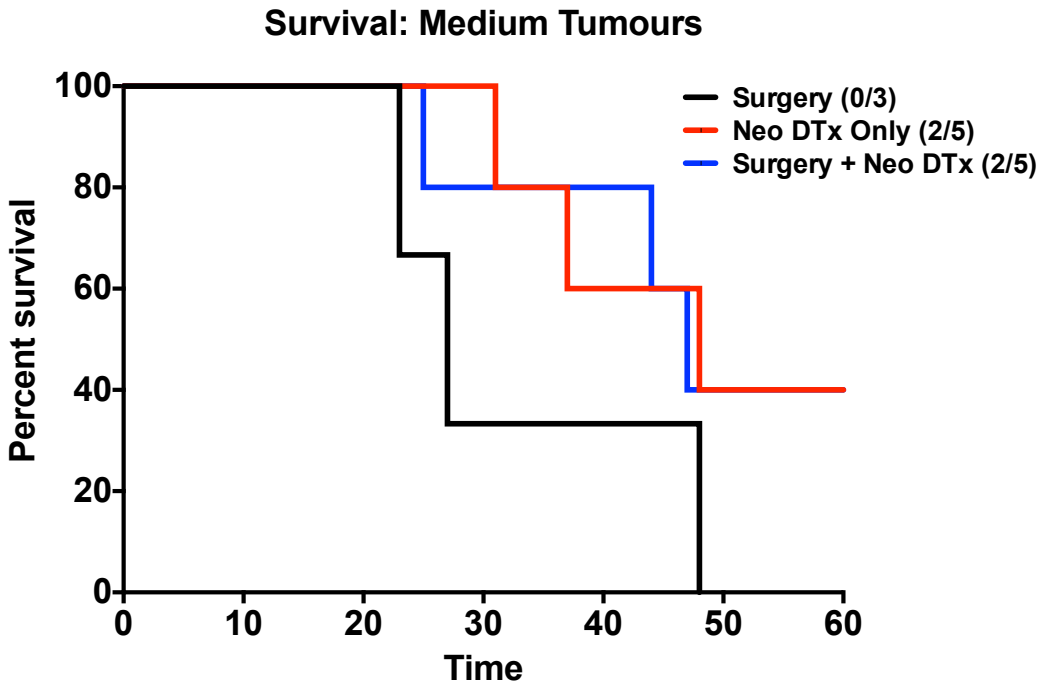

Figure 37: Survival of Medium Sized CT44 Tumours

Comparison of survival data for the surgery only group and groups treated with DTx at a medium sized CT44 tumour.

4.2.4.1.3 Adjuvant Small Tumours

The final timeline (Figure 38) observed the effect of DTx given post-surgery on tumour growth (Figure 39) and survival (Figure 34). Results showed that this group had a survival rate of 40% (2/5), the same as for the timeline 2 groups. The tumour growth rate for M2 was very high with surgery or DTx having little effect. The two survivors happened to be the two that had smaller tumours after surgery compared to the others that were slightly bigger.

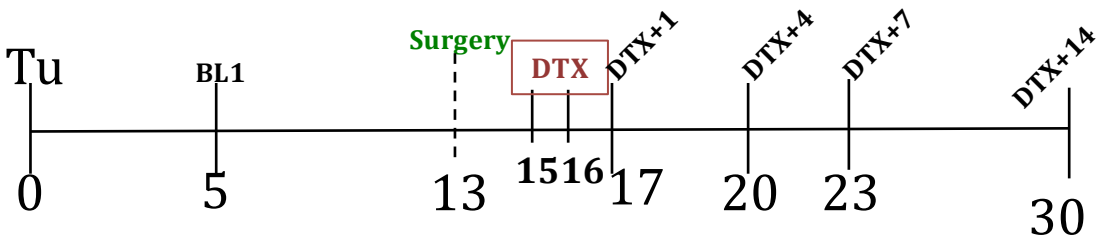

Figure 38: Timeline for Adjuvant DTx Dosing of a Small CT44 Tumour

Figure shows the timeline for this group with the respective dosing, surgery and blood collection days.

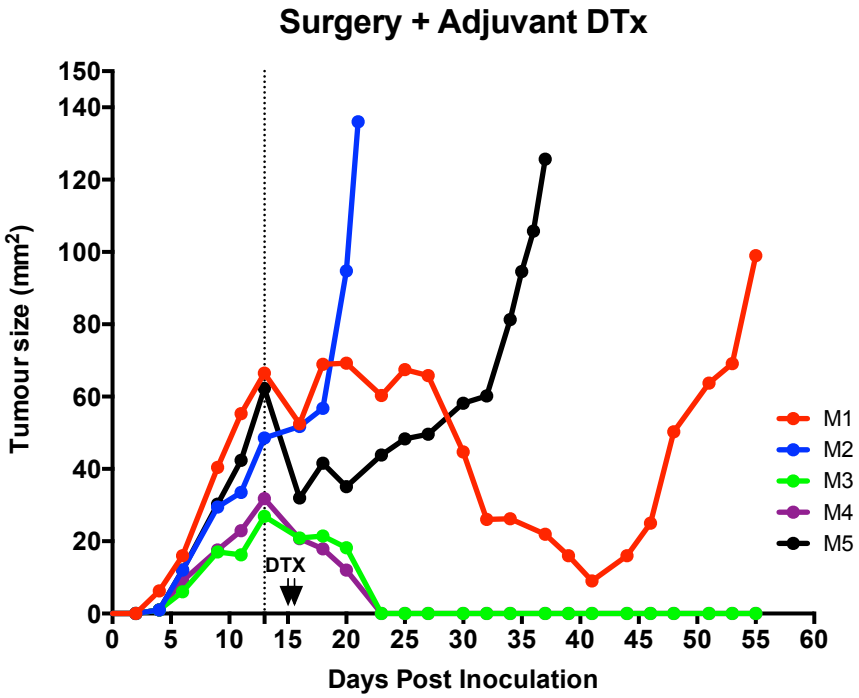

Figure 39: Adjuvant DTx Dosing of a CT44 Small Tumour

Figure shows the surgery and DTx treated at days 15/16 group. Each line represents an individual mouse. The vertical dotted line represents day of surgery and the arrows represent DTx dosing.

4.2.4.2 Flow Cytometry Analysis

Again, bloods were taken from mice at the time points specified on each timeline. The purpose of these bloods was the same as for AB1-HA to observe the depletion of Treg proportions after DTx had been given and how soon they repopulate. The increase in $CD8^+$ activation following the removal of these suppressive cells was a second objective of this analysis as well as how long these cells remained up regulated and if that correlates with a higher rate of survival.

Firstly, analysis of $CD4^+$, $CD8^+$ and $FoxP3^+$ Treg proportions (Figure 40) showed that at baseline (A), the proportion of $CD4^+$ cells were between 70-80% of total $CD3^+$ cells. The proportion of $CD8^+$ cells was between 20-30% of total $CD3^+$ cells. The Treg proportions

sat between 8-12% of total $CD4^+$ cells at baseline. Once mice had been treated with DTx, proportions were again measured at the DTx+1 time point (B) for each group and showed that the proportion of Tregs of $CD4^+$ cells had dropped down to between 1-3% for the DTx treated at small tumour groups and between 0.5-1% for the others. The proportions of both $CD4^+$ and $CD8^+$ cells did not change and remained at the same levels as their baseline readings. The surgery only group showed no change in any proportions as it was not treated with DTx. A comparison of the level of Treg depletion compared to the control levels of the surgery group are also shown (Figure 40 C) and show a significant difference between that and each treated group.

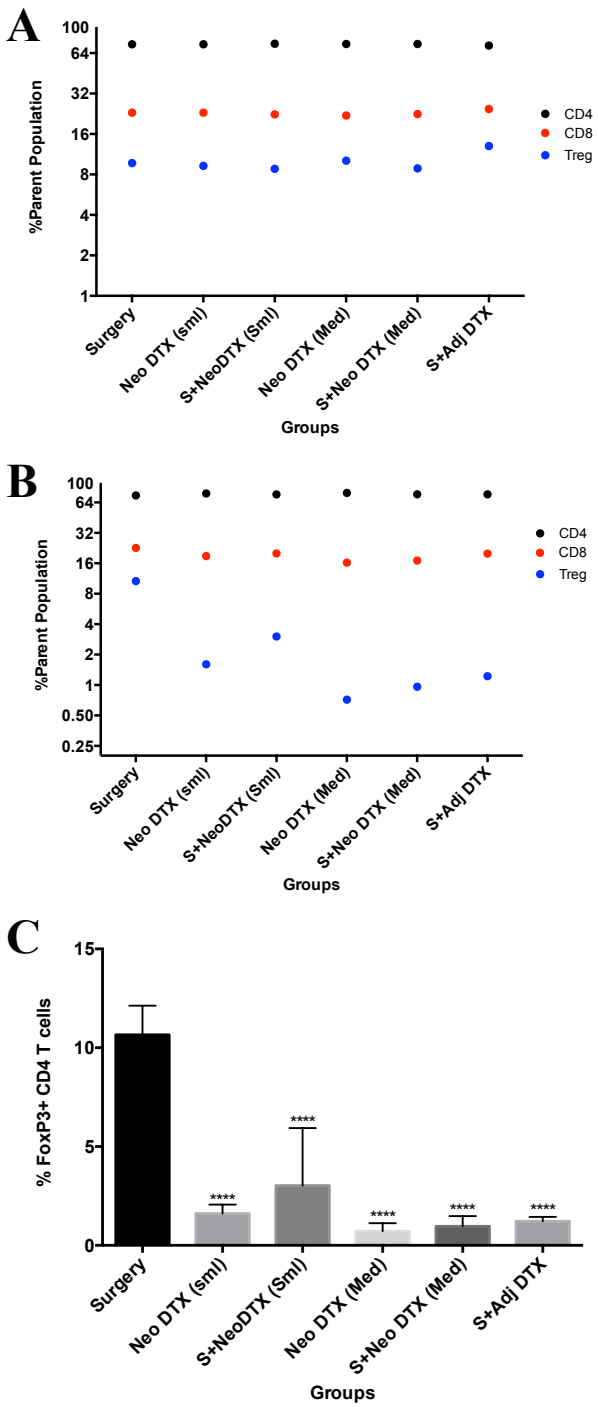

Figure 40: Baseline Proportions and Treg Depletion in the CT44 Tumour Model

Graphs showing baseline proportions for $CD4^+$, $CD8^+$ and $FoxP3^+$ cells (A) and their proportions after dosing with 5 ng/g/mouse DTx (B). Comparison of treated groups with non-DTx treated surgery group also shown (C). Each point represents a mean of all individual results for that group and was placed on a log2 scale to separate cellular proportions.

The drop in Treg proportions lead to an increase in both the proliferation and activation of $CD8^+$ cells. Activation of $CD8^+$ cells was obtained by measuring ICOS expression via flow cytometry while proliferation was done by measuring Ki67 expression and these were obtained at the DTx+4 time point (Figure 41). The baseline activation levels for $CD8^+$ cells were between 1-4% and increased up to between 25-60%. Proliferation baseline levels were between 8-12% and increased to anywhere between 30-70%. Figure 41 (A and B) is on a log2 axis to better visualise the data while proliferation was adequately represented on a linear scale. This increased level of $CD8^+$ activation remained elevated for two weeks after the DTx dose despite Treg proportions having already returned to baseline at DTx+4. A representative graph (Figure 41 C) illustrates this and is data obtained for the DTx only treated group with a medium sized tumour.

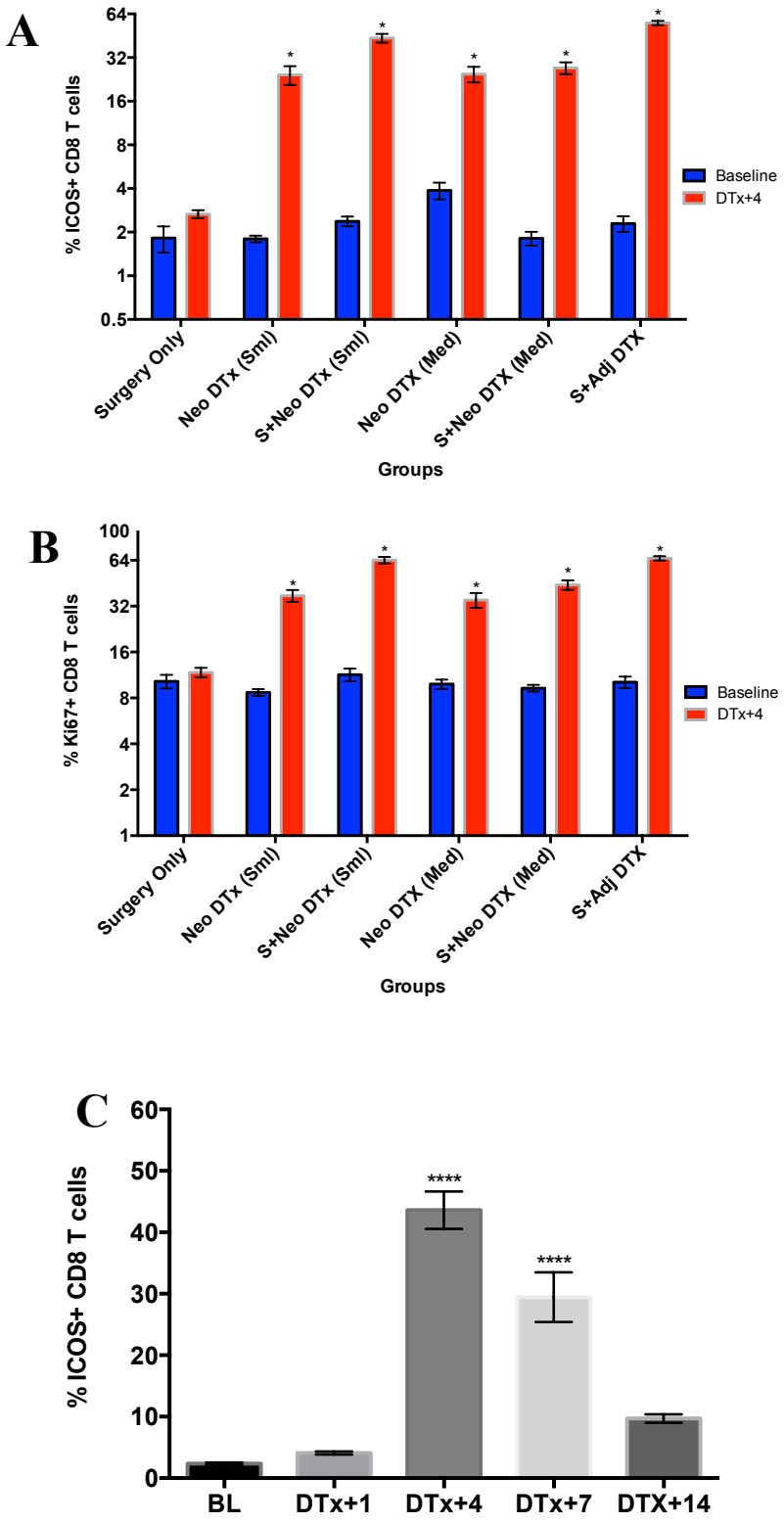

Figure 41: Increase in $CD8^+$ Activation and Proliferation

Graphs shows percentage of activated (A) and proliferating (B) $CD8^+$ T cells as well as the increased level of activation of $CD8^+$ T cells over time (C). All DTx+4/DTx+7 levels were significantly different from baseline for all groups with P-values <0.0001.

Summary

This experiment aimed to show a difference between receiving DTx only as a treatment and the combination of DTx and surgery. The surgery only control group had no survivors in those animals that developed tumours as where all other groups did have varying survival rates. When DTx was administered at a small tumour size it appeared that DTx alone was sufficient enough to result in a high survival rate with the surgery counterpart having a slightly lower survival rate. When DTx is administered to mice with medium tumours that then undergo surgical debulking the following day, the rate of survival was the same between the DTx only and surgery plus DTx groups with the group that underwent surgery receiving no survival benefit over those that didn't. The final group that received DTx post-surgery had a survival rate the same as the DTx treated mice with a medium sized tumour. This group however had one mouse that had survival extended significantly, much more than any other that had tumours reach maximum size.

The flow cytometry results show that even though a dose of 5 ng/g/mouse was used for both AB1-HA and CT44 models, Treg levels were depleted much lower in the CT44 experiment. This resulted in a much higher $CD8^+$ response with activation and proliferation significantly better than in the AB1-HA model. This was unfortunate as the aim was to determine a difference between DTx only and surgery plus DTx treatment. As the $CD8^+$ response was so great, this was not possible with some groups as survival rates were the same.

Chapter 5: Characterisation of Tregs In Lymphoid Organs

Systemic depletion of Tregs using currently available immunotherapies such as anti-CTLA-4 has been shown to increase the T-cell response to solid tumours (Tuve et al., 2007) and therefore we wanted to determine whether a similar outcome would be achieved following Treg depletion in the FoxP3.dtr mouse model.

The aims of this experiment was to determine what the baseline proportions were for CD4+ T cells, CD8+ T cells and Tregs and their activation and proliferation status in the dLNs, ndLNs, spleen and tumour. This was to determine whether the flow cytometry results obtained from blood samples in the previous section correlates with what occurs in the lymphoid organs and tumour.

To conduct this experiment, Foxp3.dtr mice were inoculated with $5x10^5$ AB1-HA cells s.c on the shaved right hand flank and were split into 8 groups (Table 1). Mice were harvested as described (Section 2.8) before treatment and 1, 4 and 7 days post treatment (DTx+1, DTx+4, DTx+7 respectively) with 2 groups harvested per time point. One group was the untreated size-matched control and the other was the DTx treated. The experimental timeline (Figure 42) shows tumours were inoculated at day 0 with the baseline harvest on day 10. DTx was administered on days 12 and 13 with the post-treatment harvests on days 14 (DTx+1), 17 (DTx+4) and 20 (DTx+7). A dose of 25 ng/g/mouse was used to ensure adequate depletion of the Tregs that would result in a significant change in CD8+ activation. All graphs are represented on a linear scale and all statistical analysis compared naïve and treatment time points with baseline levels.

Groups	No. of Mice	DTx Time point
Group 1	2	Naïve Mice
Group 2	2	Baseline Tumour Bearing
Group 3	3	Tumour Bearing DTx+1
Group 4	3	DTx Treated DTx+1
Group 5	3	Tumour Bearing DTx+4
Group 6	3	DTx Treated DTx+4
Group 7	3	Tumour Bearing DTx+7
Group 8	3	DTx Treated DTx+7

Table 1: Grouping of Mice According to DTx Time Point

Table shows the grouping of mice according to the 4 harvest time points associated with Treg depletion. For each pairing, one group received 25 ng/g/mouse DTx while the other was the untreated control.

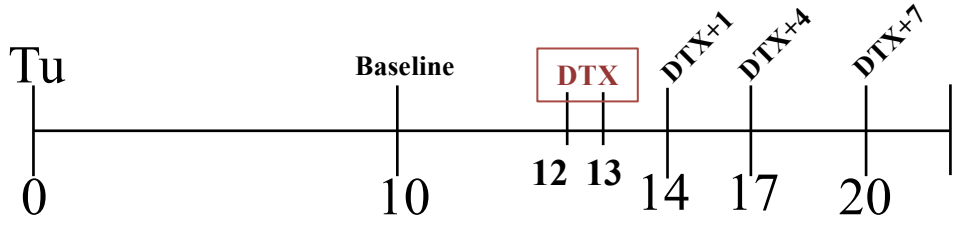

Figure 42: Timeline for Tumour and Lymphoid Harvesting

Experimental timeline for the dosing and harvesting of AB1-HA inoculated mice. DTx was administered on days 12 and 13, with tissues harvested on days 14, 17 and 20 (DTx+1, +4 and +7 respectively)

5.1 CD4+ T Cells

The CD4+ proportions for this experiment (Figure 43) showed a change from baseline once DTx had been administered. Naïve and baseline CD4+ proportions for all organs showed no significant difference while there was a drop at the DTx+1 time point at which Tregs were depleted. These proportions returned to baseline levels for blood, spleen and tumour samples with a higher proportion of CD4+ cells at DTx+4 for tumours. The lymph nodes showed a continuous decline in CD4+ proportions that correlates with the increase in CD8+ proportions (Figure 39 C and D).

CD4+ T cell activation (as represented by ICOS expression) continued to increase significantly over time with a 3-4 fold increase at DTx+7 when compared to baseline proportions (Figure 44). The tumour samples showed a decrease in ICOS+ CD4+ cells at DTx+4 that then rebounded back to the baseline proportion of 90%. The baseline proportion of ICOS+ CD4+ cells was higher in the tumours and showed the least amount of change when DTx was administered and was the only sample that showed a decrease in ICOS proportions.

The proliferation proportions of CD4+ cells represented by the marker Ki67 also increased from the DTx+4 time point for blood, spleen, dLN and ndLN samples of roughly 5-6 fold (Figure 45). Proliferation of CD4+ cells in the tumour experienced a significant decrease at DTx+1 but had returned to baseline levels by DTx+7. Again, tumours showed a much higher proportion of Ki67+ CD4+ cells at baseline when compared to the other organ samples and was the only sample showing a decrease in Ki67 proportions of CD4+ cells.

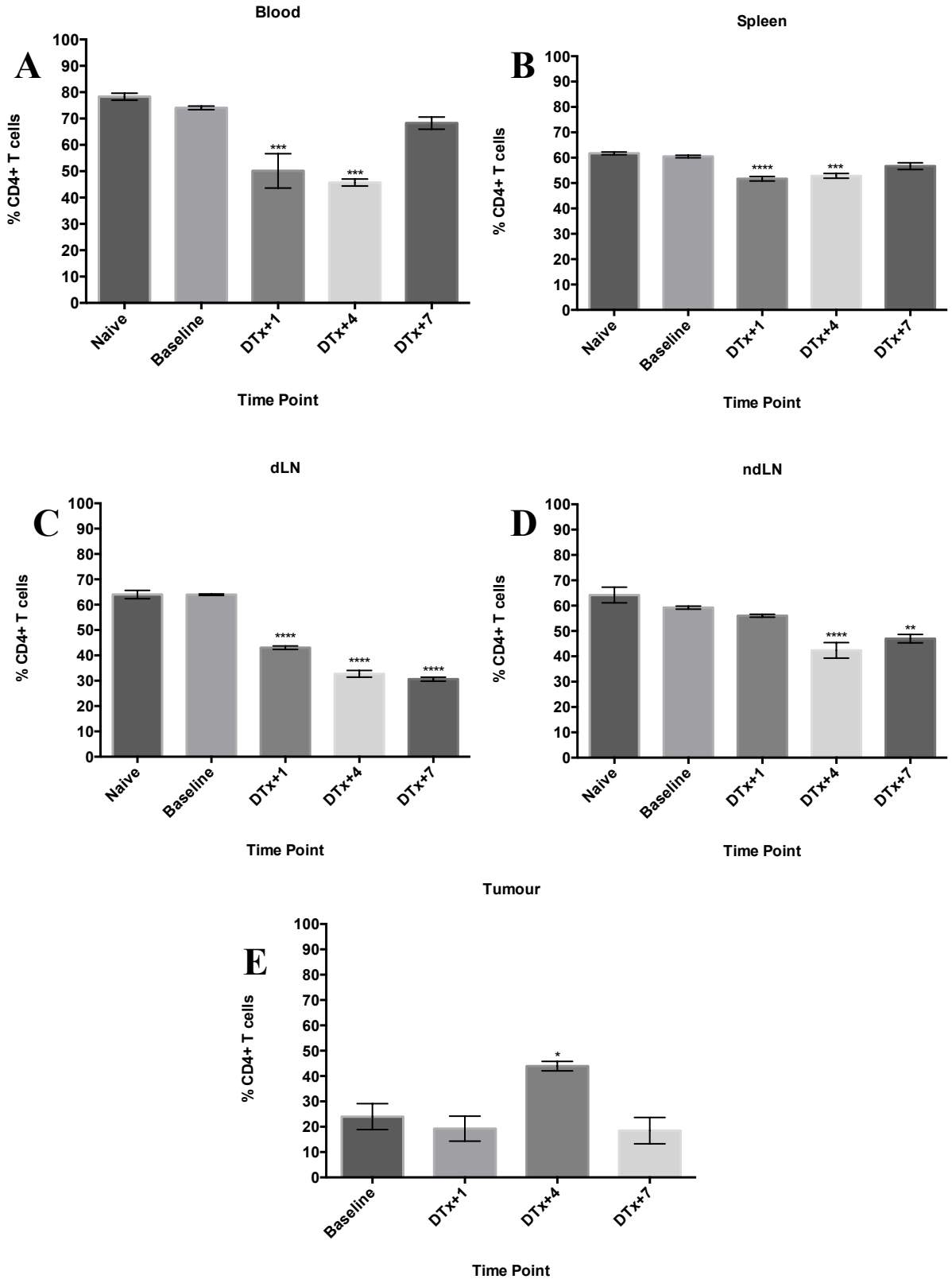

Figure 43: CD4+ T Cell Proportions Over Time

Figure shows the change in CD4+ proportions over time for blood (A), spleen (B), dLN (C), ndLN (D) and tumour (E) in mice bearing AB1-HA tumours.

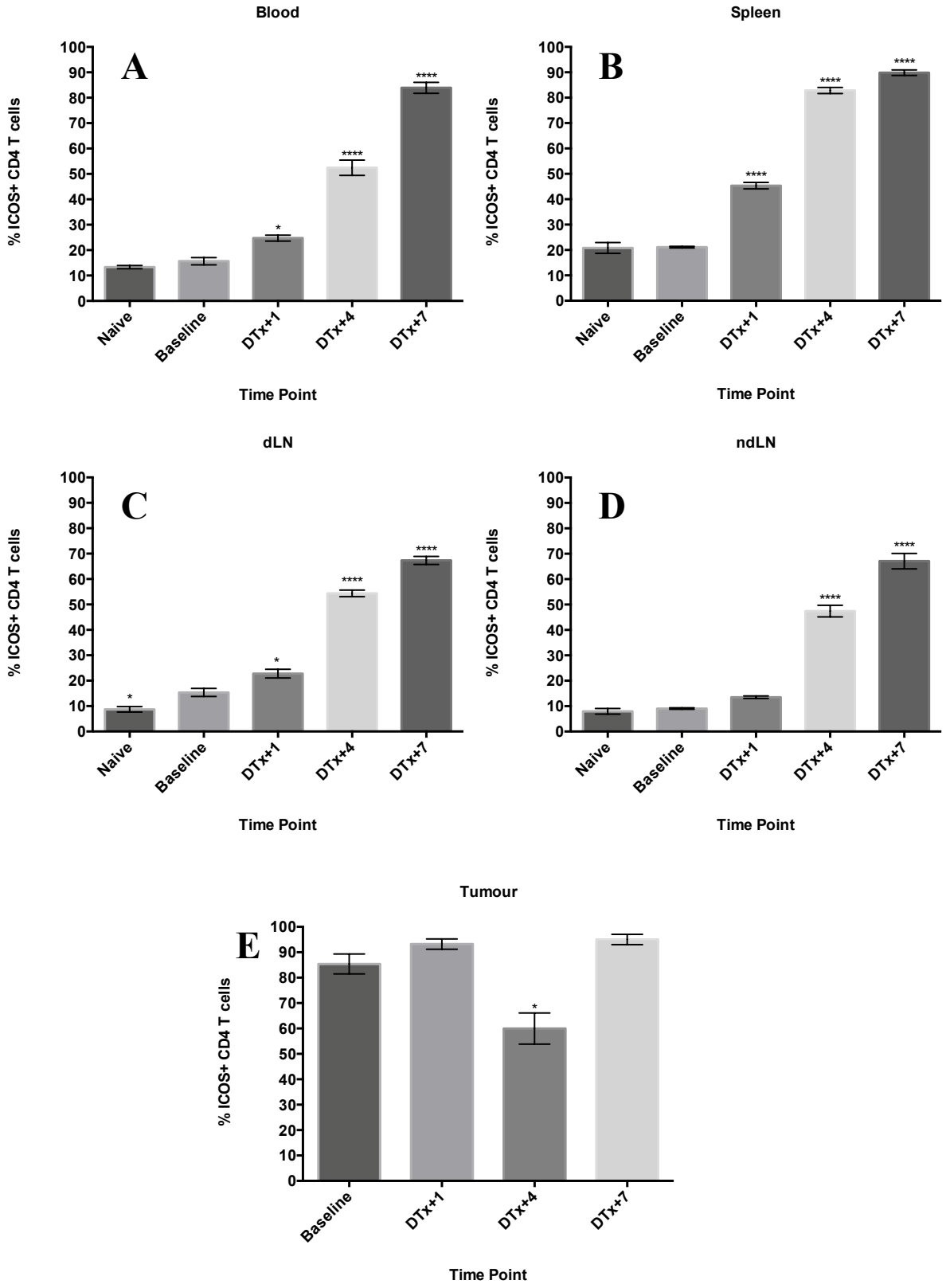

Figure 44: ICOS Expression In CD4+ T Cells Over Time

Figure shows the change in ICOS expression for CD4+ cells over time for blood (A), spleen (B), dLN (C), ndLN (D) and tumour (E) in mice bearing AB1-HA tumours.

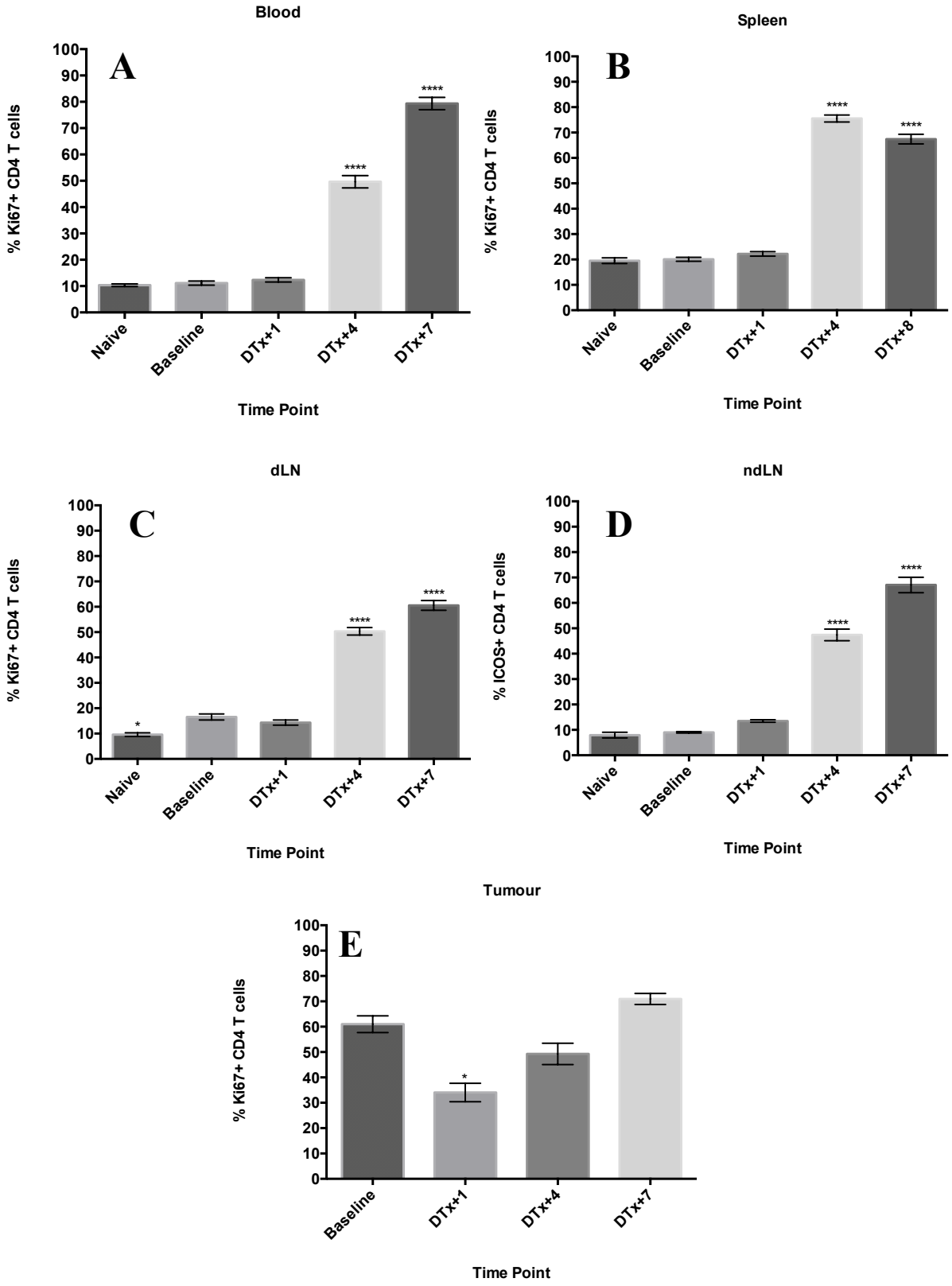

Figure 45: Ki67 Expression In CD4+ T Cells Over Time

Figure shows the change in Ki67 expression for CD4+ cells over time for blood (A), spleen (B), dLN (C), ndLN (D) and tumour (E) in mice bearing AB1-HA tumours.

5.2 FoxP3+ Tregs

The Treg proportions showed a significant decrease (p-value < 0.0001) for all tissues at the DTx+1 time point, 1 day after treatment with DTx (Figure 46). Proportions were reduced to below 1% of total CD4+ cells and started to rebound by DTx+4. By DTx+7, Treg proportions had returned to half the baseline proportion for blood, spleen and dLN tissues. The ndLN Treg proportions had returned to baseline by DTx+7 with tumour proportions remaining between 2-3% of total CD4+ cells, well below the baseline level.

The proportion of ICOS+ FoxP3+ cells did not change between naïve and baseline for blood and spleen samples however there was a significant change between the two for both lymph nodes, with the increase being 2 fold (Figure 47). Due to the high depletion of Tregs at DTx+1, there were not enough cells to obtain a reading for this time point. At DTx+4 there was an increase in ICOS+ Tregs for blood, spleen and the lymph nodes that increases further at DTx+7. The tumour samples did not have a significant increase in ICOS+ Tregs with baseline expression already at 90% of total Treg cells.

The proportion of Ki67+ Tregs (Figure 48) mirrored that seen with ICOS expression in the blood and spleen had no significant difference between naïve and baseline proportions whereas the was a difference observed in the lymph nodes. All tissues excluding tumours displayed a significant increase in the proportion of Ki67+ Tregs by DTx+4 and DTx+7. Tumours again showed the least amount of change in the Ki67+ proportion of Tregs with a decrease at DTx+4 with proportions returning to 95% at DTx+7, an increase of 15% from baseline.

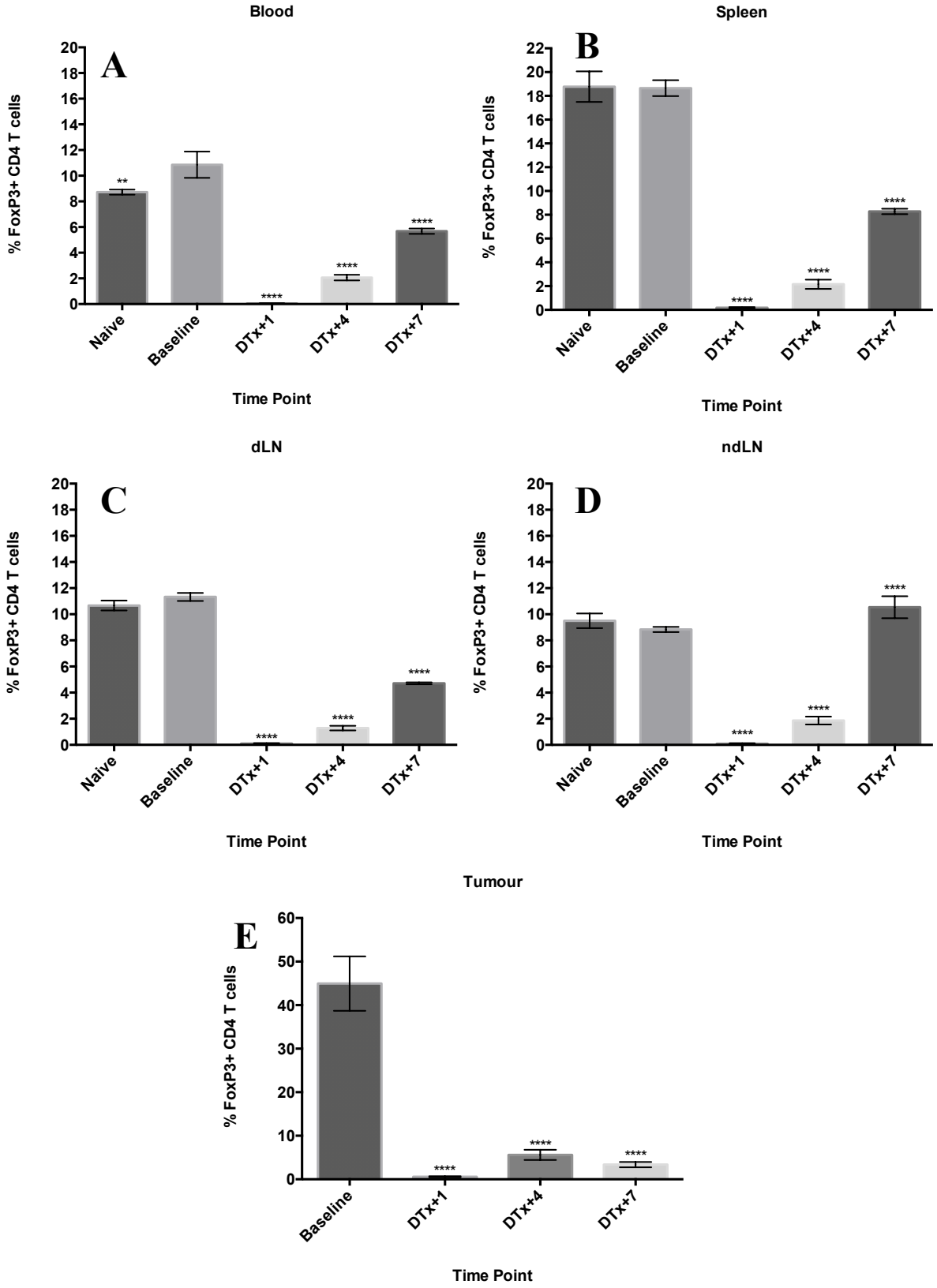

Figure 46: Treg Proportions Over Time

Figure shows the change in Treg proportions over time for blood (A), spleen (B), dLN (C), ndLN (D) and tumour (E) in mice bearing AB1-HA tumours.

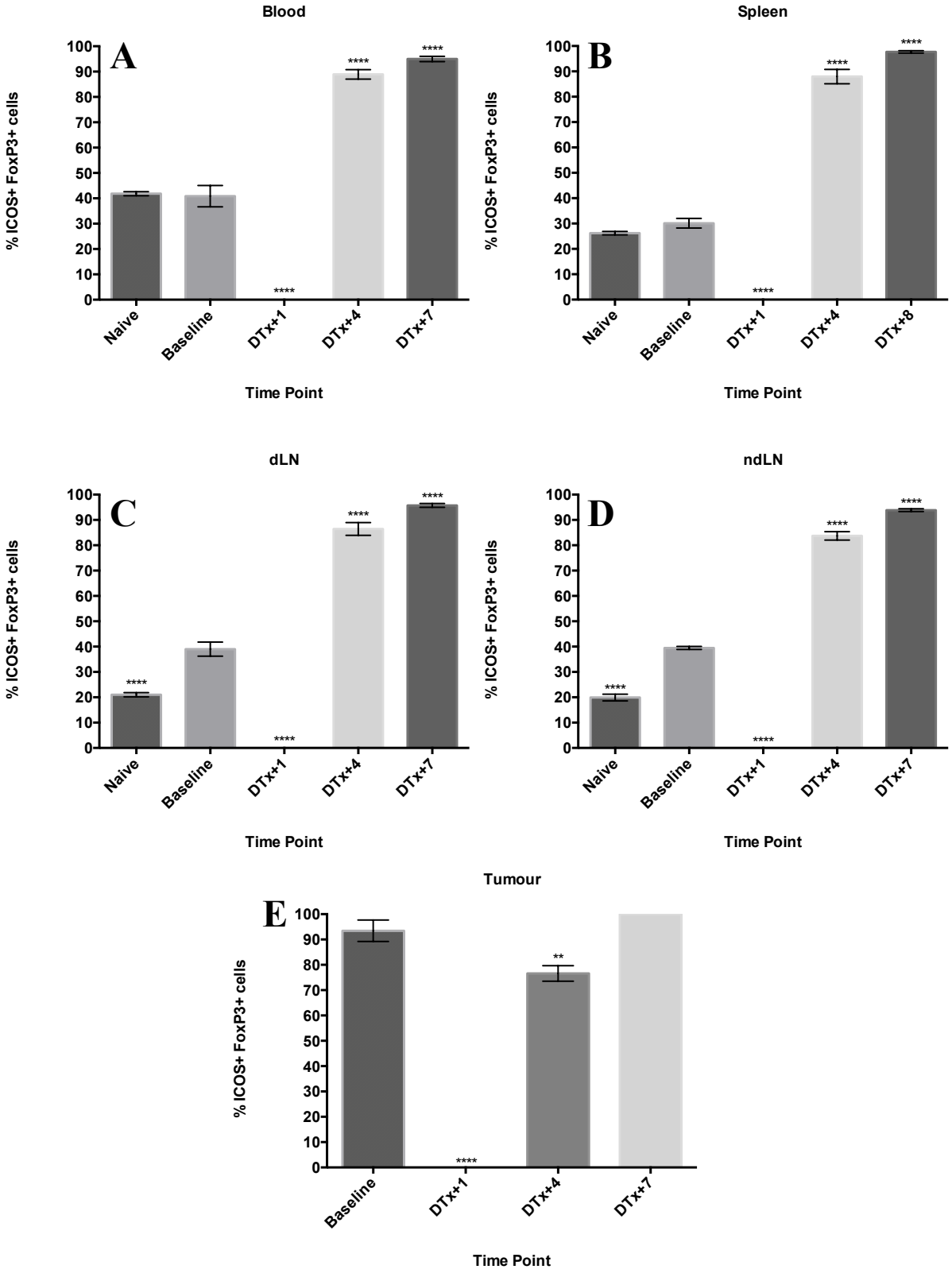

Figure 47: ICOS Expression In FoxP3+ Cells Over Time

Figure shows the change in ICOS expression in Treg cells over time for blood (A), spleen (B), dLN (C), ndLN (D) and tumour (E) in mice bearing AB1-HA tumours.

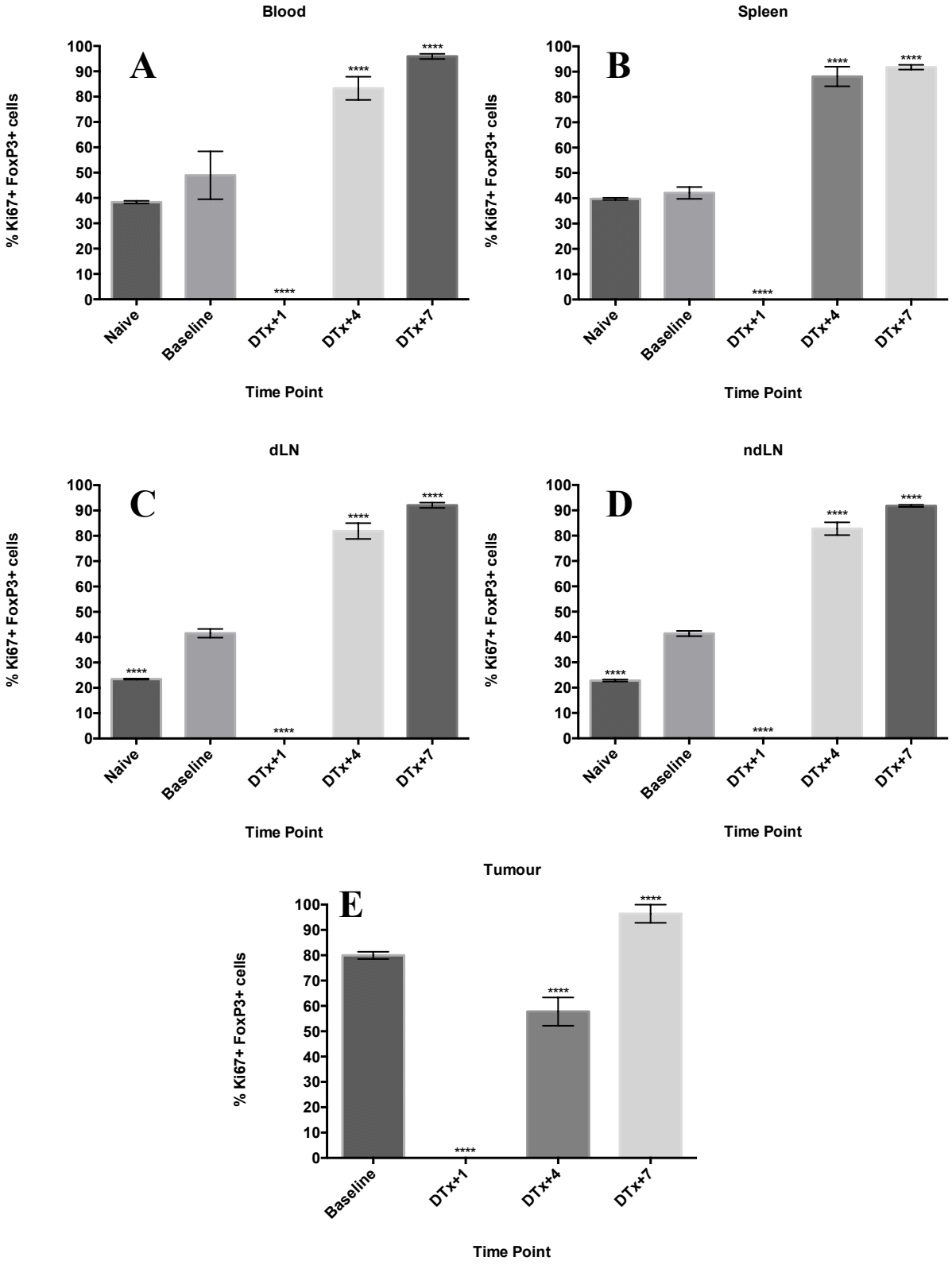

Figure 48: Ki67 Expression In FoxP3+ Cells Over Time

Figure shows the change in Ki67 expression in Treg cells over time for blood (A), spleen (B), dLN (C), ndLN (D) and tumour (E) in mice bearing AB1-HA tumours.

5.3 CD8+ T Cells

Finally, the changes in proportion in CD8+ cells as well as their percentage of activation and proliferation were analysed (Figure 49). For all tissues except the spleen, there was no significant difference between the proportion of CD8+ cells for the naïve, baseline and DTx+1 time points. At DTx+4, all tissues had a significantly higher proportion of CD8+ cells when compared to baseline proportions with the lymph node having a proportion of CD8+ cells that remained elevated through to DTx+7. The tumour displayed the largest change in CD4+ vs. CD8+ proportions with an increase up to 40% for CD8+ cells.

The most significant increase in ICOS expression in CD8+ cells was at the DTx+4 time point for the blood, spleen and lymph node tissues with an increase between 4-5 fold (Figure 50). This increase remained constant for the lymph nodes at DTx+7 but in the blood and spleen there was a small significant increase in ICOS+ CD8+ cells. While the proportion of ICOS expressing CD8+ cells did slightly decrease and then subsequently increase for the tumour samples, these changes were not significant.

The proportion of proliferating CD8+ cells was significantly higher (p-value < 0.001) for blood, spleen and lymph node tissues at the DTx+4 and DTx+7 time point (Figure 51). There was no significant difference between the proportions of proliferating CD8+ T cells at any time point within the tumour but proliferation status at baseline and DTx+1 was significantly higher (p-value < 0.001) than the corresponding levels within the other tissues.

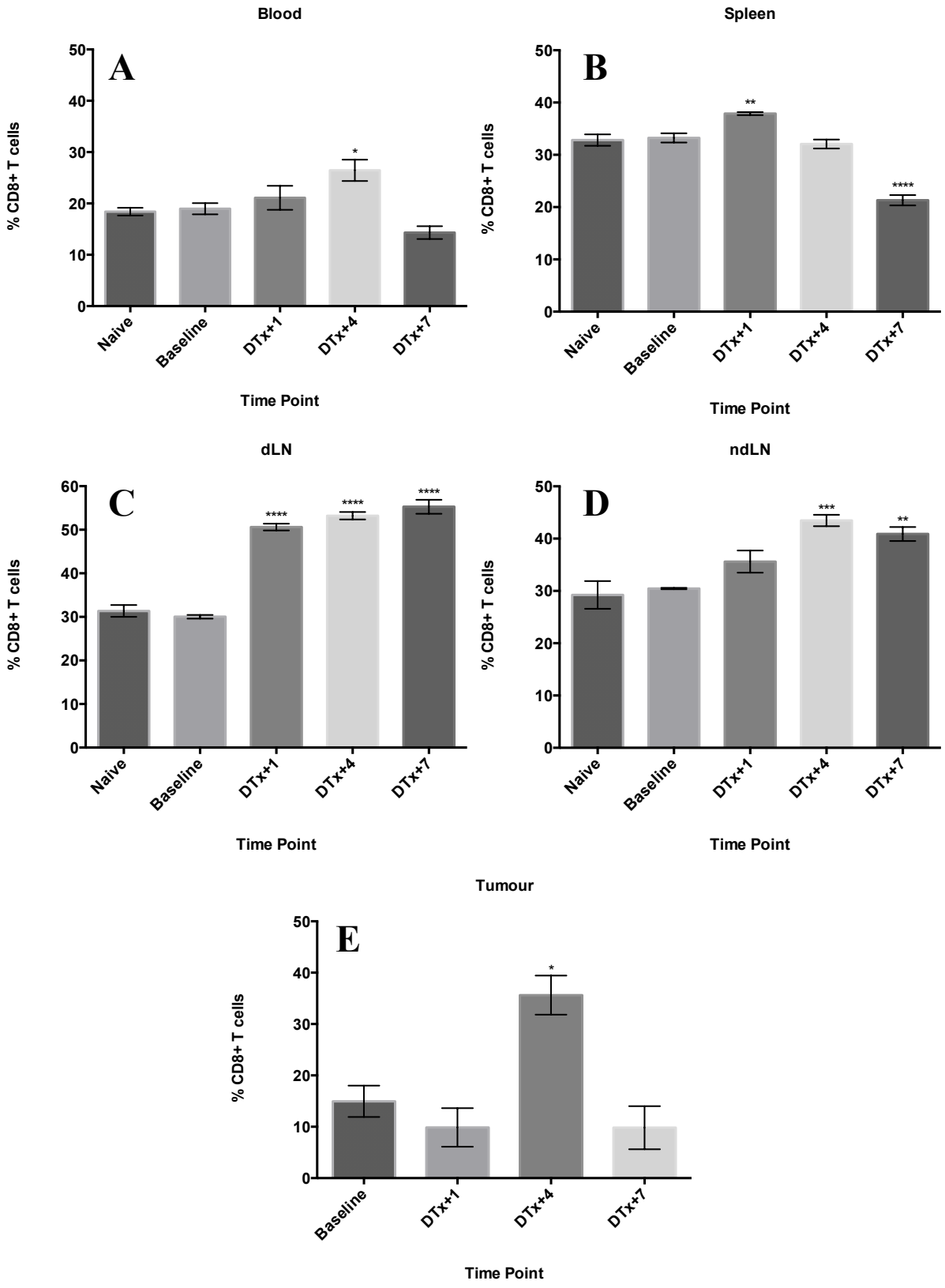

Figure 49: CD8+ Proportions Over Time

Figure shows the change in CD8+ proportions over time for blood (A), spleen (B), dLN (C), ndLN (D) and tumour (E).

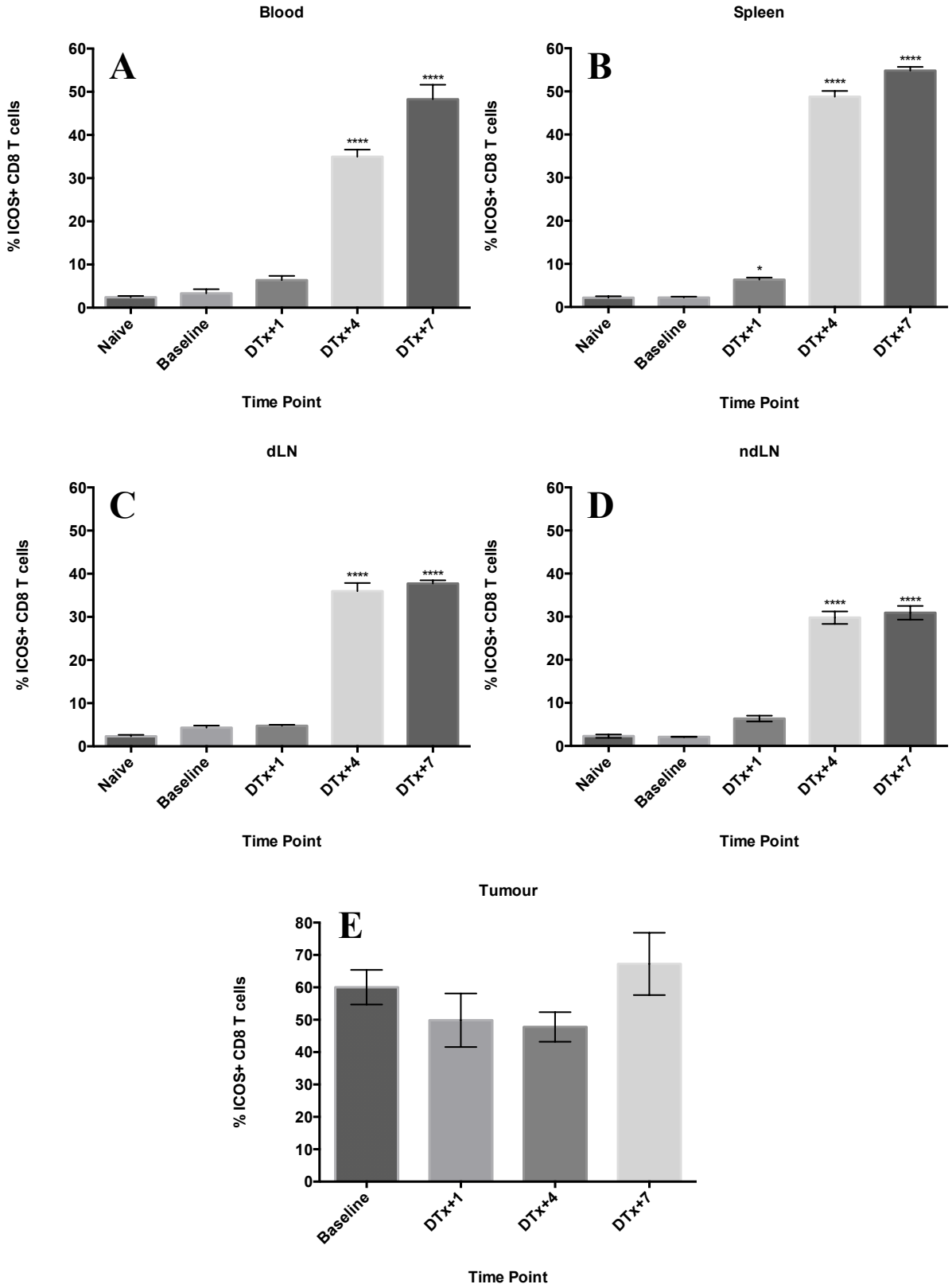

Figure 50: ICOS Expression In CD8+ Cells Over Time

Figure shows the change in ICOS expression in CD8+ cells over time for blood (A), spleen (B), dLN (C), ndLN (D) and tumour (E).

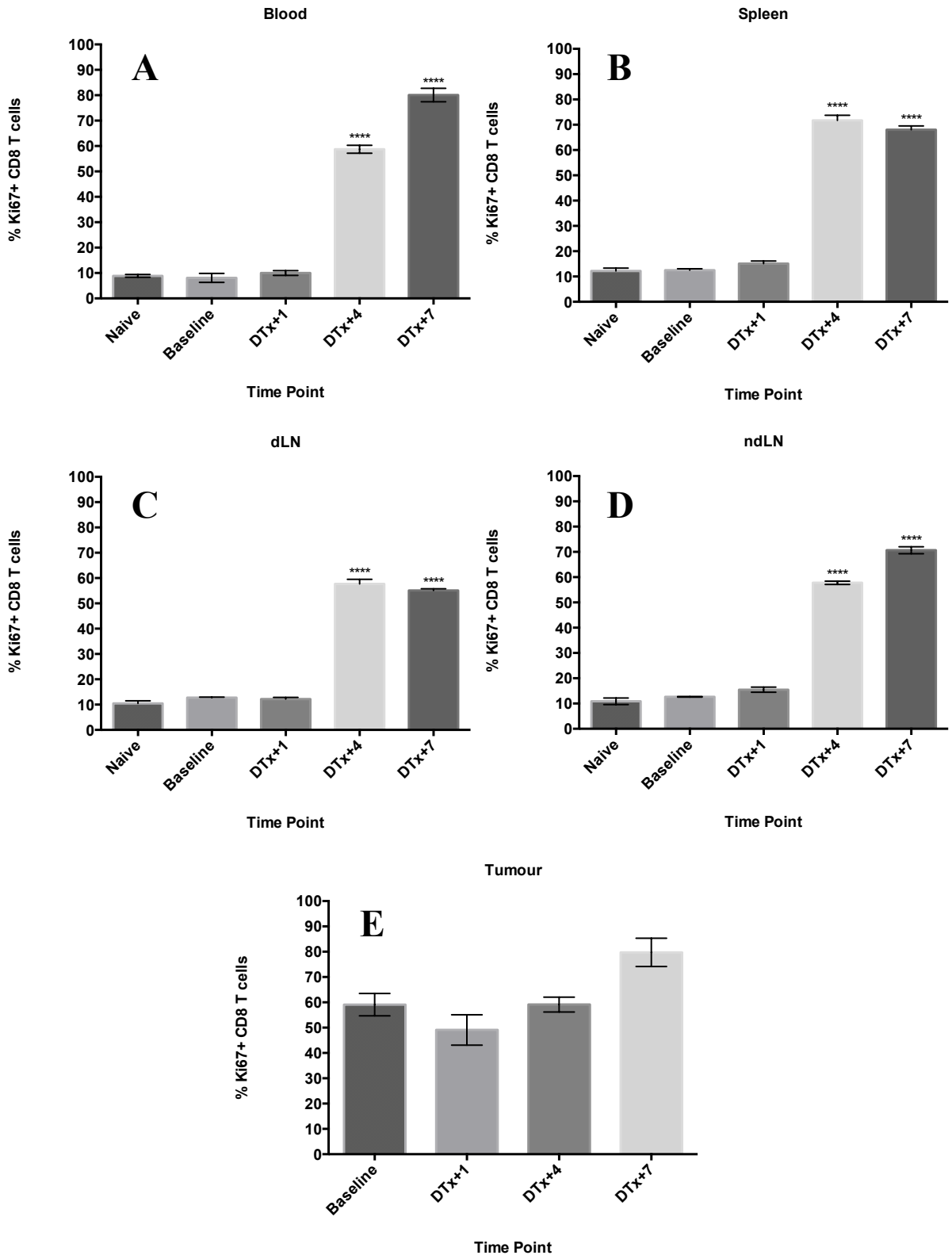

Figure 51: Ki67 Expression In CD8+ Cells Over Time

Figure shows the change in Ki67 expression in CD8+ cells over time for blood (A), spleen (B), dLN (C), ndLN (D) and tumour (E).

5.4 Treg Depletion & CD8+ T Cell Activation

The key aspects involved in this anti-tumour response is firstly the depletion of FoxP3+ Treg cells and the subsequent increase in CD8+ activation represented by a higher expression of the activation marker ICOS.

The results show that Treg baseline levels (Figure 52 A) were similar for blood, dLNs and ndLNs with proportions lying between 10-15% while proportions in the spleen were slightly higher at 18-20%. Tumour samples had the highest proportions of Tregs of total CD4+ cells with levels ranging from 25-40%. Once a dose of 25 ng/g/mouse DTx was given, Treg proportions were significantly depleted compared to baseline levels. The proportion of Tregs of total CD4+ T cells was depleted to below 1% for all organs with blood depleting the most and tumours depleting the least.

Figure 52 B shows that CD8+ activation status was significantly increased in all organs when compared to the non Treg depleted controls at the DTx+4 time point that corresponds to the highest peak in activation. The biggest difference was in the spleen and blood with activation levels increasing 4-5 fold of total CD8+ cells. Activation in the dLNs and ndLNs increased 4 fold. CD8+ activation status in the tumour had the least amount of change between baseline and DTx+4 levels with only a 2-fold increase at most.

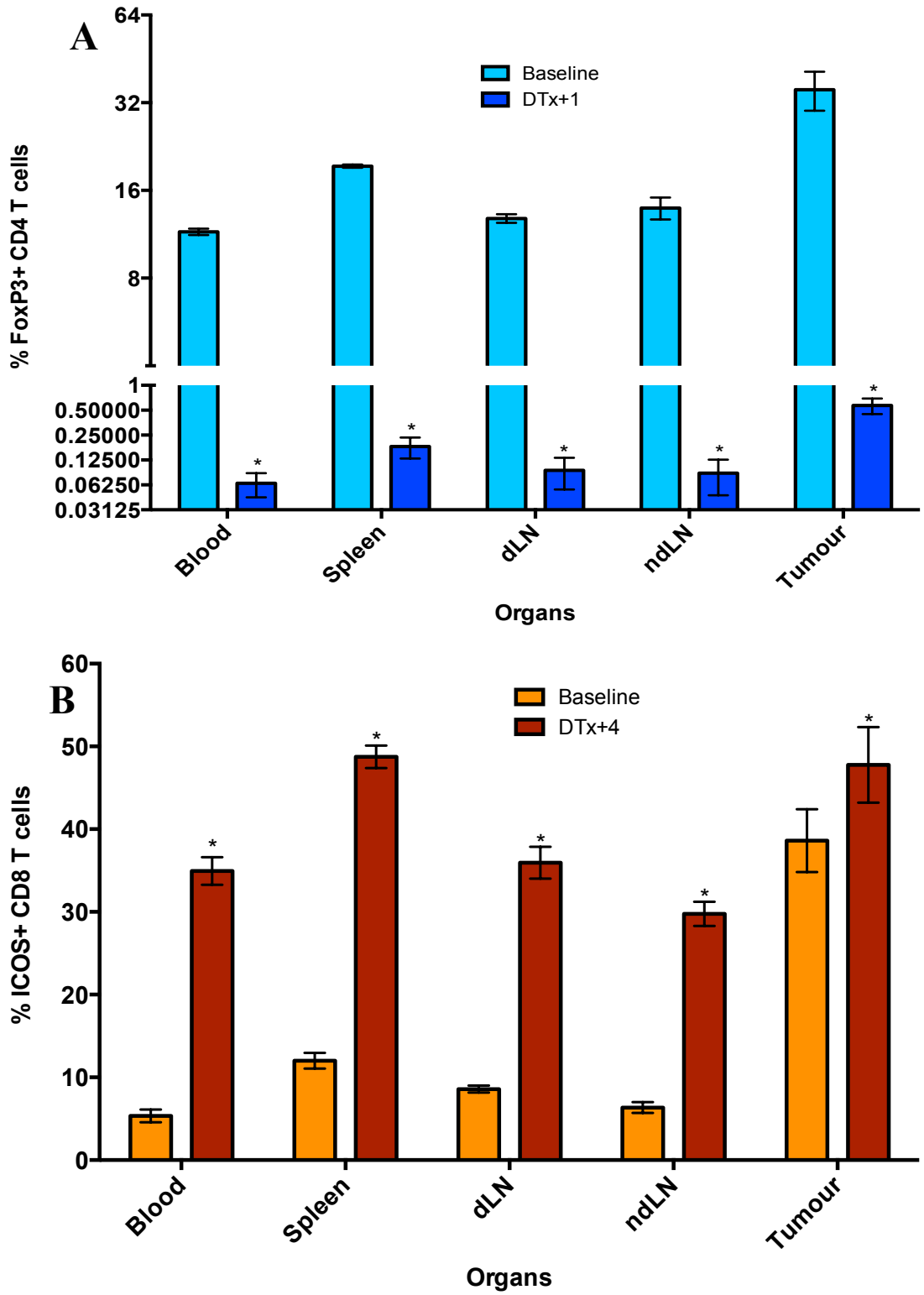

Figure 52: Treg Depletion in Lymphoid Organs, Tumours and Blood

Graphs show percentage of depleted Tregs at DTx+1 (A) and activated CD8+ T cells at DTx+4 (B). Graph A is on a log2 scale to allow for adequate visualization of the range of Treg proportions while Graph B is on a linear scale. All baseline and Treg depleted or CD8+ activated levels were significantly different for all organs with P-values <0.05.

Summary

The results from this experiment have shown that depleting the proportion of FoxP3+ Tregs in the FoxP3.dtr model mediated a number of immunological effects.

Firstly, there was a depletion of CD4+ T cells that resulted in a significant increase in activated and proliferating CD4+ cells in all tissues that remained elevated up to DTx+7.

Similarly, as Tregs were the target of this model, their proportions were depleted to below 1% for all tissues as a result of DTx administration. At DTx+4, the proportion of activated and proliferating Tregs had increased significantly to above 80% of total FoxP3+ cells and remained at that level for the DTx+7 time point. Proportions of FoxP3+ cells of CD4+ cells started to repopulate by DTx+4 and had returned to approximately half their baseline levels by DTx+7 for most tissues.

The proportion of CD8+ T cells increased significantly in the lymph nodes from the DTx+4 time point as well as in the tumour but no major changes in other tissues. Their activation and proliferation proportions increased drastically in all tissues except the tumour with changes in the percentage of activated and proliferating CD8+ cells being minor in terms of baseline levels.

Finally, of these immunological changes that resulted from DTx administration, the main focus was on the depletion of Tregs and the subsequently increase in CD8+ activation. This experiment showed that at a dose of 25 ng/g/mouse of DTx into the FoxP3.dtr mouse model inoculated with AB1-HA there is a significant depletion of Tregs in the blood, spleen, dLN, ndLN and the tumour. Baseline Treg levels for the tumour were significantly higher than the other organs while there was no difference between the dLN and ndLN. Depleted levels mirrored the baseline levels with blood having the lowest proportion of

Tregs at baseline to having the lowest proportion after treatment while in the tumours, baseline levels were the highest and remained so after DTx treatment.

CD8+ activation was significantly increased in all organs at the DTx+4 time point with the highest levels being in the spleen and the lowest being in the ndLN. The tumour had the least amount of change in CD8+ activation, with only an average increase of 9.2% between the control and treated groups. While this experiment showed a correlation between the systemic depletion of Tregs and the resulting systemic increase in CD8+ cell activation status, the intratumoural increase was the lowest of the organs analysed despite this being the pathological site and target for treatment. Further experimental research can be done to determine if a higher intratumoural dose of DTx leads to a higher increase in CD8+ activation without the resultant autoimmunity as was observed with intratumoural anti-CTLA4 (Tuve et al., 2007).

Chapter 6: Discussion

6.1 Introduction

Surgery remains a primary treatment option for many solid malignancies including melanoma and colorectal cancer but is not routinely done in others such as malignant mesothelioma. The reason being the risks often outweigh the benefits as complete resection of this tumour type is very difficult (Robinson *et al.*, 2005). There is often a recurrence of disease with surgical resection of solid cancers due to micro-metastases that have remained undetected or the inability to safely remove the entire mass (Yano *et al.*, 2009). This has resulted in the prescription of adjuvant therapies including chemotherapy, radiotherapy and immunotherapy to be used in combination with surgery to achieve a curative option in cases where complete resection is not possible (Rudd, 2010). One type of adjuvant therapy is the use of immunotherapy agents to either stimulate a stronger immune response to cancer or to remove the suppression that is imposed by these solid cancers. The role of the immune system in the fight against cancer was debated intensely but it is now well accepted that an immune response to cancer can be an effective and hopefully curative option for those malignancies currently without adequate treatments (Whiteside, 2006).

The aim of this study was to investigate the effect of removing tumour-associated immune suppression by targeting the immune suppressors Tregs and MDSCs and how this can be incorporated into debulking surgery to improve the post-surgical outcome of solid malignancies.

6.2 Pre-Clinical Models of Solid Malignancies

The cancers used in this study, mesothelioma, melanoma and colorectal cancer, were chosen because of their current treatment status in human patients. Surgery has a role in all of these cancers to either resect the entire tumour or perform partial debulking where possible and treat with adjuvant therapies. Surgery is often unsuccessful at later stages due to the diffuse nature of mesothelioma or the metastatic potential of melanoma or colorectal cancer (Cunningham *et al.*, 2010; Hiddinga *et al.*, 2013). At later stages all of these cancers are highly resistant to conventional therapies and therefore novel approaches need to be developed.

The models used in this study are not true disease state models as all tumours were grown subcutaneously with a very small chance of them metastasising to other tissues. The location of the tumours allowed for easy access for measuring as well as performing the partial debulking surgery without placing mice under excessive stress.

6.3 Kinetics of Tumour Growth

The first aim of this study was to determine the growth rates of the AB1-HA, B16-F10 and CT44 tumour cell lines that represent mesothelioma, melanoma and colorectal cancer respectively.

AB1-HA is grown in mice on a BALB/c background and forms a solid, spherical tumour when inoculated s.c. that allows for precise measurement of area to track growth. This cell line has a stable growth rate that was suitable for surgery as it allows for flexibility in terms of experimental planning. The variability of growth from one day to another is not so great that it will influence the results.

In contrast, the B16-F10 tumour cell line is a mouse melanoma line that is grown *in vivo* on C57BL/6J mice and forms aggressively progressing solid tumours when inoculated s.c (Culp *et al.*, 2006). In this study the growth of B16-F10 was delayed for 8 days post inoculation with established tumours reaching maximum size 10 days later.

There was also a high rate of tumour ulceration associated with the growth of this tumour than has been observed previously (Kline *et al.*, 2012; van Elsas *et al.*, 1999). The cause of this ulceration was not investigated due to time constraints but a correlation between tumour ulceration and the level of serum matrix metalloproteinase-8; a protein responsible for degradation of type I collagen has been shown to occur specifically in melanoma patients. This may present a possible target to reduce this incidence (Vihinen *et al.*, 2008).

The growth of the CT44 solid tumour resulted in tumours at a size of 50 mm^2 by day 10 with maximum allowable sizes reached up to 23 days after inoculation. This growth rate was slower than both AB1-HA and B16-F10 with tumours not forming a spherical mass but rather an elongated malignancy that was shown in debulking experiments to display metastatic potential by growing towards the peritoneal cavity. The slower rate of growth of this tumour *in vivo* may relate to its immunogenic nature. For example, a version of the wild type CT26 was engineered to secrete granulocyte and macrophage colony-stimulating factor (CSF). That results in the generation of CTLs that mainly recognise an antigen present on CT26, gp70 that is also present on CT44 cell lines derived from that (Huang *et al.*, 1996).

The growth kinetics of these solid tumours were used in the timing of subsequent experiments and provided a better idea of when to perform debulking surgery. The aim was to have tumours at least 50 mm^2 in size to ensure they were established.

6.4 Surgical Debulking of Solid Tumours

To investigate the hypothesis that debulking surgery is a relevant and successful treatment option in combination with an adjuvant immunotherapy, debulking models had to be established. A protocol for the partial debulking of AB1-HA solid tumours has been established previously (Broomfield *et al.*, 2005) and we sought to apply this principle to both the B16-F10 and CT44 tumour models.

The surgical debulking of AB1-HA is simple to perform due to the solid, round morphology of the tumour that has minimal bleeding and short recovery times. In contrast, debulking surgery performed on B16-F10 tumours proved challenging, as tumours were less solid and sizes more variable than AB1-HA or CT44. While difficult, surgical debulking of this tumour model was possible however several factors resulted in this model being removed from further investigations. Those that received any debulking surgery did not survive past day 20 and this was mainly a result of extensive tumour ulceration. The healing of surgical wounds was also slowed possibly due to constant grooming by the mice that occasionally lead to complete removal of sutures. In these instances the mice were no longer included in this study.

The CT44 tumour cell line responded well to debulking surgery and is a suitable model to test as patients with late stage colorectal carcinoma often experience recurrence of the disease following surgery. One cause being that the disease has either metastasised to other regions or that a complete resection was not possible (Cunningham *et al.*, 2010).

The immunogenic nature of this tumour is more pronounced with the addition of debulking surgery as there was a 13.3% rate of complete tumour regression. One immune stimulating characteristic of debulking surgery is the trauma caused at the tumour site and the release of tumour antigens into systemic circulation. This release allows for higher rates of cross-presentation of tumour antigens to APCs in the lymph nodes and a subsequent stronger CTL response to the tumour (Brown *et al.*, 2012; Khong *et al.*, 2013; Lake *et al.*, 2005). This correlates with what was mentioned previously with variants of CT44 based on a wild type cell line version that was specifically engineered to cause the generation of tumour-specific CTLs. The process of debulking surgery may enhance this response. There may be TAAs associated with CT44 that are better recognised by the immune system than those present on AB1-HA or B16-F10 (Khazaie *et al.*, 2006).

Based on the response to debulking surgery, the AB1-HA and CT44 tumour cell lines were chosen to proceed with subsequent studies and the partial debulking of these cancers was representative of what occurs in human patients particularly at later stages of these cancers.

6.5 Debulking Surgery With Transient MDSC and Treg Depletion

With the debulking models established for two tumours where complete resection of the cancer is often difficult, appropriate adjuvant therapies are needed to ensure a curative option is available. The immune suppression associated with the presence of a solid tumour can be attributed to many factors and cell types with two of these being MDSCs and Tregs.

6.5.1 Characterisation and Depletion of MDSCs

The heterogeneity of MDSCs proved troublesome to both characterise and target as a proposed immunotherapy. MDSCs are commonly described as being CD11b+ Gr-1+ in mice and so a method of negative gating in flow cytometry to remove DCs, T and B lymphocytes was used to further define this population. While the majority of MDSCs are found in the bone marrow, small populations are present in both the blood and spleen of mice (Kong *et al.*, 2013). This study showed that MDSC proportions in the blood were generally comprised of the Gr-1 high phenotype for both naïve and tumour bearing mice with a significant increase in Gr-1 high and Gr-1 low phenotypes when a solid tumour was present. The proportions in the spleen were reversed with a high Gr-1 low phenotype while the other proportions remain low. The spleen did not show a significant change in the proportion of any MDSC phenotype when comparing naïve and tumour bearing mice.

The primary mechanisms for MDSC immune suppression are cell-to-cell contact with the interaction of surface markers and the local secretion of immune mediators such as arginase-1 and iNOS with their primary role being within the tumour (Kong *et al.*, 2013). Due to the available cell number when harvesting tumours for flow cytometry analysis, characterising MDSC proportions within sold tumours was not possible as part of this project it remains however a potential source of vital information into the role of MDSCs within these tumour models.

The depletion of MDSCs was attempted in a preliminary experiment conducted by Dr Andrea Khong (UWA School of Medicine and Pharmacology) by trialing the use of two compounds, namely anti-Gr-1 antibody and ATRA. The results of that study showed that the anti-Gr-1 antibody was successful in depleting MDSCs that had a high

expression of the Gr-1 antigen but did not effect the more suppressive population that have an intermediate expression of this molecule (Dolcetti *et al.*, 2010). The use of ATRA resulted in a greater proportion of Gr-1 high MDSCs with a slight increase in the intermediate population. Tumour growth was not delayed or affected by either treatment with all tumours progressing at the same rate as the controls. This result could potentially be improved by further optimisation of the treatment compounds as well as exploration of other routes of administration. An example might be giving these intratumourally to focus the effect within the tumour instead of a systemic dose. The focus of the remainder of the study was on the role of Tregs in immune suppression as a mouse model allowing their targeted depletion has been established previously.

6.5.2 Depletion of Tregs to Enhance the Tumour Immune Response

The role of Tregs in cancer immunology has been well studied and Treg-mediated immune suppression is a crucial evasion strategy employed by solid cancers to limit the immune response (Chen *et al.*, 2005). This indicates Tregs as a target for immunotherapies to improve the outcomes of cancer currently without a cure. Presently, treatments to deplete or alter Treg activation include low dose cyclophosphamide, anti-CD25 antibody and the CTLA-4 antibody. The problem with these compounds is that as well as targeting Tregs, they also target activated effector T cells in the case of anti-CD25. Low dose cyclophosphamide is not as effective in human patients as it was in mouse models of cancer (Zou, 2006).

Therefore to analyse the effect of specific Treg depletion in combination with partial debulking surgery, the FoxP3.dtr mouse model was utilised. This allows for the administration of DTx that results in a transient depletion of only FoxP3+ Tregs and can be done in a dose dependent manner (Kim *et al.*, 2007). This combination of Treg

depletion and 75% debulking surgery was conducted on both the AB1-HA and CT44 tumour models.

6.5.2.1 Treg Depletion in the AB1-HA Tumour Model

The effect of Treg depletion was tested as a single treatment and in combination with debulking surgery. A further test was conducted to determine the effect on tumour growth when DTx is administered at different time points that correlate with a difference in size of the tumour either before or after surgery. The surgery only control had 100% of tumours grow to maximum size. Those that underwent the 75% debulking surgery indicated that AB1-HA is not extensively immunogenic and a strong immune response does not result from debulking surgery alone. When DTx was given once a small tumour had established, either with or without debulking surgery, there was one survivor that received DTx only while all other mice from this time line had tumours progress to maximum size. This difference was not significant and flow cytometry analysis of the increase in the proportion of activated CD8+ T cells show that at DTx+4 activation reaches its peak level and starts decreasing before partial debulking surgery is done.

In contrast, a high rate of tumour regression was observed in DTx treated mice bearing medium sized tumours and in combination with surgery. The DTx only group had a rate of survival of 25% of those that had a palpable tumour while in combination with surgery this was extended to 60%. The timing of administration of DTx correlated with a peak in CD8+ T cell activation only two days after debulking surgery when tumours were smaller in size. The trauma of debulking surgery could have caused the amount of TAAs in the system to reach a threshold level that is required for that an anti-tumour immune response (Robinson *et al.*, 1999). This availability of TAAs as well as the

activation of CTLs to an effective level led to the complete regression of tumours. It also resulted in the induction of memory T cells that prevented a rechallenge with AB1 from establishing a new solid tumour.

The outcome of giving DTx post-surgery on a small tumour was also investigated. This resulted in a survival rate of 33.3% of the mice that had palpable tumours for which surgery could be performed. As TAAs would be abundant at the time of administration of DTx, the reason there was no effective response could be timing. When peak CD8+ T cell activation occurred, it had been 8 days post-surgery which would have allowed tumours to re-establish and begin exponential growth getting to a size that would have resisted an immune response to the tumour.

In the AB1-HA model, once Tregs had been depleted the resultant increase in CTL activation remained at a higher than baseline level at least two weeks after DTx had been given. This is in spite of Treg activation and proliferation having increased dramatically by DTx+4 with the proportion of Tregs of total CD4+ T cells already back to the baseline level. This indicates that despite the high rate of both activated and proliferating Tregs in the systemic circulation, they are not capable of shutting down a CTL response immediately. It is a process that occurs over time, lasting much longer than it took to initiate that immune response.

6.5.2.2 Treg Depletion in the CT44 Tumour Model

With the aim of showing translatability of this approach to other tumour models, the work whereby Tregs are depleted either with or without debulking surgery was carried out in the CT44 tumour model. Based on the response to debulking surgery in which a small number of tumours completely regressed, the hypothesis was that the immune

response would be more effective towards this tumour than it was against AB1-HA. The same time lines were investigated by administering DTx either at a small, medium or small after surgery tumour to determine when the best time point was for Treg depletion. Further investigation was done to determine if there is a difference between those receiving only DTx and those receiving the combination.

The DTx stock used for CT44 study appeared to be more effective than seen previously with AB1-HA, resulting in greater Treg depletion. This correlated with CD8+ T cell activation that was much higher and remained elevated for longer (>2 weeks) and was thus able to improve the survival rate without the need for surgery.

Near complete regression occurred in one tumour that only received debulking surgery, possibly due to a strong CD4+ and CD8+ T cell response that eventually shut down (Klein *et al.*, 2003). At the stage of a small tumour, the resultant immune response was capable of causing complete regression in 80% of the established tumours with a 60% survival rate for the combination with debulking surgery. The higher CTL response due to a greater depletion of Treg proportions may have masked the potentially important role of debulking surgery at this time. This could be rectified by optimising the new DTx stock and using a lower dose to bring Tregs to between 2-3% of total CD4+ cells.

The DTx treated at a medium tumour stage showed that there was a survival rate of 40% for both the DTx only and the DTx plus surgery groups. Survival was extended for those who received the debulking surgery with 40% of the mice having a noticeable delay in tumour progression. Despite the availability of tumour antigens post-surgery as well as peak CTL activation occurring soon after, the percentage of regressed tumours was less than expected as this group performed the best in the AB1-HA tumour model.

Tregs depleted post-surgery resulted in a survival rate of 40% with a noticeable delay in growth for a further 40% of tumours. The two tumours that regressed correlated with smaller tumour sizes at time of surgery. This may indicate the size of established tumours is a representation of the suppressive effect they impose on the immune system with larger malignancies being more resistant to an effective immune response because they have already overcome immunosurveillance (Narendra *et al.*, 2013).

In summary, the result of this work showed that debulking surgery alone offers no survival benefit in terms of a complete regression in either the AB1-HA or CT44 tumour models. Treg depletion using the FoxP3.dtr mouse model increases the activation and proliferation status of CD8+ T cells and does improve survival that is further increased when done in combination with debulking surgery. The best response for the AB1-HA tumour model was the combination of debulking surgery and Treg depletion just prior to surgery. Survival rates for CT44 were best when depletion occurred at smaller tumour sizes irrespective of debulking surgery. There may be a correlation between tumour size when DTx was administered and survival. This can be further investigated to determine the threshold size of tumours and whether they will regress or not. The correlation between the extent of CD8+ activation and tumour regression was unclear as similar activation levels resulted in the regression of some tumours but not others. With all analysis of immune responses done from blood samples, these processes had to be investigated in both the lymphoid organs and the tumour itself to determine if these immune responses occurring are a representation of the systemic response taking place locally in these tissues.

6.6 Characterisation of Tregs in the Tumour and Lymphoid Organs

We then sought to investigate whether DTx administration depleted Tregs in other lymphoid organs in the same manner as we observed for peripheral blood. In terms of CD4+ T cell proportions, a possible explanation for the decrease observed was due to a depletion of FoxP3+ CD4+ T cells. Those are the only cell type affected in this model (Kim *et al.*, 2007). The increase in both activated and proliferating CD4+ included both FoxP3+ and FoxP3- populations. It is possible that the removal of Tregs removes suppression imposed on CD4+ T cells that allows them to promote activation and proliferation of the CTLs both in systemic circulation and intratumourally (Whiteside, 2006). Comparison of CD4+ T cell proportions showed a significantly lower percentage in the tumour with these cells having both high proportions of activated and proliferating cells. These CD4+ T cells may have roles in both the expansion and cytolytic capabilities of CTLs as well as the overall regulation of the immune response (Kennedy *et al.*, 2008).

Treg proportions varied between tissues with proportions in the blood and lymph nodes being between 8-12% of total CD4+ T cells at baseline. Treg proportions in the spleen were 2-fold higher than in the blood and lymph nodes, whereas the proportion in tumours were 4-fold higher. A higher density of Tregs was expected in the tumour and is often used as a marker for disease outcome in human cancers with a larger proportion of tumour-infiltrating Tregs correlating with a negative prognosis (Savage *et al.*, 2013). Following Treg depletion the activation and proliferation of Tregs increased significantly in all tissues except the tumour. A possible reason that tumour-infiltrating Tregs are already highly activated or proliferating could be due to the ability of solid tumours to recruit and maintain active Tregs intratumourally (Evans *et al.*, 2006).

Lastly, the activation and proliferation status of CD8+ T cells was characterised to determine the systemic CTL response that resulted from Treg depletion. Blood showed the lowest proportion of CD8+ T cells with the spleen having the highest at baseline. The greatest change occurred in the lymph nodes. While there was a significant increase in proportion of CD8+ T cells in both the dLN and ndLN when compared to blood, the maximum increase was observed in the dLN. A possible explanation is that APCs are tracking from the site of the tumour straight to the dLN due to its proximity to the tumour site. The presentation of antigen via cross-presentation to CD8+ T cells results in a massive expansion of this population (van der Bruggen *et al.*, 2006). CD8+ T cell proportions in the tumour were the lowest of all tissues with a significant increase at the DTx+4 time point. This may indicate that removal of suppressive Tregs results in an increase in TILs to that area, a phenomenon that has previously been correlated with a positive prognosis and increased survival in cancer (Mahmoud *et al.*, 2011). Both activation and proliferation increased in all lymphoid tissues and the blood following Treg depletion and remained so up to the final time point of DTx+7. The tumour sample experienced little change in either activated or proliferating proportions of CD8+ T cells possibly due to the fact that these were already highly activated/proliferating.

The overall impression from this work indicated that the proportions of CD4+ T cells, CD8+ T cells and Tregs as well as their activation/proliferation status was comparable between the blood and lymphoid tissues. Their proportions within blood give a good representative picture of what is happening systemically when depletion of Tregs is used as a form of immunotherapy. A clearer idea of the immune response within tumours was also established at the different time points involved with transient Treg depletion.

Chapter 7: Conclusion

7.1 Conclusion

Solid cancers such as malignant mesothelioma and colorectal cancer are incredibly difficult to treat at later stages of the disease as they often become treatment resistant. By introducing partial resection surgery in combination with an adjuvant immunotherapy we have the opportunity to induce the immune system to respond to TAAs that remain in order to eradicate micro-metastases that may have formed. Two potential immunotherapy targets are MDSCs and Tregs, which have both been implicated in the ability of solid tumours to evade host immune responses. Both of these populations are involved in suppression of the immune system that prevents an appropriate CTL response to tumours that have already adapted to evade the immune response. This study showed that removal of Treg suppression could allow CTLs to both infiltrate and impact on solid tumours and that although Tregs return to baseline soon after transient depletion, the CTL response remains active. This potentially provides a window for a second immunotherapy agent. Finally, it was shown that transient Treg depletion could successfully be combined with surgical debulking to further improve the survival rate and overall outcome of solid malignancies.

7.2 Future Directions of This Study

There are several areas presented in this study that can be further investigated. The systemic depletion of MDSCs resulted in no survival benefit despite the literature indicating a major role for this cell type in immune suppression (Gabrilovich *et al.*, 2009; Srivastava *et al.*, 2012). The treatments used may be further optimised and the possibility of treating locally by targeting the tumour directly may produce a more positive result.

Systemic depletion of Tregs proved very effective in controlling tumour growth but the potential for autoimmunity remains a barrier that needs to be overcome. Investigation of intratumoural Treg depletion in the FoxP3.dtr model may alleviate this if a dose can be given to contain the CTL response locally to the tumour without the systemic effects observed in this study. Researchers are already investigating this with other Treg depleting compounds (Needham *et al.*, 2006).

As surgery is still a primary treatment option for many solid cancers, novel surgical models need to be established to test partial resection on a variety of cancers. How this can be combined with adjuvant therapies to improve outcomes or reduce the extent to which surgery has to be done can be investigated. This may lead to less invasive procedures and a shorter recovery time for patients. This was the first study investigating the effect of Treg depletion and surgical debulking in colorectal cancer using the FoxP3.dtr mouse model and showed translatability between this model and the AB1-HA model. Furthermore, this model provided a proof on concept that systemic removal of Tregs is beneficial with new insights on how best to combine surgery with the timing of transient Treg depletion.

Chapter 8. Appendix

Table 2: Reagents

Reagent	Working Stock	Source	Catalog No.
100 U/mL Benzylpenecillin	-	SCGH Pharmacy (Nedlands, WA)	-
10x BD FACS ™ Lysing Solution	Diluted 1:10 with H_20	BD Bioscience (Lane Cove, NSW)	349202
10x BD Pharm Lyse™	Diluted 1:10 with H_20	BD Bioscience (Lane Cove, NSW)	555899
10x Permeabilisation Buffer	Diluted 1:10 with H_20	Jomar Bioscience (Stepney, SA)	00-8333-56
1x Phosphate Buffer Saline	2x PBS tablets dissolved in 400 ml ddH20	Sigma-Aldrich (Castle Hill, NSW)	P4417
2-Mercaptoethanol	-	Sigma-Aldrich (Castle Hill, NSW)	M7522
20mM Gibco® Hepes	-	Sigma-Aldrich (Castle Hill, NSW)	H3375-1KG
3x BD Stabilising Fixative™	Diluted 1:3 with H_20	BD Bioscience (Lane Cove, NSW)	338036
50 mg/mL Geneticin® Selective Antibiotic	-	Life Technologies (Mulgrave, VIC)	10131027
50 ug/mL Gentamicin	-	SCGH Pharmacy (Nedlands, WA)	-
Cellstripper™	-	Corning Cellgro (Manassas, VA)	25-056-CI
Collagenase Type ll Powder	Dissolve Collagenase in 50 ml of R2 media and DNase into 10 ml R2 Media. Add both together and make up to 100 ml with R2 media to give a 10x Tumour Digest	Worthington Biochemical (Templestowe,VIC)	LS004174
DNase Type l Grade ll		Roche Applied Science (Castle Hill, NSW)	10104159001
Diphtheria Toxin	Dissolve Diphtheria Toxin powder in ddH_20 at a concentration of 1 mg/ml and store at -80^oC	Sigma-Aldrich (Castle Hill, NSW)	D0564-1MG
Fixation/Permeabilisation Concentrate	Made up to 1x Fix/Perm solution by adding 1 part Fixation/Permeabilisation Concentrate to 3 parts Fixation/Permeabilisation Diluent	Jomar Bioscience (Stepney, SA)	00-5123-43
Fixation/Permeabilisation Diluent		Jomar Bioscience (Stepney, SA)	00-5223-56

Foetal Calf Sera	-	Life Technologies (Mulgrave, VIC)	-
Gibco® DMEM High Glucose Cell Culture Media w/ L-glutamine	-	Life Technologies (Mulgrave, VIC)	11965-092
Gibco® GlutaMAX Supplement	-	Life Technologies (Mulgrave, VIC)	35050-061
Gibco® RPMI 1640 Cell Culture Media w/ L-glutamine	-	Life Technologies (Mulgrave, VIC)	11875-093
2%FCS/PBS	Prepared by adding 2% v/v of FCS into 1x PBS	Sigma-Aldrich (Castle Hill, NSW)	-
1000 U/mL Heparin		Pfizer (West Ryde, NSW)	AUST R 49232
Trypsin 0.12%	-	Sigma-Aldrich (Castle Hill, NSW)	59430C

Table 3: Treg Panel

Antibody Marker	Fluorophore	Isotype	Clone	Dilution	Source	Catalog No.
CD3	PE-Cy7	Hamster IgG	145-2C11	1:500	BioLegend (San Diego, CA)	100320
CD4	PerCP-CY5.5	Rat IgG2b	GK1.5	1:500	BioLegend (San Diego, CA)	100434
CD8	APC-ef780	Rat IgG2a	53-6.7	1:500	Jomar Bioscience (Stepny, SA)	47-0081
FoxP3	FITC	Rat IgG2a	FJK-16s	1:100	Jomar Bioscience (Stepny, SA)	11-5773
ICOS	APC	Hamster IgG	C398.4A	1:200	BioLegend (San Diego, CA)	313510
Ki67	PE	Mouse IgG1	MOPC-21	1:20	BD Bioscience (Lance Cove, NSW)	556027

Table 4: MDSC Panel

Antibody Marker	Fluorophore	Isotype	Clone	Dilution	Source	Catalog No.
CD11b	PerCP-CY5.5	Rat IgG2b	M1/70	1:100	BioLegend (San Diego, CA)	101228
CD11c	AF488	Hamster IgG	N418	1:100	BioLegend (San Diego, CA)	117311
CD19	PE-Cy7	Rat IgG2a	1D3	1:100	BD Bioscience (Lance Cove, NSW)	552854
CD3	PE-Cy7	Rat IgG2b	145-2C11	1:500	BioLegend (San Diego, CA)	100320
Gr-1	PE	Rat IgG2b	RB6-8C5	1:1000	Jomar Bioscience (Stepny, SA)	12-5931-81

Table 5: Compensation Beads

Compensation Beads	Catalog No.
Negative Control	Comes with positive controls
Anti-Mouse	552843
Anti-rat/hamster	552845

Chapter 9: References

Anraku, M., Cunningham, K. S., Yun, Z., Tsao, M. S., Zhang, L., Keshavjee, S., . . . de Perrot, M. (2008). Impact of tumor-infiltrating T cells on survival in patients with malignant pleural mesothelioma. *Journal of Thoracic and Cardiovascular Surgery, 135*(4), 823-829.

Australian Institute of Health and Welfare. (2012). *Cancer in Australia: an overview*. Canberra.

Baumgartner, J. M., Gonzalez, R., Lewis, K. D., Robinson, W. A., Richter, D. A., Palmer, B. E., . . . McCarter, M. D. (2009). Increased Survival From Stage IV Melanoma Associated With Fewer Regulatory T Cells. *Journal of Surgical Research, 154*(1), 13-20.

Bograd, A. J., Suzuki, K., Vertes, E., Colovos, C., Morales, E. A., Sadelain, M., & Adusumilli, P. S. (2011). Immune responses and immunotherapeutic interventions in malignant pleural mesothelioma. *Cancer Immunology Immunotherapy, 60*(11), 1509-1527.

Broomfield, S., Currie, A., van der Most, R. G., Brown, M., van Bruggen, I., Robinson, B. W. S., & Lake, R. A. (2005). Partial, but not complete, tumor-debulking surgery promotes protective antitumor memory when combined with chemotherapy and adjuvant immunotherapy. *Cancer Research, 65*(17), 7580-7584.

Brown, Matthew, Van Der Most, Robbert, Vivian, Justin B., Lake, Richard A., Lama, Irma, Robinson, Bruce W. S., & Currie, Andrew J. (2012). Loss of antigen cross-presentation after complete tumor resection is associated with the generation of protective tumor-specific CD8+ T-cell immunity. *1*(7), 1094.

Cancer Research UK. (2012). *How many different types of cancer are there?* London.

Carrato, Alfredo. (2008). Adjuvant treatment of colorectal cancer. *Gastrointestinal cancer research, 2*(4), 6.

Chen, M. L., Pittet, M. J., Gorelik, L., Flavell, R. A., Weissleder, R., von Boehmer, H., & Khazaie, K. (2005). Regulatory T cells suppress tumor-specific CD8 T cell cytotoxicity through TGF-beta signals in vivoi. *Proceedings of the National Academy of Sciences of the United States of America, 102*(2), 419-424.

Chen, W. J., Jin, W. W., Hardegen, N., Lei, K. J., Li, L., Marinos, N., . . . Wahl, S. M. (2003). Conversion of peripheral CD4(+)CD25(-) naive T cells to CD4(+)CD25(+) regulatory T cells by TGF-beta induction of transcription factor Foxp3. *Journal of Experimental Medicine, 198*(12), 1875-1886.

Corthay, A. (2009). How do Regulatory T Cells Work? *Scandinavian Journal of Immunology, 70*(4), 326-336.

Culp, W. D., Neal, R., Massey, R., Egevad, L., Pisa, P., & Garland, D. (2006). Proteomic analysis of tumor establishment and growth in the B16-F10 mouse melanoma model. *Journal of Proteome Research, 5*(6), 1332-1343.

Cunningham, D., Atkin, W., Lenz, H. J., Lynch, H. T., Minsky, B., Nordlinger, B., & Starling, N. (2010). Colorectal cancer. *Lancet, 375*(9719), 1030-1047.

Davis, M. Manning, LS. Whitaker, D. Garlepp, MJ. Robinson, BWS. (1992). Establishment of a Murine Model of Malignant MEsothelioma. *International Journal of Cancer, 52*, 6.

Dolcetti, L., Peranzoni, E., Ugel, S., Marigo, I., Gomez, A. F., Mesa, C., . . . Bronte, V. (2010). Hierarchy of immunosuppressive strength among myeloid-derived suppressor cell subsets is determined by GM-CSF. *European Journal of Immunology, 40*(1), 22-35.

Dranoff, G. (2004). Cytokines in cancer pathogenesis and cancer therapy. *Nature Reviews Cancer, 4*(1), 11-22.

Dunn, G. P., Bruce, A. T., Ikeda, H., Old, L. J., & Schreiber, R. D. (2002). Cancer immunoediting: from immunosurveillance to tumor escape. *Nature Immunology, 3*(11), 991-998.

Elmageed, Z. Y. A., Gaur, R. L., Williams, M., Abdraboh, M. E., Rao, P. N., Raj, M. H. G., . . . Ouhtit, A. (2009). Characterization of Coordinated Immediate Responses by p16(INK4A) and p53 Pathways in UVB-Irradiated Human Skin Cells. *Journal of Investigative Dermatology, 129*(1), 175-183.

Evans, C., Dalgleish, A. G., & Kumar, D. (2006). Review article: immune suppression and colorectal cancer. *Alimentary Pharmacology & Therapeutics, 24*(8), 1163-1177.

Evans, C., Galustian, C., Kumar, D., Hagger, R., Melville, D. M., Bodman-Smith, M., . . . Dalgeish, A. G. (2009). Impact of surgery on immunologic function: comparison between minimally invasive techniques and conventional laparotomy for surgical resection of colorectal tumors. *American Journal of Surgery, 197*(2), 238-245.

Flinsenberg, T. W. H., Compeer, E. B., Boelens, J. J., & Boes, M. (2011). Antigen cross-presentation: extending recent laboratory findings to therapeutic intervention. *Clinical and Experimental Immunology, 165*(1), 8-18.

Gabrilovich, D. I., & Nagaraj, S. (2009). Myeloid-derived suppressor cells as regulators of the immune system. *Nature Reviews Immunology, 9*(3), 162-174.

Gyorki, David, Gyorki, Margaret, Callahan, Jedd, & Wolchok, Charlotte. (2013). The delicate balance of melanoma immunotherapy. *Clinical & Translational Immunology, 2*(8), 8.

Harrison, S., & Benziger, H. (2011). The molecular biology of colorectal carcinoma and its implications: A review. *Surgeon-Journal of the Royal Colleges of Surgeons of Edinburgh and Ireland, 9*(4), 200-210.

Heath, W. R., Belz, G. T., Behrens, G. M. N., Smith, C. M., Forehan, S. P., Parish, I. A., . . . Villadangos, J. A. (2004). Cross-presentation, dendritic cell subsets, and the generation of immunity to cellular antigens. *Immunological Reviews, 199*(1), 9-26.

Hegmans, Jpjj, Hemmes, A., Hammad, H., Boon, L., Hoogsteden, H. C., & Lambrecht, B. N. (2006). Mesothelioma environment comprises cytokines and T-regulatory cells that suppress immune responses. *European Respiratory Journal, 27*(6), 1086-1095.

Hiddinga, B. I., & van Meerbeeck, J. P. (2013). Surgery in Mesothelioma - Where Do We Go after MARS? *Journal of Thoracic Oncology, 8*(5), 525-529.

Huang, Alex Y, Gulden, Pamela H, Woods, Amina S, Thomas, Matthew C, Tong, Caryn D, Wang, Wei, . . . Jaffee, Elizabeth M. (1996). The Immunodominant Major Histocompatibility Complex Class I-Restricted Antigen of a Murine Colon Tumor Derives from an Endogenous Retroviral Gene Product. *Proceedings of the National Academy of Sciences of the United States of America, 93*(18), 9730-9735.

Ismail-Khan, Roohi, Robinson, Lary A., Williams, Jr Charles C., & Garrett, Christopher R. (2006). - Malignant pleural mesothelioma: a comprehensive review. *Cancer Control, - 13*(- 4), - 63.

Janeway, C. A. (2001). How the immune system works to protect the host from infection: A personal view. *Proceedings of the National Academy of Sciences of the United States of America, 98*(13), 7461-7468.

Joffre, O. P., Segura, E., Savina, A., & Amigorena, S. (2012). Cross-presentation by dendritic cells. *Nature Reviews Immunology, 12*(8), 557-569.

Kennedy, R., & Celis, E. (2008). Multiple roles for CD4(+) T cells in anti-tumor immune responses. *Immunological Reviews, 222*, 129-144.

Khazaie, K., & von Boehmer, H. (2006). The impact of CD4(+)CD25(+) Treg on tumor specific CD8(+) T cell cytotoxicity and cancer. *Seminars in Cancer Biology, 16*(2), 124-136.

Khong, A., Brown, M. D., Vivian, J. B., Robinson, B. W. S., & Currie, A. J. (2013). Agonistic Anti-CD40 Antibody Therapy is Effective Against Postoperative Cancer Recurrence and Metastasis in a Murine Tumor Model. *Journal of Immunotherapy, 36*(7), 365-372.

Kim, J. M., Rasmussen, J. P., & Rudensky, A. Y. (2007). Regulatory T cells prevent catastrophic autoimmunity throughout the lifespan of mice. *Nature Immunology, 8*(2), 191-197.

Kim, R., Emi, M., & Tanabe, K. (2007). Cancer immunoediting from immune surveillance to immune escape. *Immunology, 121*(1), 1-14.

Klein, L., Trautman, L., Psarras, S., Schnell, S., Siermann, A., Liblau, R., . . . Khazaie, K. (2003). Visualizing the course of antigen-specific CD8 and CD4 T cell responses to a growing tumor. *European Journal of Immunology, 33*(3), 806-814.

Kline, J., Zhang, L., Battaglia, L., Cohen, K. S., & Gajewski, T. F. (2012). Cellular and Molecular Requirements for Rejection of B16 Melanoma in the Setting of Regulatory T Cell Depletion and Homeostatic Proliferation. *Journal of Immunology, 188*(6), 2630-2642.

Kong, Y. Y., Fuchsberger, M., Xiang, S. D., Apostolopoulos, V., & Plebanski, M. (2013). Myeloid Derived Suppressor Cells and Their Role in Diseases. *Current Medicinal Chemistry, 20*(11), 1437-1444.

Lake, R. A., & Robinson, B. W. S. (2005). Opinion - Immunotherapy and chemotherapy - a practical partnership. *Nature Reviews Cancer, 5*(5), 397-405.

Le Voyer, T. E. (2003). - Colon cancer survival is associated with increasing number of lymph nodes analyzed: a secondary survey of intergroup trial INT-0089. *Journal of Clinical Oncology, - 21*(- 15), - 9.

Lee, C. W., Murray, N., Anderson, H., Rao, S. C., & Bishop, W. (2009). Outcomes with first-line platinum-based combination chemotherapy for malignant pleural mesothelioma: A review of practice in British Columbia. *Lung Cancer, 64*(3), 308-313.

Lee, J. M., Seo, J. H., Kim, Y. J., Kim, Y. S., Ko, H. J., & Kang, C. Y. (2012). The restoration of myeloid-derived suppressor cells as functional antigen-presenting cells by NKT cell help and all-trans-retinoic acid treatment. *International Journal of Cancer, 131*(3), 741-751.

Lin, Yung-Chang, Lin, Jayashri, Mahalingam, Jy-Ming, Chiang, Po-Jung, Su, Yu-Yi, Chu, Hsin-Yi, . . . Chiu, Chun-Yen. (2013). Activated but not resting regulatory T cells accumulated in tumor microenvironment and correlated with tumor progression in patients with colorectal cancer. *International Journal of Cancer, 132*(6), 10.

Liu, Y. A., & Zeng, G. (2012). Cancer and Innate Immune System Interactions: Translational Potentials for Cancer Immunotherapy. *Journal of Immunotherapy, 35*(4), 299-308.

Mahmoud, S. M. A., Paish, E. C., Powe, D. G., Macmillan, R. D., Grainge, M. J., Lee, A. H. S., . . . Green, A. R. (2011). Tumor-Infiltrating CD8(+) Lymphocytes Predict Clinical Outcome in Breast Cancer. *Journal of Clinical Oncology, 29*(15), 1949-1955.

Marzo, A. L., Lake, R. A., Robinson, B. W. S., & Scott, B. (1999). T-cell receptor transgenic analysis of tumor-specific CD8 and CD4 responses in the eradication of solid tumors. *Cancer Research, 59*(5), 1071-1079.

Mohiuddin, K., & Swanson, S. J. (2013). Maximizing the Benefit of Minimally Invasive Surgery. *Journal of Surgical Oncology, 108*(5), 315-319.

Narendra, B. L., Reddy, K. E., Shantikumar, S., & Ramakrishna, S. (2013). Immune system: a double-edged sword in cancer. *Inflammation Research, 62*(9), 823-834.

Needham, D. J., Lee, J. M., & Beilharz, M. W. (2006). Intra-tumoural regulatory T cells: A potential new target in cancer immunotherapy. *Biochemical and Biophysical Research Communications, 343*(3), 684-691.

Nefedova, Y., Fishman, M., Sherman, S., Wang, X., Beg, A. A., & Gabrilovich, D. I. (2007). Mechanism of all-trans retinoic acid effect on tumor-associated myeloid-derived suppressor cells. *Cancer Research, 67*(22), 11021-11028.

Niederkorn, J. Y. (2009). Immune escape mechanisms of intraocular tumors. *Progress in Retinal and Eye Research, 28*(5), 329-347.

Nowak, A. K., Lake, R. A., & Robinson, B. W. S. (2006). Combined chemoimmunotherapy of solid tumours: Improving vaccines? *Advanced Drug Delivery Reviews, 58*(8), 975-990.

Prados, J., Alvarez, P. J., Melguizo, C., Rodriguez-Serrano, F., Carrillo, E., Boulaiz, H., . . . Aranega, A. (2012). How is Gene Transfection Able to Improve Current Chemotherapy? The Role of Combined Therapy in Cancer Treatment. *Current Medicinal Chemistry, 19*(12), 1870-1888.

Radzi, R., Osaki, T., Tsuka, T., Imagawa, T., Minami, S., & Okamoto, Y. (2012). Morphological Study in B16F10 Murine Melanoma Cells after Photodynamic Hyperthermal Therapy with Indocyanine Green (ICG). *Journal of Veterinary Medical Science, 74*(4), 465-472.

Read, J. (2013). Recent advances in cutaneous melanoma: towards a molecular model and targeted treatment. *Australasian Journal of Dermatology, 54*(3), 163-172.

Remon, J., Lianes, P., Martinez, S., Velasco, M., Querol, R., & Zanui, M. (2013). Malignant mesothelioma: New insights into a rare disease. *Cancer Treatment Reviews, 39*(6), 584-591.

Robinson, B. W. S., & Lake, R. A. (2005). Medical progress - Advances in malignant mesothelioma. *New England Journal of Medicine, 353*(15), 1591-1603.

Robinson, B. W. S., Lake, R. A., Nelson, D. J., Scott, B. A., & Marzo, A. L. (1999). Cross-presentation of tumour antigens: Evaluation of threshold, duration, distribution and regulation. *Immunology and Cell Biology, 77*(6), 552-558.

Robinson, B. W. S., Musk, A. W., & Lake, R. A. (2005). Malignant mesothelioma. *Lancet, 366*(9483), 397-408.

Rudd, R. M. (2010). Malignant mesothelioma. *British Medical Bulletin, 93*(1), 105-123.

Rus, H., Cudrici, C., & Niculescu, F. (2005). The role of the complement system in innate immunity. *Immunologic Research, 33*(2), 103-112.

Salama, P., Phillips, M., Grieu, F., Morris, M., Zeps, N., Joseph, D., . . . Iacopetta, B. (2009). Tumor-Infiltrating FOXP3(+) T Regulatory Cells Show Strong Prognostic Significance in Colorectal Cancer. *Journal of Clinical Oncology, 27*(2), 186-+.

Sankpal, U. T., Pius, H., Khan, M., Shukoor, M. I., Maliakal, P., Lee, C. M., . . . Basha, R. (2012). Environmental factors in causing human cancers: emphasis on tumorigenesis. *Tumor Biology, 33*(5), 1265-1274.

Savage, P. A., Malchow, S., & Leventhal, D. S. (2013). Basic principles of tumor-associated regulatory T cell biology. *Trends in Immunology, 34*(1), 33-40.

Savina, A., & Amigorena, S. (2007). Phagocytosis and antigen presentation in dendritic cells. *Immunological Reviews, 219*, 143-156.

Spagnolo, F., & Queirolo, P. (2012). Upcoming strategies for the treatment of metastatic melanoma. *Archives of Dermatological Research, 304*(3), 177-184.

Srivastava, M. K., Zhu, L., Harris-White, M., Kar, U., Huang, M., Johnson, M. F., . . . Sharma, S. (2012). Myeloid Suppressor Cell Depletion Augments Antitumor Activity in Lung Cancer. *Plos One, 7*(7).

Sterman, D. H., & Albelda, S. M. (2005). Advances in the diagnosis, evaluation, and management of malignant pleural mesothelioma. *Respirology, 10*(3), 266-283.

Taams, L. S., Palmer, D. B., Akbar, A. N., Robinson, D. S., Brown, Z., & Hawrylowicz, C. M. (2006). Regulatory T cells in human disease and their potential for therapeutic manipulation. *Immunology, 118*(1), 1-9.

Tuve, S., Chen, B. M., Liu, Y., Cheng, T. L., Toure, P., Sow, P. S., . . . Lieber, A. (2007). Combination of tumor site-located CTL-associated antigen-4 blockade and systemic regulatory T-cell depletion induces tumor-destructive immune responses. *Cancer Research, 67*(12), 5929-5939.

Umansky, V., & Sevko, A. (2012). Overcoming immunosuppression in the melanoma microenvironment induced by chronic inflammation. *Cancer Immunology Immunotherapy, 61*(2), 275-282.

van der Bruggen, P., & Van den Eynde, B. J. (2006). Processing and presentation of tumor antigens and vaccination strategies. *Current Opinion in Immunology, 18*(1), 98-104.

van Elsas, A., Hurwitz, A. A., & Allison, J. P. (1999). Combination immunotherapy of B16 melanoma using anti-cytotoxic T lymphocyte-associated antigen 4 (CTLA-4) and granulocyte/macrophage colony-stimulating factor (GM-CSF)-producing vaccines induces rejection of subcutaneous and metastatic tumors accompanied by autoimmune depigmentation. *Journal of Experimental Medicine, 190*(3), 355-366.

Vesely, Matthew D., & Schreiber, Robert D. (2013). Cancer immunoediting: antigens, mechanisms, and implications to cancer immunotherapy. *Annals of the New York Academy of Sciences, 1284*(1).

Vignali, D. A. A., Collison, L. W., & Workman, C. J. (2008). How regulatory T cells work. *Nature Reviews Immunology, 8*(7), 523-532.

Vihinen, P., Koskivuo, I., Syrjanen, K., Tervahartiala, T., Sorsa, T., & Pyrhonen, S. (2008). Serum matrix metalloproteinase-8 is associated with ulceration and vascular invasion of malignant melanoma. *Melanoma Research, 18*(4), 268-273.

Whiteside, T. L. (2006). Immune suppression in cancer: Effects on immune cells, mechanisms and future therapeutic intervention. *Seminars in Cancer Biology, 16*(1), 3-15.

Wolchok, J. D., Kluger, H., Callahan, M. K., Postow, M. A., Rizvi, N. A., Lesokhin, A. M., . . . Sznol, M. (2013). Nivolumab plus Ipilimumab in Advanced Melanoma. *New England Journal of Medicine, 369*(2), 122-133.

Wolf, A. M., Wolf, D., Steurer, M., Gastl, G., Gunsilius, E., & Grubeck-Loebenstein, B. (2003). Increase of regulatory T cells in the peripheral blood of cancer patients. *Clinical Cancer Research, 9*(2), 606-612.

Yano, H., Moran, B. J., Cecil, T. D., & Murphy, E. M. (2009). Cytoreductive surgery and intraperitoneal chemotherapy for peritoneal mesothelioma. *Ejso, 35*(9), 980-985.

Youn, J. I., & Gabrilovich, D. I. (2010). The biology of myeloid-derived suppressor cells: The blessing and the curse of morphological and functional heterogeneity. *European Journal of Immunology, 40*(11), 2969-2975. doi: 10.1002/eji.201040895

Zou, W. P. (2006). Regulatory T cells, tumour immunity and immunotherapy. *Nature Reviews Immunology, 6*(4), 295-307.